Contact Structures and Classifications of Legendrian and Transverse Knots

by

LAURA STARKSTON

LSTARKST@FAS.HARVARD.EDU

ADVISOR: ANDREW COTTON-CLAY

HARVARD UNIVERSITY DEPARTMENT OF MATHEMATICS
Cambridge, Massachusetts

CONTENTS

1. Introduction

Topology is centered around a simple problem: classify shapes and spaces, without paying strict attention to the angles and distances of the space. While topologists can typically ignore many of the details of the geometry of a space, and ask broader questions, there are times when geometric structures can tell us something about a space from a topological perspective. Conversely, many geometric problems can be answered using purely topological techniques. Contact topology exemplifies this unexpected relationship. While originally contact structures were studied as rigid geometric objects, significant advances have been made by looking at them from a topological perspective. In the other direction, the geometry of contact structures can be used to answer important questions in topology.

For many decades, contact structures were viewed as strictly geometric and analytic structures. They originally arose as solutions to differential equations that arose in various applications including optics, thermodynamics, and control-theory. Many of the known theorems from before the 1980s were proven by solving equations and making tricky geometric arguments. This changed dramatically with the development of new topological ways of thinking about contact structures.

A contact structure on a space associates a plane to each point in the space, such that the planes vary smoothly as one moves through different points in space, and the planes are always twisting in some direction so that a non-integrability condition is satisfied. The exact definition will be given in the next section which introduces much of the basic terminology and essential theorems.

The first change in the study of contact topology that I will discuss is Giroux's theory of convex surfaces. This new theory allowed mathematicians to keep track of significantly fewer details, without losing any meaningful information about the contact structure. It reduced a rigid set of geometric data to a flexible set of topological data. This made it possible to employ "cut-and-paste" techniques, which are often utilized by topologists. By cutting the space into basic building blocks, and looking at Giroux's reduced information about the contact structure along the boundary surfaces where the cuts were made, one can make very strong assertions about the entire contact structure.

It is quite impressive how much one can prove about a space given relatively little data. In sections 3-5 of this paper, I will look at how we can use these cut-and-paste techniques to say something about Legendrian and transverse knots, mathematical knots that satisfy certain properties with respect to the contact structure. A mathematical knot is simply a closed loop that can be knotted up in any way, before attaching the two ends together. A Legendrian knot is a knot in the space which always just brushes tangentially against each of the planes in the contact structure. A transverse knot is one which goes through the contact plane at each point.

There has been considerable work in the study of mathematical knots in the last century. Knot theory seeks to classify mathematical knots up to isotopy (meaning that two knots are equivalent if they can be stretched, contracted, tangled, and untangled until that they are identical without breaking open the closed loop). While mathematicians can play with knot diagrams for years to attempt to stretch and untangle two knots in all possible ways they can think of, they need a rigorous mathematical proof to ensure that two knots are actually distinct. The way mathematicians prove such things is by using knot invariants. A knot invariant is a mathematical object associated to a knot, that will always have the same value for two pictures of equivalent knots, regardless of how different the pictures may look.

In the context of contact topology, we look only at subclasses of knots: Legendrian or transverse, and impose a stronger equivalence relation. Two Legendrian (resp. transverse) knots are equivalent (Legendrian (resp. transversely) isotopic) if through stretching, contracting, tangling, and untangling we can get from one to the other where the knots remain Legendrian (resp. transverse) during the stretching, etc. The contact structure puts restrictions on which knots are Legendrian

and transverse. Thus, knowing something about the Legendrian or transverse knots can provide information about a contact structure and the space it is on. While my focus will be on the study of Legendrian and transverse knots in the standard contact structure on the standard Euclidean space $\mathbb{R}^3$ or the three sphere S^3, these results can be applied to obtain information about more general contact manifolds (through surgery along Legendrian and transverse knots). It is important to keep in mind that these seemingly restricted results are part of a larger conversation about contact structures and their applications.

In this paper we explore techniques to begin to classify Legendrian and transverse knots. We first introduce the "classical invariants" which essentially count the number of times contact planes twist in different ways as one moves along the knot. These invariants provide a fairly simple way to distinguish different classes of Legendrian and transverse knots. However, for many years, it was difficult to tell whether these invariants were all that was needed for the classification, or whether there were more intricate details. The question can be formulated as: are there two Legendrian (resp. transverse) knots which have the same topological knot type and same values for their classical invariants, which are not Legendrian (resp. transversely) isotopic? A mathematical knot type which has two such Legendrian (resp. transverse) knots will be called Legendrian (resp. transversely) nonsimple.

Examples of Legendrian knot classes that were not completely determined by general knot type and the classical invariants, were first discovered through new invariants developed by Chekanov [3] right near the turn of the millenium. However, Chekanov's invariants were incapable of finding transverse knots which were not determined by classical invariants. Until about 2007 it remained a mystery whether there were any such examples of transverse knots. In 2007 two different techniques were employed to discover examples of transversely nonsimple knots. One of these methods was the cut-and-paste techniques utilizing convex surface theory. This was carried out by Etnyre and Honda in a series of papers that concluded with a definitive proof of the existence of certain transversely nonsimple knots. These results and techniques are covered in sections 4 and 5. Near the same time, Birman and Menasco used techniques in braid theory to classify certain transverse knots, resulting in the discovery of another set of transversely nonsimple knots.

These results were significant breakthroughs, but there are limitations to the scope of the techniques used. They are only effective in knots satisfying certain patterns, or with limited complexity. However the knowledge that transversely nonsimple knots could be found lead to a search for other invariants of Legendrian and transverse knots through more algebraic methods. A number of powerful algebraic invariants were introduced in general knot theory in the last decade, and recently there have been efforts to apply these methods to find Legendrian and transverse knot invariants. Plamenevskaya discovered one such invariant [25] by looking at Khovanov homology (a relatively new and powerful invariant in knot theory). While this invariant has useful relations to other aspects of contact topology, unfortunately there are no known examples on which it is able to identify transversely nonsimple knots. Ozsváth, Szabó, and Thurston defined another transverse invariant using combinatorial knot Floer homology [24]. This has turned out to be quite effective at finding transversely nonsimple knots [22]. I will discuss this invariant and its implications in the last section of this paper.

While significant advances have been made in the last five years in the classification of Legendrian and transverse knots, there is still considerable work to be done in identifying exactly how and why knots are distinguished by these new invariants. We would like to understand when these invariants are effective at identifying nonsimple knots, and why certain invariants are effective in certain situations. Once we understand the relations between these invariants, we will have a broader understanding of the classification of Legendrian and transverse knots. This will feed into more general advances in contact topology, which can be applied to find new solutions to problems in

topology and in the fields of mechanics, optics, and dynamics which originally motivated the study of contact structures.

The purpose of this paper is to give an introduction to the study of contact topology through these significant turning points in methodology and to bring diverse techniques together to begin the search for connections between these methods. Along the way we supply more details than can be found in the literature, and discuss some slight generalizations of the results obtained by geometric methods. The next section provides an overview of some of the important concepts in contact topology. For the reader with no previous knowledge of contact topology, further introductory material can be found in Etnyre's lecture notes [7], [8] or *An Introduction to Contact Topology* by Geiges [11]. The third section introduces more of the geometric tools. The fourth section establishes some conventions and proves some classification results using these geometric tools. The fifth section proves that positive cables of the $(2,3)$ torus knot are transversely non-simple, a slight generalization of the proof by Etnyre and Honda. The sixth section introduces algebraic tools used to define effective transverse invariants, and the last section discusses how to use these tools to find examples of transversely nonsimple knots. After estabilishing the basics of contact topology, the reader can look either at the algebraic or the geometric sections first, although one's appreciation of the algebraic invariants and intuition for how to apply them will be better established after learning the geometric cut-and-paste techniques.

2. Contact Topology Basics

This section summarizes the basic definitions of contact topology and introduces some of the powerful theorems that provide a base of tools for doing contact topology. Many of these theorems have technical proofs with a different flavor than the proofs in the main sections of this thesis. Some of these proofs have been included, some simply sketched, and some omitted. It is not necessary to look up these proofs to understand the rest of the paper, but for those wishing to learn more of the detailed background there are a few introductory sources which include these proofs, including the book by Geiges [11], and the lecture notes by Etnyre [7], [8].

2.1. **What is a contact structure?** A contact structure is a field of hyperplanes on an odd dimensional manifold that satisfies a certain twisting condition, or non-integrability condition. We will formalize this concept through a few definitions. First, some notation. If M is a manifold, for each $p \in M$, T_pM is the tangent space to M at p and $TM = \cup_{p \in M} T_pM$ is the tangent bundle of M.

Definition 1. *A* hyperplane field ξ *on M is a smooth subbundle of the tangent bundle TM such that $\xi_p = T_pM \cap \xi$ is a vector space of codimension 1 in T_pM.*

Note that we can locally define ξ as the kernel of a 1-form by the following argument. Choose a Riemannian metric g on M which provides an inner product $g_p(\cdot, \cdot)$ on each tangent space that varies smoothly with $p \in M$. Then we can define $\xi^\perp$, which will be a line-bundle over M, and is thus trivializable on a local neighborhood U. Let X be a non-zero vector field over U in $\xi^\perp|_U$. Using this trivialization, we can define $\alpha_U = g(X, \cdot)$ on U. Then at any point $p \in M$, and for any $v_p \in \xi_p$, $\alpha_U(p)(v_p) = g_p(X_p, v_p) = 0$ since X_p is orthogonal to v_p. Conversely if $\alpha_U(q)(w_q) = 0$ then $g_q(X_q, w_q) = 0$ so w_q is orthogonal to X_q. Since $\xi_q^\perp$ is one-dimensional, it is spanned by X_q so $w_q \in (\xi_q^\perp)^\perp = \xi_q$. Thus $\ker(\alpha_U) = \xi|_U$.

Furthermore, if ξ is co-orientable, meaning that TM/ξ is orientable and thus trivial (since it is a line bundle), then there is a global 1-form α such that $\ker(\alpha) = \xi$.

Finally, notice that α only uniquely defined for ξ if we mod out by multiplication of α by a nonzero function $f : M \to R$.

Definition 2. *Suppose* $\dim M = 2n + 1$. *A hyperplane field ξ is said to be* maximally non-integrable *if for every 1-form α such that $\alpha = \xi$ (locally or globally) we have that*

$$\alpha \wedge (d\alpha)^n \neq 0$$

(where $\neq 0$ means is never 0). Namely, $\alpha \wedge (d\alpha)^n$ is a volume form on M. In this case ξ is called a contact structure *on M. The pair (M, ξ) is called a* contact manifold.

Note that the term maximally non-integrable comes from the fact that there is no integral submanifold of ξ, a manifold whose tangent bundle coincides with ξ. Furthermore, there is not even a submanifold whose tangent bundle agrees with ξ on a small neighborhood of M.

Although we have defined contact structures for a general odd-dimensional manifold, for the rest of this paper we will focus on co-orientable 3-dimensional manifolds. In this case, the contact structure ξ will be a field of 2-dimensional planes such that $\xi = \ker \alpha$ and $\alpha \wedge d\alpha \neq 0$.

We also want a way to classify contact structures up to some kind of equivalence relation. The relevant equivalence relation is whether two contact manifolds are *contactomorphic*.
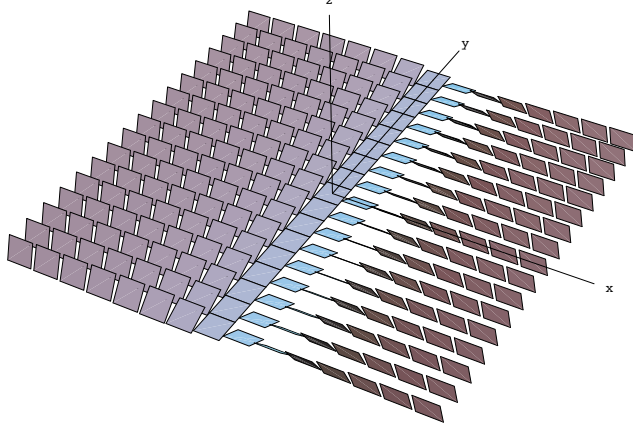
FIGURE 1. The standard contact structure on $\mathbb{R}^3$.

Definition 3. *A* contactomorphism *from* (M, ξ) *to* (M', ξ) *is a diffeomorphism* $\phi : M \to M'$ *such that for all* $p \in M$, $d\phi_p(\xi_p) = \xi'_{\phi(p)}$. *If there is such a contactomorphism between* (M, ξ) *and* (M', ξ') *we say the are* contactomorphic.

2.2. **Examples.**

2.2.1. *The standard contact structure on* $\mathbb{R}^3$. Consider $\mathbb{R}^3$ with standard coordinates (x, y, z) and $\alpha = dz - ydx$. Since

$$\alpha \wedge d\alpha = (dz + xdy) \wedge (dx \wedge dy) = dx \wedge dy \wedge dz \neq 0$$

$\xi = \ker \alpha$ is a contact structure on $\mathbb{R}^3$. This is known as the *standard contact structure* on $\mathbb{R}^3$ and is denoted $(\mathbb{R}^3, \xi_{std})$. The planes are horizontal (orthogonal to $\frac{\partial}{\partial z}$) at $x = 0$ and they rotate as x increases or decreases limiting towards vertical planes as $x \to \pm\infty$. See figure 1. At a point (x, y, z) the contact plane is spanned by $\{\frac{\partial}{\partial x}, -x\frac{\partial}{\partial z} + \frac{\partial}{\partial y}\}$.

In other literature, the standard contact structure is given as $\xi' = \ker(dz - ydx)$ which is spanned by $\{\frac{\partial}{\partial y}, y\frac{\partial}{\partial z} + \frac{\partial}{\partial x}\}$. This is not a problem because $(\mathbb{R}^3, \xi_{std})$ is contactomorphic to $(\mathbb{R}^3, \xi')$ via $\phi : (\mathbb{R}^3, \xi_{std}) \to (\mathbb{R}^3, \xi')$ where $\phi(x, y, z) = (y, -x, z) = (x', y', z')$. Indeed this is a contactomorphism because

$$d\phi_{(x,y,z)}\left(\frac{\partial}{\partial x}\right) = \begin{bmatrix} 0 & -1 & 0 \\ 1 & 0 & 0 \\ 0 & 0 & 1 \end{bmatrix}\begin{bmatrix} 1 \\ 0 \\ 0 \end{bmatrix} = \begin{bmatrix} 0 \\ 1 \\ 0 \end{bmatrix} = \frac{\partial}{\partial y'}$$

and

$$d\phi_{(x,y,z)}\left(-x\frac{\partial}{\partial z} + \frac{\partial}{\partial y}\right) = \begin{bmatrix} 0 & -1 & 0 \\ 1 & 0 & 0 \\ 0 & 0 & 1 \end{bmatrix}\begin{bmatrix} 0 \\ -1 \\ x \end{bmatrix} = \begin{bmatrix} 1 \\ 0 \\ x \end{bmatrix} = x\frac{\partial}{\partial z'} + \frac{\partial}{\partial x'} = y'\frac{\partial}{\partial z'} + \frac{\partial}{\partial x'}$$
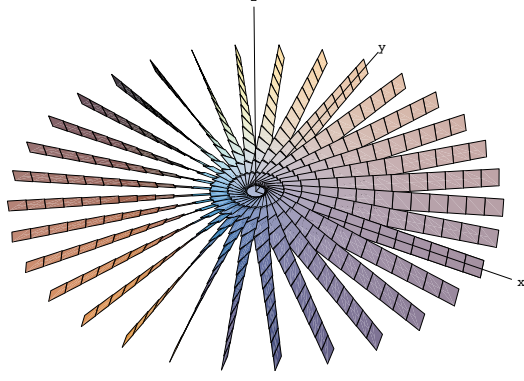
FIGURE 2. The rotationally symmetric contact structure on $\mathbb{R}^3$

2.2.2. *The rotationally symmetric contact structure on* $\mathbb{R}^3$. We can also take a radially symmetric contact structure on $\mathbb{R}^3$, by letting $\alpha_{rot} = dz - ydx + xdy$. Letting $\xi_{rot} = \ker(\alpha_{rot})$, $(\mathbb{R}^3, \xi_{rot})$ is also a contact structure since

$$\alpha \wedge d\alpha = (dz - ydx + xdy) \wedge (-dy \wedge dx + dx \wedge dy) = 2dx \wedge dy \wedge dz \neq 0$$

In this case the planes at $x = y = 0$ are horizontal, and they twist out radially, limiting towards vertical planes as the radius limits to infinity, as in figure 2. The contact plane at (x, y, z) is spanned by $\{x\frac{\partial}{\partial x} + y\frac{\partial}{\partial y}, y\frac{\partial}{\partial z} + \frac{\partial}{\partial x}\}$ when $y \neq 0$, by $\{x\frac{\partial}{\partial x} + y\frac{\partial}{\partial y}, x\frac{\partial}{\partial z} - \frac{\partial}{\partial y}\}$ when $x \neq 0$, and by $\{\frac{\partial}{\partial x}, \frac{\partial}{\partial y}\}$ when $x = y = 0$.

This is also contactomorphic to the standard contact structure via $\phi : (\mathbb{R}^3, \xi_{rot}) \rightarrow (\mathbb{R}^3, \xi_{std})$ defined by $\phi(x, y, z) = (2y, -x, xy + z) = (x'', y'', z'') \in (\mathbb{R}^3, \xi_{std})$. Then

$$
\begin{aligned}
d\phi_{(x,y,z)}\left(x\frac{\partial}{\partial x} + y\frac{\partial}{\partial y}\right) &= \begin{bmatrix} 0 & 2 & 0 \\ -1 & 0 & 0 \\ y & x & 1 \end{bmatrix} \begin{bmatrix} x \\ y \\ 0 \end{bmatrix} \\
&= \begin{bmatrix} 2y \\ -x \\ 2xy \end{bmatrix} \\
&= 2y\frac{\partial}{\partial x''} - x\frac{\partial}{\partial y''} + 2xy\frac{\partial}{\partial z''} \\
&= x''\frac{\partial}{\partial x''} + y''\left(\frac{\partial}{\partial y''} - x''\frac{\partial}{\partial z}\right)
\end{aligned}
$$

$$d\phi_{(x,y,z)}\left(y\frac{\partial}{\partial z} + \frac{\partial}{\partial x}\right) = \begin{bmatrix} 0 & 2 & 0 \\ -1 & 0 & 0 \\ y & x & 1 \end{bmatrix}\begin{bmatrix} 1 \\ 0 \\ y \end{bmatrix}$$

$$= \begin{bmatrix} 0 \\ -1 \\ 2y \end{bmatrix}$$

$$= 2y\frac{\partial}{\partial z''} - \frac{\partial}{\partial y''}$$

$$= -\left(\frac{\partial}{\partial y''} - x''\frac{\partial}{\partial z''}\right)$$

So

$$d\phi((\xi_{rot})_{(x,y,z)}) = \text{span}\left\{x''\frac{\partial}{\partial x''} + y''\left(\frac{\partial}{\partial y''} - x''\frac{\partial}{\partial z}\right), -\left(\frac{\partial}{\partial y''} - x''\frac{\partial}{\partial z''}\right)\right\}$$

$$= \text{span}\left\{\frac{\partial}{\partial x''}, \frac{\partial}{\partial y''} - x''\frac{\partial}{\partial z''}\right\}$$

$$= (\xi_{std})_{\phi(x,y,z)}$$

So indeed ϕ is a contactomorphism from $(\mathbb{R}^3, \xi_{rot})$ to $(\mathbb{R}^3, \xi_{std})$. Therefore we are justified in interchanging the two contact structures when referring to the standard contact structure on $\mathbb{R}^3$.

2.2.3. *The standard contact structure on S^3.* Now we would like to extend the standard contact structure on $\mathbb{R}^3$ to S^3. View S^3 as the subset of $\mathbb{R}^4$ with coordinates (x_1, y_1, x_2, y_2) satisfying $x_1^2 + y_1^2 + x_2^2 + y_2^2 = 1$. Let

$$\alpha = (x_1 dy_1 - y_1 dx_1 + x_2 dy_2 - y_2 dx_2)|_{S^3}$$

and let $\xi = \ker\alpha$. An equivalent way to define this contact structure is through the complex structure on $\mathbb{R}^4 = \mathbb{C}^2$. Let J be the complex structure given by $J(x_i) = y_i$, $J(y_i) = -x_i$. Let $f = x_1^2 + x_2^2 + y_1^2 + y_2^2$. Then $S^3 = f^{-1}(1)$ so

$$T_{(x_1,y_1,x_2,y_2)}S^3 = \ker(df_{(x_1,y_1,x_2,y_2)}) = \ker(x_1 dx_1 + y_1 dy_1 + x_2 dx_2 + y_2 dy_2)$$

I claim that $\xi = T_{(x_1,y_1,x_2,y_2)}S^3 \cap J(T_{(x_1,y_1,x_2,y_2)}S^3)$.

First note that for $v \in T_{(x_1,y_1,x_2,y_2)}S^3$, $v \in J(T_{(x_1,y_1,x_2,y_2)}S^3)$

$$\iff -Jv \in \ker(df_{(x_1,y_1,x_2,y_2)})$$

$$\iff df_{(x_1,y_1,x_2,y_2)} \circ -J(v) = 0$$

$$\iff v \in \ker(df_{(x_1,y_1,x_2,y_2)} \circ J)$$

So $T_{(x_1,y_1,x_2,y_2)}S^3 \cap J(T_{(x_1,y_1,x_2,y_2)}S^3) = \ker(df_{(x_1,y_1,x_2,y_2)} \circ J)$. However

$$df_{(x_1,y_1,x_2,y_2)} \circ J = -2x_1 dy_1 + 2y_1 dx_1 - 2x_2 dy_2 + 2y_2 dx_2 = 2\alpha$$

so $\xi = T_{(x_1,y_1,x_2,y_2)}S^3 \cap J(T_{(x_1,y_1,x_2,y_2)}S^3)$. Furthermore, we can check this is a contact structure and it is an extension of the standard contact structure on $\mathbb{R}^3$.

First we check that this is a contact structure:

$$\alpha \wedge d\alpha = (x_1 dy_1 - y_1 dx_1 + x_2 dy_2 - y_2 dx_2) \wedge (2dx_1 \wedge dy_1 + 2dx_2 \wedge dy_2)$$

$$= 2(x_1 dy_1 \wedge dx_2 \wedge dy_2 - y_1 dx_1 \wedge dx_2 \wedge dy_2 + x_2 dx_1 \wedge dy_1 \wedge dy_2 - y_2 dx_1 \wedge dy_1 \wedge dx_2)$$

Note that $x_1\frac{\partial}{\partial x_1} + y_1\frac{\partial}{\partial y_1} + x_2\frac{\partial}{\partial x_2} + y_2\frac{\partial}{\partial y_2} \in \ker(\alpha \wedge d\alpha)$. Then at any $(x_1, y_1, x_2, y_2) \in S^3$, $\ker(\alpha \wedge d\alpha)_{(x_1,y_1,x_2,y_2)}$ is a linear one dimensional subspace of the tangent space so

$$\ker(\alpha \wedge d\alpha)_{(x_1,y_1,x_2,y_2)} = \mathrm{span}(x_1\frac{\partial}{\partial x_1} + y_1\frac{\partial}{\partial y_1} + x_2\frac{\partial}{\partial x_2} + y_2\frac{\partial}{\partial y_2}) = (T_{(x_1,y_1,x_2,y_2)}S^3)^\perp$$

and thus $\alpha \wedge d\alpha$ is nonvanishing on TS^3.

By deleting a point and then taking the stereographic projection, one can similarly compute that $(S^3 \setminus \{p\}, \xi|_{S^3 \setminus \{p\}})$ is contactomorphic to $(\mathbb{R}^3, \xi_{std})$.

2.3. **Tight and Overtwisted Contact Structures.** A division between two types of contact structures was developed as more became known about contact structures. This is the classification of contact structures as *tight* or *overtwisted*.

Definition 4. *A contact manifold (M, ξ) is* overtwisted *if there exists an embedded disk $D \subset M$ such that $T_pD = \xi_p$ for every $p \in \partial D$ (D is called an* overtwisted disk*). A contact manifold is* tight *if it is not overtwisted.*

An example of an overtwisted contact manifold is $(\mathbb{R}^3, \xi_o)$, $\xi = \ker(\cos r dz + r \sin r d\theta)$ (in cylindrical coordinates on $\mathbb{R}^3$ (r, θ, z)). In this case, the contact planes twist radially, but the contact planes are horizontal i.e. $\xi = \ker(\pm dz)$ whenever $r = n\pi$, $n \in \mathbb{Z}_+$. Therefore a flat disk $D = \{z = 0\} \cap \{r \leq \pi\}$ has tangent space $\ker(dz)$ at every point, and thus the tangent planes coincide with the contact planes along ∂D. Therefore $(\mathbb{R}^3, \xi_o)$ is overtwisted. It is true, though considerably more difficult to prove that the standard contact structure on $\mathbb{R}^3$ (and its extension to S^3) is tight.

The reason that we are interested in the distinction between tight and overtwisted contact structures is because overtwisted contact structures are essentially classified by their homotopy type. This is given by the following significant theorem of Eliashberg.

Theorem 1 (Eliashberg [5])**.** *Let M be a closed, compact 3-manifold. Let H be the set of homotopy classes of oriented plane fields on M and C_0 be the set of isotopy classes of oriented overtwisted contact structures on M. The inclusion map C_0 into H gives a homotopy equivalence.*

Because we have a reasonably good hold on how to classify overtwisted contact structures, the more interesting contact manifolds to investigate are the tight ones. There are examples of tight contact structures which disallow Eliashberg's result from extending to all contact structures. We must use more subtle geometric techniques to classify tight contact structures. Most of the techniques discussed in this paper will involve cutting and pasting pieces of contact manifolds, and will rely heavily on the theory of convex surfaces, which will be introduced later in this chapter.

There is a stronger condition one can ask of a contact manifold than simply being tight:

Definition 5. *A contact manifold (M, ξ) is* universally tight *if its universal cover $(\widetilde{M}, \widetilde{\xi})$ is tight. $\widetilde{M}$ is simply the universal cover of M in the topological sense, and $\widetilde{\xi}$ is obtained by pulling back ξ along the covering map $\pi : \widetilde{M} \to M$.*

There are certain contact structures which become overtwisted when pulled back to a cover, but if a contact manifold has a tight cover then it must be tight. This implies that every cover of a contact manifold that is universally tight is tight. Some of the classifications results of tight contact structures on 3-manifolds include a description of which contact structures are universally tight. This allows us to look at covering spaces of contact manifolds to understand the base space, which can be useful if the cover is a simpler contact manifold to classify.

9
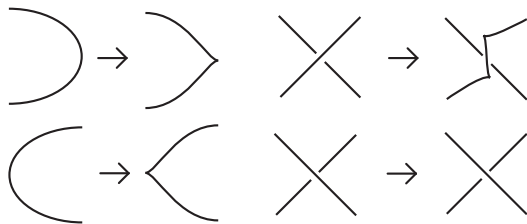
FIGURE 3. Changing a knot diagram to a Legendrian front projection.

2.4. **Legendrian and Transverse knots in** $(\mathbb{R}^3, \xi_{std})$**.** In addition to classifying contact structures on 3-manifolds up to contactomorphism, we can also classify certain classes submanifolds of a contact manifold up to isotopy within that class. By understanding knots in $(\mathbb{R}^3, \xi_{std})$ (or equivalently (S^3, ξ_{std})) which preserve some information about the contact structure, we gain a considerable amount of information about general contact three-manifolds. There are two kinds of knots, which keep track of some of the information of the contact structure: Legendrian knots and transverse knots.

Definition 6. *A knot K in (M, ξ) is* Legendrian *if $T_pK \subset (\xi)_p$ for all $p \in K$; i.e. the knot is everywhere tangent to the contact planes.*

K is transverse *if $T_pK \pitchfork (\xi)_p$ for all $p \in K$ and T_pK and K intersects ξ positively; i.e. the knot is never tangent to the contact planes, and the orientation of its tangent vector agrees with the normal orientation to ξ.*

Definition 7. *Two Legendrian (resp. transverse) knots K, K' are* Legendrian (resp. transversely) *isotopic if there is a one-parameter family of Legendrian (resp. transverse) knots K_t, $t \in [0, 1]$ such that $K_0 = K$ and $K_1 = K'$.*

It is often convenient to look at projections of knots onto $\mathbb{R}^2$. In $(\mathbb{R}^3, \xi_{std})$ there are two fairly natural projections to consider. The first is the *front projection* which sends (x, y, z) to (y, z).

Recall that the contact planes are given by $\ker(dz + xdy)$. Since a Legendrian knot is tangent to the contact planes, the value of the x coordinate is completely determined by the slope in the (y, z) projection:

$$(1) \qquad \qquad x = -\frac{dz}{dy}$$

The only slope that is not allowable in the front projection of a Legendrian knot is a completely vertical slope. Furthermore whenever we have a crossing, the larger slope must pass under the smaller slope because of equation 1. The only kind of singularities allowable for the projection of a smooth knot are cusps with well-defined tangent spaces and transverse crossings. If we want to turn a general knot diagram into a Legendrian knot diagram, we can do this by changing vertical slopes to cusps and adjusting crossings as in figure 3. Note also that we can make these adjustments arbitrarily small, meaning that we can C^0 approximate any knot by a Legendrian knot.

There are Legendrian Reidemeister moves for the front projection. It is possible to get from any Legendrian front projection to any other Legendrian front projection of a Legendrian isotopic knot through these Legendrian Reidemeister moves together with isotopy within Legendrian front projections. These moves are given in figure 4. This shows that any knot can be realized as a
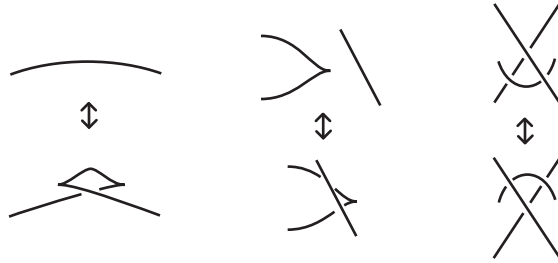
FIGURE 4. Legendrian Reidemeister moves for the front projection

FIGURE 5. We can find a Legendrian knot arbitrarily close to any knot in $\mathbb{R}^3$ by approximating it with sprials which appear here as zig-zags in the front projection.

Legendrian knot. Furthermore, any knot in $\mathbb{R}^3$ can be C^0 approximated by a Legendrian knot. To do this we add zig-zags in the front projection which spiral around the knot in $\mathbb{R}^3$ as in figure 5.

In the case of transverse knots we have only an inequality for the x value:

$$(2) \qquad x > -\frac{dz}{dy}$$

Therefore a transverse knot is not completely determined by its front projection, however it is determined up to transverse isotopy. The front projection of a transverse knot can never have vertical slopes pointing downwards (since any lift to $\mathbb{R}^3$ would have negative intersection number with all contact planes). If the front projection of a transverse knot has oriented tangent vector $a\frac{\partial}{\partial x} - \frac{\partial}{\partial z}$ there are restrictions on the x coordinate of the transverse knot in $(\mathbb{R}^3, \xi_{std})$. If $a > 0$ then $x > a$ and if $a < 0$ then $x < a$. This determines which is the overcrossing if two such segments, one where $a > 0$ and the other where $a < 0$, cross. Figure 6 shows these disallowed choices. Furthermore we cannot have cusps in the front projection of transverse knots since this would indicate that the tangent vector to the transverse knot at the point projecting to the cusp is $a\frac{\partial}{\partial x}$, which is not transverse to any contact plane. Thus the only allowable singularities in front projections of transverse knots are isolated double points from crossings.

There are only two transverse Reidemeister moves in the front projection (since there is no way to add in a Reidemeister I twist without having a cusp or downward pointing tangent vector). These are given by figure 7.

The second useful projection of knots in $(\mathbb{R}^3, \xi_{std})$ is the *Lagrangian projection* which sends (x, y, z) to (x, y). While Lagrangian projections are incredibly useful in certain contexts (e.g. Chekanov's combinatorial contact homology invariant of Legendrian knots [3]), we will primarily use the Lagrangian projection simply to give another perspecitve from which to view a knot. Lagrangian

FIGURE 6. Segments that cannot show up in the front projection of a transverse knot.
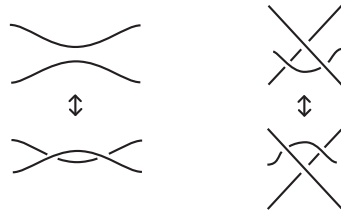
FIGURE 7. Transverse Reidemeister moves in the front projection

diagrams are slightly more problematic to work with because it is difficult to recognize which diagrams are allowable as Lagrangian projections of Legendrian or transverse knots.

2.5. **Classical invariants of Legendrian and transverse knots.** There are two invariants of Legendrian knots and one of transverse knots that are reasonably simple to compute and use to distinguish Legendrian or transverse knots of the same topological knot type. For Legendrian knots these invariants are the Thurston-Benniquin number, tb, and the rotation number, r. For transverse knots we have the self-linking number. The Thurston-Benneqin number essentially measures the twisting of the contact planes around the Legendrian knot, with respect to the framing induced by a Seifert surface. The rotation number counts the number of times the direction of the Legendrian knot rotates around in a trivialization of the contact planes on a Seifert surface for K. The self-linking number of a transverse knot is the linking number of K with a pushoff in a direction of the contact planes. The formal definitions of these "classical invariants" follow.

Definition 8. *Let K be a Legendrian knot, and let Σ be a Seifert surface for K. Let X be a vector field on K which is transverse to ξ and let K' be the pushoff of K in the direction determined by X. Then the* Thurston-Bennequin number $tb(K)$ *is the signed intersection number of K' with Σ.*

Equivalently, let ν be the normal bundle to K. Then $\nu \cap \xi|_K$ is a line bundle. Then $tb(K)$ is the twisting of this line bundle with respect to the Seifert framing. More generally, the twisting *of K relative a given framing F, $t(K,F)$ is the twisting of $\nu \cap \xi|_K$ with respect to F.*

Definition 9. *Let K be Legendrian and Σ a Seifert surface. Then we can find a trivialization of $\xi|_\Sigma \cong \Sigma \times \mathbb{R}^2$. This induces a map $\phi : K \to \mathbb{R}^2 \setminus 0$ which sends $p \in K$ to the oriented tangent vector to K which lies in ξ_p which is identified with $\mathbb{R}^2$ under the trivialization. The* rotation number $r(K)$ *is the winding number of ϕ around 0.*

Equivalently, let Y be a non-zero vector field on Σ which lies in $\xi|_\Sigma$ and let Z be a non-zero vector field tangent to K and defined on K. The rotation number is the twisting of Z relative to Y in ξ.

In other words, the rotation number is the obstruction to extending Z to a non-zero vector field over all of Σ.

Definition 10. *Let K be a transverse knot, Σ a Seifert surface for K, and Z a non-zero section of $\xi|_{\Sigma}$. Let K' be the pushoff of K in the direction of Z. The* self-linking number, $sl(K)$ *is the linking number of K with K'.*

Equivalently, let V be a non-zero vector field in $\xi \cap T\Sigma$ along K. The self-linking number is the obstruction to extending V over Σ to a non-zero vector field.

A useful bound on the classical invariants is the Bennequin inequality:

Theorem 2 (Bennequin Inequality). *Let K be a Legendrian knot and let Σ be a Seifert surface for K. Then*

$$tb(K) + |r(K)| \leq -\chi(\Sigma)$$

(where χ indicates Euler characteristic). If K' is a transverse knot and Σ' is a Seifert surface for K' then

$$sl(K') \leq -\chi(\Sigma')$$

A proof can be found in any introduction to contact topology including [11] and [8].

2.6. **Standard Neighborhood Theorems.** Contact structures can only make distinctions between manifolds on a global scale. Darboux's theorem shows that locally contact structures on 3-manifolds are all the same. More careful argumentation shows that every Legendrian knot has a neighborhood which is contactomorphic to a standard neighborhood of a Legendrian knot. These classical results use rather different techniques than we will use for most of the other proofs in this paper. A sketch of the proof is included here. For a more detailed proof of a more general result see [11].

Theorem 3 (Darboux's Theorem). *Let (M, ξ) be a contact 3-manifold, and let $p \in M$. Then there is a neigbhorhood of p contactomorphic to a neighborhood of 0 in $(\mathbb{R}^3, \xi_{std})$.*

To extend this to neighborhoods of Legendrian knots, instead of just neighborhoods of points, we need a standard Legendrian neighborhood to compare to. Let $X = R^2 \times S^1$ be parametrized by (x, y, z), $z \in [0, 1)$. Take the contact structure $\xi_0 = \ker(\cos(2\pi z)dx + \sin(2\pi z)dy$. Then $K_0 = \{(0, 0, z)\}$ is a Legendrian knot in (X, ξ_0). Let $N_0 = \{(x, y, z) \in X : x^2 + y^2 < 1\}$. Using this notation we have the following:

Theorem 4 (Legendrian Standard Neighborhood Theorem). *If K is a Legendrian knot in a contact manifold (M, ξ), then there is a neighborhood $N(K)$ and a contactomorphism $\phi : N(K) \to N_0$ which sends K to K_0.*

Note that in N_0 the contact planes twist once around K_0 with respect to the Seifert surface framing given by the $x > 0$ part of the xz plane. However, the contactomorphism may twist the planes around the Legendrian knot arbitrarily many times with respect to the Seifert surface framing. The number of times is determined by the Thurston-Bennequin number of the Legendrian knot.

sketch of proof. Keep track of the line bundle which is orthogonal to the contact planes and the line bundle in the contact planes which is orthogonal to the Legendrian knot. The direct sum of these makes up the normal bundle to the Legendrian knot. Find a map of the normal bundle of the given knot to the normal bundle of the standard Legendrian knot which preserves this split into the two summands. If $\mathcal{N}K_0$ and $\mathcal{N}K$ denote the normal space to the standard Legendrian knot and the given Legendrian knot respectively, we have an isomorphism $\Phi : \mathcal{N}K \to \mathcal{N}K_0$, which preserves some of the information of the contact structure.

One can embed a neighborhood of the 0-section of the normal bundle of a knot into the 3-manifold so that the 0-section goes to the knot and the normal spaces are orthogonal to the knot. Let U_0 and U be these neighborhoods in $\mathcal{N}K_0$ and $\mathcal{N}K$ respectively. Call these embeddings $f_0 : U_0 \to N_0$ and $f : U \to N(K)$ (N_0 and $N(K)$ are neighborhoods of K_0 and K respectively). Using these embeddings for the normal spaces of the given Legendrian knot and the standard Legendrian knot, together with the map between the normal bundles of these two knots, we obtain a diffeomorphism of neighborhoods of the two knots: $f_0 \circ \Phi \circ f^{-1}$.

Then we use Gray's stability theorem (below) to show that the contact structure induced by this diffeomorphism is isotopic to the standard Legendrian contact structure through an isotopy that fixes K_0. Adjusting the diffeomorphism according to this isotopy provides the desired contactomorphism. $\square$

A standard trick that is used in contact topology to switch between smooth families of contact structures and isotopies of the contact manifold is Gray's stability theorem:

Theorem 5 (Gray stability)**.** *Let ξ_t ($t \in [0,1]$) be a smooth family of contact structures on a closed manifold M. Then there is an isotopy ψ_t of M such that $T\psi_t(\xi_0) = \xi_t$ for each $t \in [0,1]$.*

2.7. **Surfaces in a contact manifold.** In this section we give a brief survey of some of the most important definitions and theorems about surfaces in a contact manifold. For more details and proofs see [12], [14], and [17].

Suppose S is a surface in (M, ξ), a contact 3-manifold. Because ξ is maximally non-integrable the set of singularities $E = \{p \in S : T_pS = \xi_p\}$ contains no open set of S. For all $p \in S \setminus E$, $T_pS \cap \xi_p$ is a line. There is a foliation of $S \setminus E$ whose leaves are the integral submanifolds of $TS \cap \xi|_{S \setminus E}$. The *characteristic foliation* S_ξ is a singular foliation on S made up of these leaves together with the singularities on E.

The characteristic foliation also determines the contact structure in a neighborhood of the surface:

Theorem 6 ([7])**.** *Let (M_i, ξ_i) be a contact manifold and S_i an embedded surface for $i = 0, 1$. If there is a diffeomorphism $f : S_0 \to S_1$ that preserves the characteristic foliation, then f can be extended to a contactomorphism on a neighborhood of S_0.*

The characteristic foliations encode a large amount of information about the contact structure. Often we do not need to know all of this information to make effective geometric arguments. Giroux introduced the theory of convex surfaces to capture the most essential information about the characteristic foliation.

Definition 11. *A vector field X on a contact manifold (M, ξ) is a* contact vector field *if its flow preserves ξ.*

A surface S is convex *if there is a contact vector field everywhere transverse to S. Equivalently, S is convex exactly when there is a neighborhood $N = S \times I$ in M such that ξ is invariant in the I direction.*

Giroux proved that any closed surface can be C^∞ approximated by a convex surface [12]. Honda extended this result to surfaces S with Legendrian boundary providing the twisting of the contact planes around the boundary relative the framing induced by the surface F_S satisfies $t(\partial S, F_S) \leq 0$.

The reason convex surfaces are useful, in addition to being prevalent is that we need not look at the entire characteristic foliation. On convex surfaces we can focus instead on only a few curves called the dividing set.

Definition 12. *Given a convex surface S with a transverse contact vector field X, the* dividing set Γ_S *is the set of points p such that $X(p) \in \xi(p)$. The isotopy type of Γ_S is independent of choice of X so the dividing set is well defined up to isotopy.*

If Y denotes the positively-oriented normal vector-field to $\xi|_S$ and X is the contact vector field transverse to S, then $f : S \to \mathbb{R}$ defined by $f(p) = \langle Y_p, X_p \rangle$ is a smooth function on S, where $\Gamma_S = f^{-1}(0)$. Therefore generically, Γ_S is a one-dimensional submanifold of S, namely a collection of closed curves and arcs with endpoints on ∂S. Furthermore Γ_S is the boundary dividing R_+, the set where the orientation of X coincides with the orientation of the positive normal to ξ, from R_- the set where the orientations disagree. Also note that Γ_S is always transverse to the characteristic foliation because otherwise we would violate the non-integrability of the contact structure.

The prevalence of convex surfaces, and the usefulness of dividing curves in measuring twisting is shown in the following theorem.

Theorem 7 (Kanda [17]). *If γ is a Legendrian curve in a surface S then S may be isotoped relative γ so that it is convex if and only if the twisting of the contact planes relative the framing given by S has the property $t_S(\gamma) \leq 0$. Then if S is convex*

$$t_S(\gamma) = -\frac{1}{2}\#(\gamma \cap \Gamma_S)$$

While there cannot be any open neighborhood in S where TS matches up with ξ, there can be one-dimensional submanifolds of singularities.

Definition 13. *Suppose S is a convex surface. A* Legendrian divide *of S is a curve $\gamma \subset S$ such that $TS|_\gamma = \xi_\gamma$.*

Notice that a Legendrian divide can never intersect the dividing curves (otherwise the contact vector field would be both transverse and tangent to S). Thus Legendrian divides are "parallel" to dividing curves. Heuristically, the Legendrian divides alternate with the dividing curves in the direction of twisting. As the contact planes twist, the alternate between being tangent to S (Legendrian divides) and being transverse to S (dividing curves).

The Giroux flexibility theorem shows why it is only the dividing curves, instead of the exact characteristic foliation that we need to consider in contact topology. We will say that Γ_S *divides* a foliation $\mathcal{F}$ of S if there is an I-invariant contact structure on $S \times I$ such that $\mathcal{F} = \xi|_{S \times \{0\}}$.

Theorem 8 (Giroux Flexibility [12]). *Suppose S is a convex surface in (M, ξ) with contact vector field X transverse to S. Suppose $\mathcal{F}$ is a singular foliation on S divided by Γ_S. Then there is an isotopy ϕ_t, $t \in [0, 1]$, of S such that*

(1) $\phi_0(S) = S$

(2) $\phi_t(S)$ *is transverse to X for all* $t \in [0, 1]$

(3) *The characteristic foliation of* $\phi_1(S)$ *is* $\mathcal{F}$

Therefore convex surfaces are determined up to isotopy by their dividing sets. A useful theorem that follows from Giroux's flexibility theorem is the Legendrian realization principle (LRP). This theorem, originally proven by Kanda and reformulated by Honda, allows us to isotope a convex surface so that almost any curve, and certain collections of curves on that surface, become Legendrian.

Theorem 9 (Legendrian Realization Principle). *Suppose S is a convex surface with contact vector field X transverse to S and C is a collection of curves on S satisfying the following properties:*

- *C is transverse to* Γ_S
- *Every endpoint of C lies on* Γ_S
- *Every component of* $S \setminus (\Gamma_S \cup C)$ *has a piece of* Γ_S *on its boundary*

Then there exists an isotopy ϕ_t, $t \in [0, 1]$ *such that*

(1) $\phi_t(S)$ *is convex for all* $t \in [0, 1]$

(2) $\phi_0 = id$

(3) $\phi_1(\Gamma_S) = \Gamma_{\phi_1(S)}$

(4) $\phi_1(C)$ *is Legendrian*

In particular if C is a closed curve on S with non-empty transverse intersection with Γ_S, then C can be realized as a Legendrian curve as in the above theorem.

In tight contact manifolds there are certain restrictions on the topology of the dividing set on a convex surface. This is formalized by Giroux's criterion for determining which convex surfaces have tight neighborhoods:

Theorem 10 (Giroux's criterion [14]). *If* $S \neq S^2$ *is a convex surface (closed or compact with Legendrian boundary) in a contact manifold* (M, ξ) *then S has a tight neighborhood if and only if* Γ_S *has no homotopically trivial curves. If* $S = S^2$ *then it has a tight neighborhood if and only if there is only one dividing curve.*

This significantly reduces the possibilities for the dividing set on a surface that lies in a tight contact structure. We can get other restrictions on the dividing sets of convex surfaces by looking at the relations between the dividing curves of two intersecting convex surfaces.

Lemma 1. *Suppose* S_1 *and* S_2 *are convex surfaces that intersect transversely at a Legendrian curve* $\gamma = S_1 \cap S_2$. *Then the points where* Γ_{S_1} *intersect* γ *alternate with the points where* Γ_{S_2} *intersect* γ *as in figure 8.*

By the Legendrian realization principle, we can almost always isotope the surfaces so that their intersection is Legendrian. Specifically, if the curve $\gamma = S_1 \cap S_2$ intersect the dividing curves of S_1 or S_2 nontrivially, it can be realized as a Legendrian curve.

Proof. Since $\gamma = S_1 \cap S_2$ is Legendrian, it has a neighborhood isotopic to $D^2 \times S^1$ parametrized by (x, y, t) with contact structure given by $\ker(\cos(2\pi nt)dx + \sin(2\pi nt)dy)$ where n is determined by the number of times the dividing curves of S_1 or S_2 intersect γ. Essentially, n is the twisting of γ
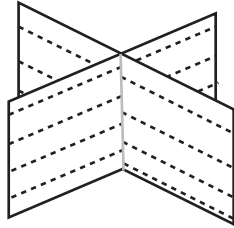
FIGURE 8. The dividing curves alternate at the intersection of two convex surfaces
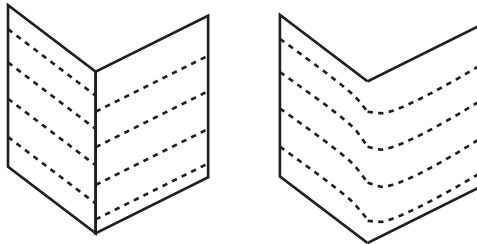
FIGURE 9. Rounding the edge of the intersection of two convex surfaces with Legendrian boundary

with respect to the framing given by S_1 or S_2. Since S_1 and S_2 are always transverse, they cannot twist around each other and thus the framings induced by either yields the same value for n. The contact planes make on half-twist around γ with respect to S_1 from one point of $\gamma \cap \Gamma_{S_1}$ to the next, with a singularity in between. Since S_2 is transverse to S_1 the singularities of the contact planes along γ alternate between S_1 and S_2 as they twist, and the dividing curves meet γ in between where the transverse contact vector field intersects the contact planes nontrivially.

More formally, we can show that this alternation occurs in the standard neighborhood of a Legendrian knot with twisting n, $(D^2 \times S^1, \ker(\cos(2\pi nt)dx + \sin(2\pi nt)dy))$. We may assume by an isotopy of the contact manifold and choice of coordinates that the surfaces are given by $S_1 = \{x = 0\}$ and $S_2 = \{y = 0\}$ in a small neighborhood of γ, and the transverse contact vector fields are given by $\frac{\partial}{\partial y}$ and $\frac{\partial}{\partial x}$ respectively. In this case the dividing curves of S_1 are given by $S_1 \cap \{t = \frac{k}{2n} : k \in \{0, 1, \cdots, n-1\}\}$ and the dividing curves of S_2 are given by $S_2 \cap \{t = \frac{2k+1}{4n} : k \in \{0, 1, \cdots, n-1\}\}$. These alternate as shown in figure 8. After a contact isotopy, this extends to the general case. $\square$

Lemma 2. *If S_1 and S_2 are convex surfaces with Legendrian boundary, which intersect along their boundaries, then we can smooth out the corner where the two surfaces meet. The dividing curves which alternate along $S_1 \cap S_2$ will always connect up as in figure 9.*

This can be proven rigorously as in the previous lemma by looking explicitly at the standard neighborhood $D^2 \times S^1$ and replacing the corner with a quarter of a small cylinder.
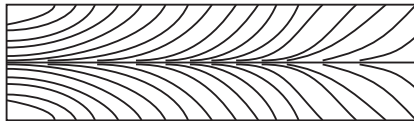
FIGURE 10. The characteristic foliation on the annulus A and the positive and negative transverse pushoffs of L

2.8. **Transverse Pushoffs.** Because Legendrian knots are more rigid than transverse knots, it is typically easier to compute invariants of Legendrian knots than of transverse knots. We can relate the Legendrian invariants of a knot to the transverse invariants of a controlled transverse approximation: the transverse pushoff.

Definition 14. *Given a Legendrian knot L, let $A = S^1 \times [-\varepsilon, \varepsilon]$ be the embedded annulus where $S^1 \times \{0\} = L$, and $TA|_L = \xi|_L$, We can make ε sufficiently small so that the characteristic foliation on A is as in figure 10. Then the* positive (resp. negative) transverse pushoff *is $T_+(L) = S^1 \times \{\frac{\varepsilon}{2}\}$ (resp. $T_-(L) = S^1 \times \{-\frac{\varepsilon}{2}\}$).*

The negative transverse pushoff will be oriented negatively with respect to the contact structure. Since we have defined transverse knots to be positively oriented with respect to the contact structure we will mainly look at the positive transverse pushoff, though negative transverse knots have corresponding results.

The following lemma gives the relation between the classical Legendrian and transverse invariants.

Lemma 3. *Let L be a Legendrian knot,*

$$sl(T_+(L)) = tb(L) - r(L)$$

Proof. The idea of the proof is to compute each invariant in terms of the twisting of various vector fields around each other, and then relate the vector fields for a Legendrian knot and its transverse pushoff.

Let K be a Legendrian knot, and $A = S^1 \times [-\varepsilon, \varepsilon]$ be the annulus from the definition of transverse pushoff. Let Σ be a Seifert surface for K. Let σ be a non-zero vector field on Σ which lies in $\xi|_\Sigma$, then restricted to K. Let τ be a vector field in $\xi|_K$ always transverse to TK. Let ν be the vector field of outward unit normals to Σ, then restricted to K.

The rotation number is the twisting of positive vectors in TK with respect to σ. This is equivalent to the twisting of τ, which is always transverse to TK, to σ. Therefore $r(K) = t(\tau, \sigma)$.

The Thurston Bennequin number measures the twisting of the contact planes with respect to the Seifert surface. Since ν is orthogonal to the Seifert surface and τ is in $\xi|_K$ and is always transverse to TK (and thus always stays on one side of TK), $tb(K) = t(\tau, \nu)$.

Now we can find corresponding vector fields for the transverse knot $T_+(K)$. Let Σ' be the Seifert surface for $T_+(K)$ obtained by adding on the small part of A from K to $T_+(K)$ to Σ. Let σ_+, τ_+,

and ν_+ be the vector fields obtained by pushing σ, τ, and ν along A in the $[-\varepsilon, \varepsilon]$ direction. Then σ_+ is the non-zero vector field in $\xi|_{\Sigma'}$ which extends σ. ν_+ is the outward normal to Σ' and is isotopic to ν since K and $T_+(K)$ are topologically isotopic. σ_+, τ_+, and ν_+ rotate around each other in the same relations as σ, τ, and ν.

The self-linking number of $T_+(K)$ is the linking number of $T_+(K)$ with a pushoff in the direction of a non-zero section of $\xi|_{\Sigma'}$. σ_+ is one such section. Therefore to measure the self-linking number we can simply measure the twisting of σ_+ with respect to the tangent space to Σ' or equivalently with respect to $\nu_+ = \nu$. The equation comes from the following:

$$
\begin{aligned}
sl(T_+(K)) &= t(\sigma_+, \nu_+) \\
&= t(\sigma_+, \tau_+) + t(\tau_+, \nu_+) \\
&= t(\sigma, \tau) + t(\tau, \nu) \\
&= -r(K) + tb(K)
\end{aligned}
$$

$\square$

3. Stabilization, Bypasses, and Thickening

3.1. **Stabilization of Legendrian Knots in** (S^3, ξ_{std})**.** The simplest way to change the Legendrian isotopy type of a knot is to add a twist in the knot so that as it moves through the contact structure, the planes have additional twisting. We formalize this notion in *stabilization*. Given a Legendrian knot L, there are two kinds of stabilization operations which change the classical invariants, $tb(L)$ and $r(L)$. *Positive stabilization* of L, denoted $S_+(L)$, is given by the following transformation shown in the front projection and top projection:
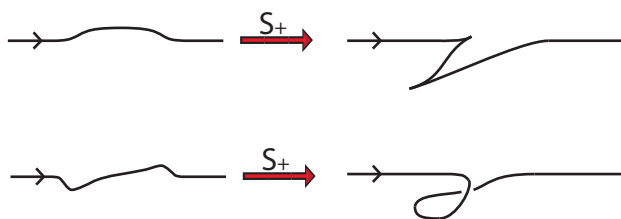
FIGURE 11. The front projection (above) and top projection (below) of a positive stabilization

and *negative stabilization* of L, denoted by $S_-(L)$ is given by:
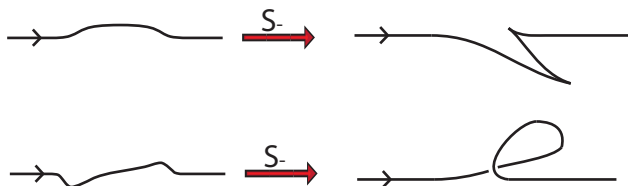
FIGURE 12. The front projection (above) and top projection (below) of a negative stabilization

Stabilization is a well-defined operation because, in a front projection of a knot, we can move the stabilization across a cusp or a crossing to a different part of the diagram through Legendrian Reidemeister moves. For the same reason, positive and negative stabilizations commute: $S_+ \circ S_- = S_- \circ S_+$.

If we compare the Seifert surface of the stabilized knot to that of the unstabilized knot, we see that the stabilization adds in a twisted disk, which we will call the *stabilization disk*. See figure 13.

Examining the twisting of the contact planes along the stabilizing disks (Figure 14) we can see that the framing given by the stabilization disk makes an additional full twist as it passes through the two cusps of the stabilized knot with respect to the Seifert surface obtained by gluing the stabilization disk to a Seifert surface for the unstabilized knot. Thus the twisting of the planes with respect to a Seifert surface for the stabilized knot has one more negative twist than for the unstabilized knot. This happens for both positive and negative stabilizations.

$$tb(S_+(L)) = tb(S_-(L)) = tb(L) - 1$$
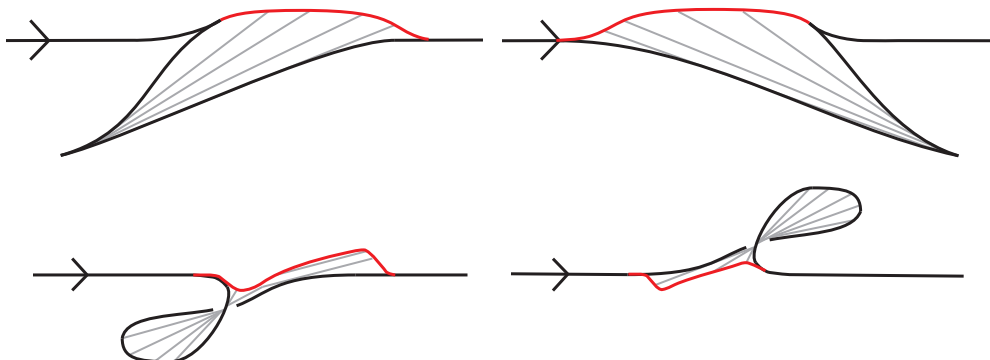
FIGURE 13. The stabilization disks in the front projection (above) and top projection (below) under positive (left) and negative (right) stabilization.
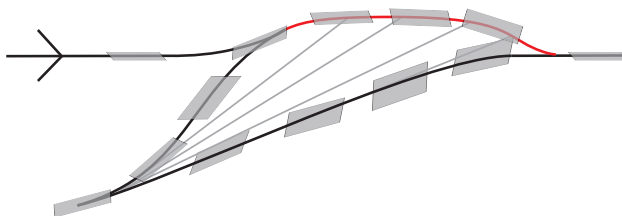
FIGURE 14. The twisting of the contact planes around the stabilized portion of a knot with respect to the framing given by the Seifert surface obtained by gluing the stabilizing disk to a Seifert surface for the unstabilized knot.

More generally we have the formula $tb(L) = \text{writhe}(\pi(L)) - \frac{1}{2}\{\text{number of cusps in } \pi(L)\}$ where $\pi(L)$ is the front projection of the knot. This formula comes from examining the twisting of the contact planes locally near crossings and cusps as in this specific case for stabilizations.

We can also compute the rotation number of the stabilizations. It is easiest to see this from the top projections since the contact planes are all oriented the same way from this perspective, so the rotation number is simply the number of times the knot winds around counterclockwise in the top projection minus the number of times the knot winds around clockwise in the top projection. Therefore

$$r(S_+(L)) = r(L) + 1$$
$$r(S_-(L)) = r(L) - 1$$

Using stabilizations, we can easily make the Thurston-Bennequin number of a knot arbitrarily small. However, for a given knot type K, there is a maximal Thurston-Bennequin number achieved by that knot, denoted $\overline{tb}(K)$, which is an invariant of the knot type. To determine whether we can increase the Thurston-Bennequin number of a knot, we see if we can *destabilize* the knot (the inverse

operation of stabilization). While we can always perform positive or negative stabilizations on any Legendrian knot, we cannot always destabilize. To study this in greater detail, we look at a notion from the study of convex surfaces within contact structures: bypass disks.

3.2. **Types of singularities of a characteristic foliation.** A *singularity* occurs in a characteristic foliation of a surface S when the contact plane coincides with the tangent plane to the surface.

For each singularity, we can classify it as elliptic or hyperbolic. In order to do this, we will see that we must perturb the surface slightly so that certain transversality conditions are met at the singularity. Suppose $s \in S$ is the singularity. We first find a small neighborhood U of s in S such that we can trivialize the vector bundle $TM|_U$ under a map $\phi : TM|_U \to U \times \mathbb{R}^3$ such that at each $x \in S$, $T_x S \subset T_x M$ maps to $\{x\} \times \mathbb{R}^2 \times \{0\}$. We can shrink and perturb U so that

(1) s is the only singularity in U
(2) $\phi(\xi_x)$ is not perpendicular to $\phi(T_x S) = \{x\} \times \mathbb{R}^2 \times \{0\}$ for any $x \in U$.

Then we can define a map $f : U \to \mathbb{R}^2$ in the following way. For each $x \in U$, let n_x be the line orthogonal to $\phi(\xi_x) \subset \{x\} \times \mathbb{R}^3$. Because $\phi(\xi_x)$ is not perpendicular to $\{x\} \times \mathbb{R}^2 \times \{0\}$ at any $x \in U$, n_x intersects $\{x\} \times \mathbb{R}^2 \times \{1\}$ exactly once, at a point $(x, (u_x, v_x, 1)) \in \{x\} \times \mathbb{R}^3$. Let $f(x) = (u_x, v_x) \in \mathbb{R}^2$. Note that f maps a point in U to $(0,0)$ if and only if that point is a singularity, because $n_x \cap \{x\} \times \mathbb{R}^2 \times \{1\} = (x, (0,0,1)$ if and only if $n_x = \{(x, (0,0,t)) : t \in \mathbb{R}\}$, namely when $n_x = \phi(\xi_x)^\perp$ is perpendicular to $\{x\} \times \mathbb{R}^2 \times \{0\}$. We may assume that f is transverse to the map $\mathbf{0} : U \to \mathbb{R}^2$ where $\mathbf{0}(x) = (0,0)$ for all $x \in U$, by perturbing ξ slightly, which by the Gray stability theorem 5 can equivalently be done by perturbing U slightly. We then compute the oriented intersection number of f with $\mathbf{0}$ near s. Because f is transverse to $\mathbf{0}$ and s is the only point in U which f maps to $(0,0)$, this is ± 1.

If the intersection number is $+1$ we say the singularity is *elliptic* and if it is -1 we say the singularity is *hyperbolic*. The foliations in a neighborhood of elliptic and hyperbolic singularities are illustrated in figure 15.

elliptic   elliptic   hyperbolic

FIGURE 15. Two elliptic singularities (left and center) and a hyperbolic singularity (right)

We will frequently consider convex surfaces with Legendrian boundary. When we have singularities at the boundary, we can still classify them as elliptic or hyperbolic by computing the intersection number near the singularity. In these cases the foliations look locally like figure 16.

In addition to being classified into elliptic and hyperbolic points, singularities are also classified as positive or negative. A singularity is *positive* (resp *negative*) if the orientation of the tangent plane to the surface agrees (resp. disagrees) with the orientation of the contact plane. Note that this sign is separate from the sign of the intersection number used above to classify points as elliptic or hyperbolic. Elliptic and hyperbolic singularities can both be either positive or negative in sign.

elliptic   elliptic   hyperbolic
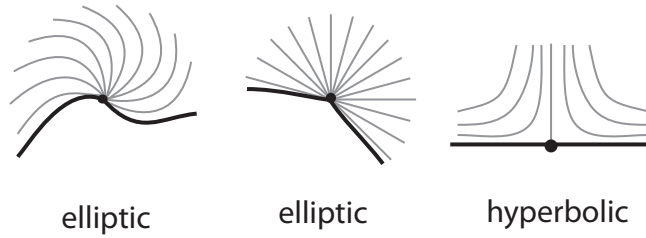
FIGURE 16. Elliptic (left) and hyperbolic (right) singularities along the boundary of a surface

In order to make sense of these definitions we need to fix an orientation for the contact planes. In the standard contact structure on $\mathbb{R}^3$ we will take $\{\frac{\partial}{\partial x}, x\frac{\partial}{\partial z} - \frac{\partial}{\partial y}\}$ to be an ordered basis for the contact planes, that gives the positive orientation.

As an example we will look at a Seifert surface for the standard Legendrian unknot in $(\mathbb{R}^3, \xi_{std})$. (Figure 17)
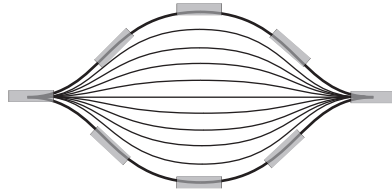
FIGURE 17. The foliation for the standard unknot in $(\mathbb{R}^3, \xi_{std})$. The two singularities are negative elliptic points.

At the cusps the tangent planes to the Seifert surface are horizontal as are the contact planes. This is because we can obtain a basis for each of these planes from

(a) the tangent vector to the cusp in the plane of the page $(\frac{\partial}{\partial y})$

(b) a vector orthogonal to the page $(\frac{\partial}{\partial x})$

(a) is clearly included in the tangent plane to the Seifert surface at the cusp. It is included in the contact plane because the unknot is Legendrian. (b) is tangent to the actual Legendrian unknot because the only way a smooth knot can have a cusp in the projection is if the tangent vector to the knot is perpendicular to the projection plane. Therefore (b) is in the tangent plane to the Seifert surface at the cusp. (b) is in the contact plane at the cusp because it is in every contact plane in $(\mathbb{R}^3, \xi_{std})$. Note that it does not matter which Seifert surface we choose for this Legendrian unknot, we will always have singularities at these two cusps.

We can choose the Seifert surface such that it does not contain the vector $\frac{\partial}{\partial x}$ at any other place, and so these cusps are the only singularities. Intersecting the contact planes with the tangent planes to the surface on its interior, we obtain the foliation which reveals that the singularities are elliptic. Finally we determine the sign of the singularities. At the cusps, the tangent plane is spanned by $\{\frac{\partial}{\partial x}, \frac{\partial}{\partial y}\}$ which we can take as a positively oriented basis at one cusp and a negatively oriented basis at the other since the upward facing side of the surface is different between the two cusps. Therefore
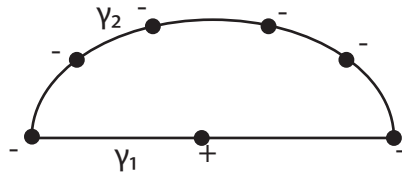
FIGURE 18. A bypass disk. The singularities are marked by points.

one singularity is positive elliptic and the other is negative elliptic (depending on the orientation we choose for the surface).

3.3. **Bypasses.** Suppose we have a Legendrian knot L. A *bypass* for L is a convex disk, D with Legendrian boundary $\partial D = \gamma_1 \cup \gamma_2$ where $D \cap L = \gamma_1$ and γ_1 and γ_2 only intersect at their two endpoints where the characteristic foliation on D has the following properties:

- There are two singularities of the same sign at the endpoints of γ_1 and γ_2 where they meet, and exactly one singularity of the opposite sign on the interior of γ_1.
- The signs of the singularities along γ_2 (including those on the endpoints) are all the same, and there are at least 3 singularities along γ_2 (including the endpoints).
- There are no singularities on the interior of D.

See figure 18 for an example.

The *sign of the bypass* is the sign of the singularity on the interior of γ_1 (the only singularity with a different sign from all the others).

The reason we are interested in bypasses here is because they show us how to destabilize a Legendrian knot.

Proposition 1. *Bypass disks with D, γ_1, γ_2 as above, are stabilization disks, where γ_1 is the stabilized portion of the boundary of D (black line in figure 13) and γ_2 is the unstabilized portion of the boundary of D (red line in figure 13).*

Proof. The full foliation of a stabilization disk is given in figure 19. To get this full picture we will examine smaller portions of the stabilization disk.

Looking at the end points where the red (unstabilized) and black (stabilized) curves meet, we see that each curve approaches the same slope in the front projection, thus forming a cusp which corresponds to a singularity. As we approach each endpoint, the tangent plane to the stabilizing disk which connects the red curve to the black curve approaches a plane spanned by a vector of that constant slope and a vector going out of the page. This span is identical to the contact plane at that point. Therefore each endpoint is a singularity. Furthermore these are elliptic points because the contact planes in a neighborhood of these points intersect the tangent planes pointing toward the endpoints.
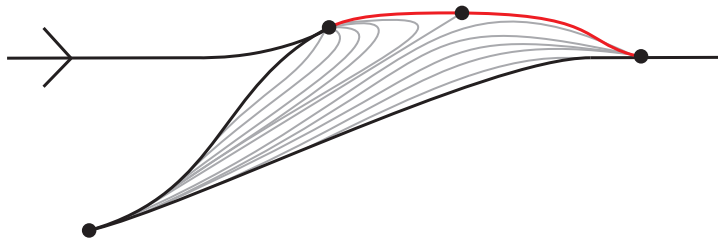
FIGURE 19. The foliation of a positive stabilizing disk.

At the cusp at the bottom of the black curve there is another singularity (the cusp indicates that the tangent plane to the surface is going into the page at that point, as the contact planes do). Again examining the foliation nearby we see that this is an elliptic singularity.

We will orient the surface such that the induced normal vector points up near the red (unstabilized) part of the boundary. We note that when the contact planes are horizontal, their positive orientation is given by $\{\frac{\partial}{\partial x}, -\frac{\partial}{\partial y}\}$ so the induced normal is $-\frac{\partial}{\partial z}$. Therefore the elliptic singularities where the red curve meets the black curve are both negative. However at the cusp at the bottom of the black curve, the surface twists so that the induced normal now points down. Therefore at the cusp in the center of the black curve there is a positive elliptic singularity.

We can choose the surface so that the tangent planes are transverse to the contact planes along the red curve at all but the endpoints and the center point at which there is a hyperbolic singularity. Since neither the surface nor the contact planes twist along the red curve, this singularity is negative like the endpoint singularities.   □

It is also useful to study bypasses of convex surfaces. A *bypass* for a convex surface S is a bypass for a Legendrian curve γ contained in S that does not intersect S anywhere except where it intersects γ. Furthermore it must have the property that it intersects, Γ_S, the dividing curves of S, at exactly the three elliptic singularities in the foliation of D along γ. See figure 20.

We can obtain a new convex surface from a bypass disk, D by looking a neighborhood of $S \cup D$, and taking the boundary component of that neighborhood that lies on the same side of S that D does. Since convex surfaces are essentially characterized by their dividing curves, understanding the surface that results from passing over a bypass disk comes down to understanding the change in the dividing curves. This change is described in the following lemma by Honda [14]

Lemma 4 (Bypass Attachment (Honda) [14]). *Assume D is a bypass for a convex surface S. Then there exists a neighborhood of $S \cup D$, diffeomorphic to $S \times [0,1]$ such that $S_i = S \times \{i\}$, $i = 0,1$ are convex, $S \times [0,\varepsilon]$ is I-invariant, $S = S \times \{\varepsilon\}$, and Γ_{S_1} is obtained from Γ_{S_0} by performing the operation depicted in Figure 20 in a neighborhood of the attaching Legendrian arc where the bypass disk meets S.*
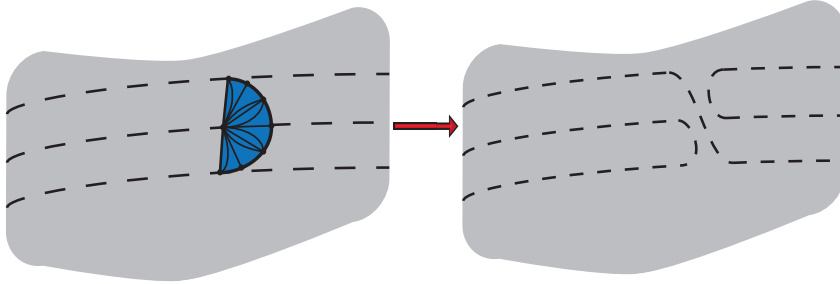
FIGURE 20. S_0 with bypass disk (left), S_1 (right). The dotted lines are the dividing curves.
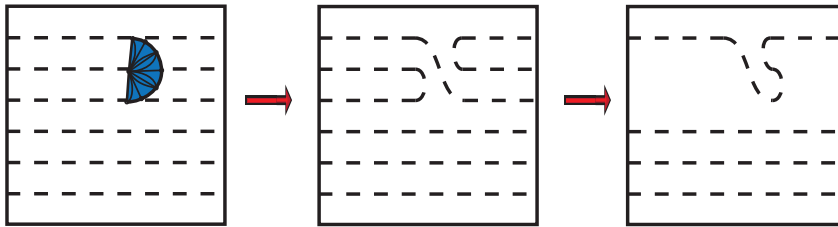
FIGURE 21. A bypass on a torus along three distinct dividing curves

When we are trying to classify knots in a contact structure, we will frequently need to understand what happens when we attach a bypass disk to a torus. The dividing curves on a torus are fairly straightforward. Since there cannot be any dividing curves that bound a disk in a tight contact structure, all dividing curves must be parallel . Since the dividing curves must split the surface into two disconnected pieces, there is an even number of components. First, we will assume the slope of the dividing curves is 0 and the bypass disk intersects the surface along a Legendrian ruling curve of slope $-\infty < r \leq -1$ (other cases come from an $SL(2,\mathbb{Z})$ transformation of this case). If there are 3 distinct dividing curves on the torus that the bypass disk intersects applying the above lemma shows us that the bypass eliminates two of the dividing curves (Figure 21).

If the torus only has two dividing curves, then the bypass changes the slope. If the slope of the dividing curves was originally 0, after the bypass is changes to -1. (Figure 22).

There is a convenient way to determine the change in slope after a bypass when there are only two dividing curves on the torus, using the Farey tessellation of the disk model of the hyperbolic plane, depicted in Figure 23, and constructed in the following way [14]. First label $(1,0)$ as $0/1 = 0$ and $(-1,0)$ as $1/0 = \infty$. Then successively, between every two points labeled p/q, p'/q' such that (p,q), (p',q') forms a $\mathbb{Z}$ basis for $\mathbb{Z}^2$ place a point at the midpoint between them labelled $(p+p')/(q+q')$. We will say $[a,b]$ in the Farey tessellation denotes the arc starting at a and moving counterclockwise until b.
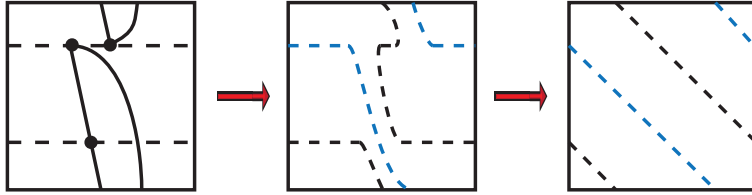
FIGURE 22. A bypass on a torus with only two dividing curves
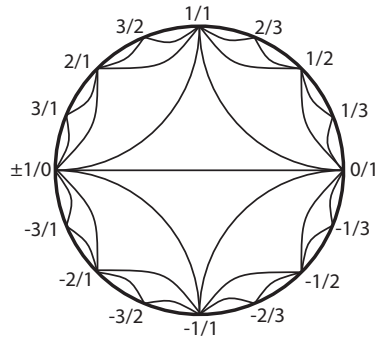
FIGURE 23. The Farey tessellation of the disk model of the hyperbolic plane

We then obtain the slope of the torus with two dividing curves after a bypass using the following lemma:

Lemma 5 (Honda [14]). *Suppose T is a convex torus with two dividing curves of slope s. Suppose there is a bypass disk D which intersects T along a Legendrian ruling curve of slope $r \neq s$. Then after the bypass, the dividing curves have slope s', which is the point on $[r, s]$ closest to r that has an edge to s.*

Now we want to know how to find bypass disks. One simple way is by finding *boundary-parallel curves*. A boundary-parallel curve is a dividing curve on a surface S which intersects ∂S twice and cuts off a disk which contains no other dividing curves.

The characteristic foliation intersects the dividing curve transversely. By flowing along the characteristic foliation, we will eventually reach a disk with Legendrian boundary which is in fact a bypass disk. Because the dividing curve is boundary parallel, it contains one singularity, so the limiting disk will end at the singularities to the left and right. Therefore this part along the boundary will be the γ_1 side of the bypass disk. Flowing out into the surface along the characteristic foliation will limit towards a Legendrian curve with singularities of the same sign. The fact that this limiting will end at a Legendrian curve is due to a lemma of Eliashberg. He shows that this happens when there are no "limit cycles" - a closed leaf in the characteristic foliation. The fact that tightness is

equivalent to the nonexistence of limit cycles is an important theorem in the classification of contact manifolds. Since we are only working in tight contact manifolds, Eliashberg's lemma applies:

Lemma 6 (Eliashberg [6]). *If V is a neighborhood in a surface, and no trajectory exiting (resp. entering) the characteristic foliation is attracted by limit cycles then the closure of the set of points which can be reached from V by flowing along the characteristic foliation has a natural structure of a Legendrian polygon. All vertices on the boundary are negative (resp. positive).*

One common use of boundary-parallel curves in finding bypasses is on an annulus. In the case of an annulus, there are dividing curves which begin and end on different boundary components and those which begin and end on the same boundary component. If there are dividing curves which begin and end on the same boundary component, at least one of them must be boundary parallel. When the number of dividing curves intersecting each boundary component differs, there must be such dividing curves which begin and end on the same boundary component. Half the number of intersections of the dividing curve with each Legendrian boundary component gives its twisting number. This is summed up in the following imbalance principle:

Lemma 7 (Imbalance Principle [9]). *If A is a convex annulus and $\partial A = L_1 \sqcup L_2$ is Legendrian and $t(L_1) < t(L_2)$ then there is a bypass for L_2 on A.*

3.4. **Thickening.** We will use bypasses to *thicken* solid tori which are neighborhoods of a knot. A solid torus $S^1 \times D^2$ *represents* a knot K if its core curve is isotopic to K. Taking a thicker or thinner solid torus changes the slope of the dividing curves on the boundary of the solid torus. Given a Legendrian knot K with $tb(K) = n$, a *standard neighborhood* of K is a solid torus that represents K with two dividing curves on the boundary of slope $1/n$. This standard neighborhood corresponds to the standard neighborhood of theorem 4.

The following lemmas follow from Honda's classification of tight contact structures on $T^2 \times I$ and the solid torus [14]. They describe different slopes of dividing curves that we can expect to find on the boundary of solid tori representing a knot.

Lemma 8 (Etnyre, Honda [9]). *If $T^2 \times [0,1]$ has convex boundary in standard form and the boundary slope on $T^2 \times \{i\}$ is s_i for $i = 0, 1$, then we can find convex tori parallel to $T^2 \times \{i\}$ with any boundary slope s in $[s_1, s_0]$ (if $s_0 < s_1$ then this means $[s_1, \infty] \cup [-\infty, s_0]$).*

In [14], Honda classified all tight contact structures on $T^2 \times I$ and solid tori. The main idea was to break $T^2 \times I$ into basic slices. A basic slice is a layer, $T^2 \times I$ whose two boundary slopes (from the two boundary components) form a basis for $\mathbb{Z}^2$. Honda proves that given a basic slice with boundary slopes s_0 and s_1, one can find a torus of any slope in between. Any $T^2 \times I$ can be split into a sequence of basic slices divided by tori whose slopes increase monotonically (in the sense of the above lemma), so the lemma follows.

Lemma 9 (Etnyre, Honda [9]). *If a solid torus has convex boundary where the slope of the dividing curves is $s < 0$, then we can find a convex torus parallel to the boundary of the solid torus whose dividing curves have slope s' for any $s' \in [s, 0)$.*

Proof. This follows from the fact that every Legendrian knot has a standard neighborhood. By taking arbitrarily many stabilizations, we can find standard neighborhoods whose boundaries are arbitrarily close to 0 ($-\frac{1}{n}$ as $n \to \infty$). Between each successive integer is a basic slice so we can obtain all slopes in between. □
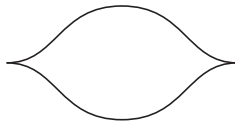
FIGURE 24. The front projection of a Legendrian unknot with $tb = -1$

To find thickenings of the torus we need to look for bypasses (equivalently destabilizations of Legendrian curves).

3.5. **Basic example: the unknot.** As an application of the tools discussed above, we will go through a proof of the fact that the unknot is Legendrian simple, namely a Legendrian unknot is determined up to Legendrian isotopy by its Thurston-Bennequin number and its rotation number.

Recall that stabilization decreases tb by 1 and changes r by ± 1. Therefore we first look at Legendrian unknots with maximal tb and then look at the stabilization/destabilization relationships between other Legendrian unknots.

We claim first that the maximal tb for the unknot, $\mathcal{U}$, $\overline{tb}(\mathcal{U}) = -1$. First if there were a Legendrian unknot U with $tb(U) = 0$ then U would bound an overtwisted disk. Since we are looking at knots in the standard tight contact structure on S^3, this cannot happen. Any Legendrian unknot with $tb > 0$ would stabilize to a Legendrian unknot of $tb = 0$ therefore $\overline{tb}(\mathcal{U}) < 0$. The front projection of a Legendrian unknot with $tb = -1$ is given by figure 24.

Next we claim that there is a unique Legendrian unknot with $tb = -1$. Suppose U is a Legendrian unknot and $tb(U) = -1$. Let D be a disk whose boundary is U. We can isotope D slightly so that it is convex since $tb(U) < 0$ (theorem 7). Furthermore

$$-1 = tb(U) = t_D(U) = -\frac{1}{2}\#(U \cap \Gamma_D)$$

therefore the dividing curves on D intersect U exactly twice. Since the dividing curves cannot bound a disk in a tight contact structure, all dividing curves on D must start and end on the boundary U. Therefore there is a single dividing curve on U so the characteristic foliation on D is unique modulo the Flexibility theorem. Then if there are two Legendrian unknots U, U' of $tb = -1$ bounding convex disks D, D' respectively, there is a map $f : S^3 \to S^3$ which sends U to U' and D to D' and is a contactomorphism when restricted to $N(D)$, a neighborhood of D (theorem 6). We can isotope f to a contactomorphism on all of S^3 because the characteristic foliation on the boundary of $\overline{N(D)}$ is the same as that on its image $\overline{N(D')}$ since f is a contactomorphism on $N(D)$. Therefore the boundary of $\overline{S^3 \setminus N(D)}$ has the same characteristic foliation as $\overline{S^3 \setminus N(D')}$. Since there is a unique tight contact structure on a 3-ball with a given characteristic foliation on its boundary, f must be a contactomorphism on $S^3 \setminus N(D)$ as well. Therefore U and U' are Legendrian isotopic.

Finally we show that all other Legendrian unknots destabilize, so every Legendrian unknot is a stabilization of the maximal tb Legendrian unknot. Suppose U is a Legendrian unknot with $tb(U) < -1$. Then U bounds a convex disk D where

$$tb(U) = t_D(U) = -\frac{1}{2}\#(U \cap \Gamma_D)$$

Therefore the dividing curves of D intersect U more than *twice* so there is more than one dividing curve on D. One of these dividing curves must be boundary parallel and therefore there is a bypass which allows U to destabilize. Therefore all Legendrian unknots are stabilizations of the unknot

depicted in figure 24 and are thus completely classified by their Thurston-Bennequin number and rotation number.

4. Cables, UTP, and Legendrian Simplicity

Throughout this section we will use the convention that curly letters will be used to denote a topological knot type, and instances of that knot type will be denoted by the standard font. For example, K and K' are knots of type $\mathcal{K}$. We will follow this convention to distinguish a knot from a knot type, and will frequently refer to a knot type as a knot.

4.1. The Uniform Thickening Property (UTP).
We begin with some important definitions. Recall that a solid torus is said to *represent* a knot type $\mathcal{K}$ if its core curve has topological knot type $\mathcal{K}$.

Definition 15. *The* contact width *of a knot $\mathcal{K}$ is*

$$w(\mathcal{K}) = \sup \frac{1}{slope(\Gamma_{S^1 \times D^2})}$$

where the supremum is taken over all embeddings of $S^1 \times D^2$ into S^3 which represent $\mathcal{K}$.

Recall that a *standard neighborhood* of a Legendrian knot K is a solid torus $N(K)$ containing K such that $\Gamma_{\partial N(K)} = \frac{1}{tb(K)}$.

Definition 16. *A knot K satisfies the* uniform thickening property (UTP) *if*

- $\overline{tb}(K) = w(K)$
- *Every embedded solid torus representing K can be thickened to a standard neighborhood of a maximal tb Legendrian knot.*

The significance of the UTP comes from the following theorem which we will prove in the last two parts of this section.

Theorem 11 (Etnyre, Honda [10])**.** *If K is a Legendrian simple knot and K satisfies the UTP, then all of its cables are Legendrian simple.*

Before we prove this theorem, we will establish some useful background and some notation.

4.2. Tight contact structures on $T^2 \times I$.
Tight contact structures on $T^2 \times I$ were classified by Honda in [14]. He first looks at what he calls *basic slices*. $(T^2 \times I, \xi)$ is a basic slice if ξ is tight, $T_i = T^2 \times \{i\}$ is convex with two dividing curves of slope s_i for $i = 0, 1$, where the minimal integral representatives s_i form a $\mathbb{Z}$ basis of $\mathbb{Z}^2$. Furthermore we require that ξ be minimally twisting, which essentially means that all the slopes of tori isotopic to T_0 and T_1 have dividing curves with slopes between s_0 and s_1. Then we have the following:

Theorem 12 (Honda [14])**.** *If $T^2 \times I$ has the boundary conditions of a basic slice, then there are exactly two minimally twisting tight contact structures, both of which are universally tight. They are distinguished by their relative half-Euler class. The Poincaré duals of the relative half-Euler classes are given by $\pm$ the difference of the shortest integer vectors corresponding to s_0 and s_1, the slopes of the dividing curves on the boundary components.*

A general $T^2 \times I$ splits into layers of basic slices. The basic slices are determined by finding the minimal sequence of jumps on the Farey tesselation from s_0 to s_1, because jumps on the Farey tesselation correspond to pairs of vectors which form a $\mathbb{Z}$ basis for $\mathbb{Z}^2$. Thickening to the next layer is equivalent to attaching a bypass (as with thickening solid tori). The sign of the bypass determines which tight contact structure you have on the basic slice. Most of the time, basic slices will only

glue to each other if the signs of the bypasses match up, or equivalently, if the signs of the Poincaré duals of the half-Euler classes match up. However there are certain blocks of basic slices where the sign can switch at the boundary, at these places we say there is a *mixing of signs*.

Lemma 10 (Honda [14])**.** *There can be mixing of signs along a torus in* $(T^2 \times I, \xi)$ *only if the dividing curves have slopes which are negative integers or the reciprocal of negative integers. If* $T^2 \times I$ *is split into blocks of basic slices where the boundary of each block is a negative integer (or the reciprocal of a negative integer), then the signs within each block are constant. However, there is a different factorization of the same* $(T^2 \times I, \xi)$ *where the signs of two adjacent blocks are switched (this is known as shuffling).*

This essentially completes the classification of tight contact structures on $T^2 \times I$. By analyzing how to split thickened tori into basic slices, one can explicitly count the number of tight contact structures on $T^2 \times I$. There are other cases to deal with when the number of dividing curves on the boundary tori is greater than 2. This ends up giving a non-rotative slice where all convex tori have the same dividing slope and the other boundary component has only 2 dividing curves. There is also the possibility that there are full rotations so the slopes of the dividing curves change and then rotate all the way around the Farey tesselation before reaching the other boundary component. In [14], Honda is able to completely classify tight contact structures on $T^2 \times I$, and count the number of tight contact structures in the minimally twisting rotative cases, using analysis of the splitting into basic slices and the shuffling lemma.

4.3. **Cables and Coordinates.** A (p,q) cable of a knot $\mathcal{K}$ is a knot $\mathcal{K}_{(p,q)}$ that sits on the boundary of $N(\mathcal{K})$, a solid torus representing $\mathcal{K}$, and wraps around $\partial N(\mathcal{K})$ p times meridonally and q times longitudinally.

We will identify this boundary torus with $\mathbb{R}^2/\mathbb{Z}^2$ under a coordinate system where the longitude has slope ∞ and the meridian has slope 0. This coordinate system will be referred to as $\mathcal{C}_{\mathcal{K}}$. Under $\mathcal{C}_{\mathcal{K}}$, $\mathcal{K}_{(p,q)}$ has slope $\frac{q}{p}$.

It will also be useful to look at solid tori representing $\mathcal{K}_{(p,q)}$, and coordinates on their boundaries. Suppose $K_{(p,q)}$ is a (p,q) cable of $\mathcal{K}$ which sits on the boundary of $N(\mathcal{K})$. Furthermore, suppose $N(\mathcal{K}_{(p,q)})$ is a solid torus representing $K_{(p,q)}$. Let A be an annulus on $\partial N(\mathcal{K})$ that intersects $\partial N(\mathcal{K}_{(p,q)})$ along its boundary, such that $\partial N(\mathcal{K}_{(p,q)}) \setminus A$ has two disjoint components, S_1, S_2, each of which is an annulus such that $A \cup S_i$ is isotopic to $\partial N(\mathcal{K})$. If we think of $\partial N(\mathcal{K})$ as $\mathbb{R}^2/\mathbb{Z}^2$ and $K_{(p,q)}$ as a line of slope $\frac{q}{p}$, we can find A as in figure 25.

Then we define $\mathcal{C}_{\mathcal{K}}^{(p,q)}$ to be the coordinate system on $\partial N(\mathcal{K}_{(p,q)})$ where the meridian has slope 0 and $A \cap \partial N(K_{(p,q)})$ has slope ∞.

On the other hand, we also have the coordinate system $\mathcal{C}_{\mathcal{K}_{(p,q)}}$ on $\partial N(\mathcal{K}_{(p,q)})$ where the meridian has slope 0 and the longitude has slope ∞. The longitude is defined by the intersection of a Seifert surface for $\mathcal{K}_{(p,q)}$ with $\partial N(\mathcal{K}_{(p,q)})$. In order to compare $\mathcal{C}_{\mathcal{K}}^{(p,q)}$ with $\mathcal{C}_{\mathcal{K}_{(p,q)}}$ we want to describe the Seifert surface for $\mathcal{K}_{(p,q)}$. Take $|p|$ copies of meridional disks of $N(K)$ and $|q|$ copies of Seifert surfaces for K whose boundaries lie on $\partial N(K)$. If we identify $N(K)$ with a square in coordinates $\mathcal{C}_{\mathcal{K}}$ then we can imagine that the meridional disks lie below the plane of the square (corresponding to inside $N(K)$), and the Seifert surfaces lie above the plane of the square (corresponding to outside $N(K)$) so that they only intersect along their boundaries on $\partial N(K)$. At each of these pq intersections add a twist to connect these pieces together into a single surface. By choosing the twists in one direction or the other, we obtain a surface whose boundary is a curve of slope $\pm\frac{q}{p}$ on $N(K)$ and is thus isotopic to $K_{(p,q)}$ as in figure 26
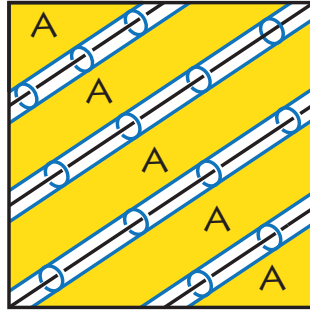
FIGURE 25. The square represents the identification of $\mathbb{R}^2/\mathbb{Z}^2$ with $\partial N(\mathcal{K})$. The black lines represent $K_{(p,q)}$. The blue cylinders represent $N(K_{(p,q)})$. The yellow regions marked A lie in the plane of the page and make up the annulus A discussed above. $N(K_{(p,q)}) \cap A$ is precisely the intersection of $\partial N(K_{(p,q)})$ with the plane of the page, so half of each cylinder lies above the page and half lies below. Note that if we take the union of A with either the piece of $\partial N_{(p,q)}$ which lies above the page or with the piece of $\partial N_{(p,q)}$ that lies below the page, we get a torus isotopic to $\partial N(K)$.
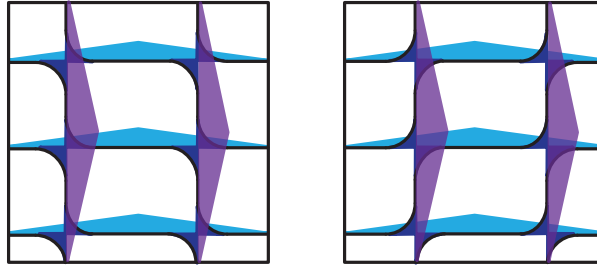
FIGURE 26. The square represents $N(K)$ the blue horizontal triangles are the $|p| = 3$ meridional disks. The purple vertical triangles are the $|q| = 2$ Seifert surfaces for K. After adding in twists at the intersections we obtain a surface whose boundary is the black line, which has slope $\pm\frac{q}{p}$ (with the sign depending on the direction of the twists).

We want to be able to switch between these two coordinate systems. The transformations between $(\mathbb{R}^2/\mathbb{Z}^2, \mathcal{C}_{\mathcal{L}}^{(p,q)})$ and $(\mathbb{R}^2/\mathbb{Z}^2, \mathcal{C}_{\mathcal{L}_{(p,q)}})$ are given by:

$$(3) \qquad \begin{bmatrix} 1 & -pq \\ 0 & 1 \end{bmatrix} : (\mathbb{R}^2/\mathbb{Z}^2, \mathcal{C}_{\mathcal{L}_{(p,q)}}) \to (\mathbb{R}^2/\mathbb{Z}^2, \mathcal{C}_{\mathcal{L}}^{(p,q)})$$

$$(4) \qquad \begin{bmatrix} 1 & pq \\ 0 & 1 \end{bmatrix} : (\mathbb{R}^2/\mathbb{Z}^2, \mathcal{C}^{(p,q)}_{\mathcal{L}}) \to (\mathbb{R}^2/\mathbb{Z}^2, \mathcal{C}_{\mathcal{L}_{(p,q)}})$$

Figure 27 shows this pictorially. When we compare this with the twisting of the contact planes we get the following lemma:

Lemma 11. *If $K_{(p,q)} \in \mathcal{K}_{(p,q)}$ is the (p,q) cable of $K \in \mathcal{K}$ then*

$$t(K_{(p,q)}, \mathcal{C}^{(p,q)}_{\mathcal{K}}) + pq = t(K_{(p,q)}, \mathcal{C}_{\mathcal{K}_{(p,q)}}) = tb(K_{(p,q)})$$
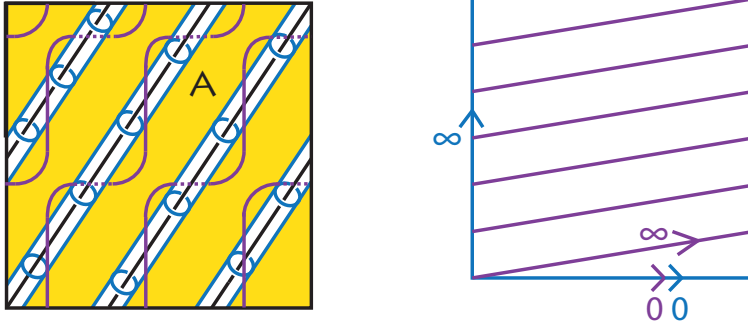
FIGURE 27. On the left we have N, the neighborhood of the (p,q) cable of a knot $\mathcal{L}$ (∂N is the blue cylinders), lying on the square which represents the boundary of a neighborhood of $\mathcal{L}$. The yellow sections are the annulus A. The purple lines are the boundary of the Seifert surface obtained by taking p meridional disks and q Seifert surfaces for $\mathcal{L}$ and adding in twists at their intersections. Thus the purple lines are the longitude of N. On the right, ∂N is identified with the square and we have coordinates $\mathcal{C}^{(p,q)}_{\mathcal{L}}$ (blue) and $\mathcal{C}_{\mathcal{L}_{(p,q)}}$ (purple).

In the case where $\mathcal{K}$ is an unknot and $\mathcal{K}_{(p,q)}$ is a torus knot, we have some further coordinate systems. An unknotted torus decomposes S^3 into two solid tori V_1 and V_2, ($\partial V_1 = -\partial V_2$). We will say that $\mathcal{U}_{(p,q)}$ lies on $\partial V_1 = -\partial V_2$. Let $\mathcal{U}_1, \mathcal{U}_2$ be the core (unknotted) curves of V_1 and V_2 respectively. Here I am using the notation that indicates that $\mathcal{U}_1$ and $\mathcal{U}_2$ are topological knot types. However I want to only allow knots that are topologically isotopic to the core curve of V_1 (or V_2) within V_1 (or V_2). Thus, even though $\mathcal{U}_1$ and $\mathcal{U}_2$ are both topological unknot types, they live in disjoint solid tori. Then the $(p,q) = (2,3)$ torus knot $K \in \mathcal{K}$ is the (p,q) cable of $\mathcal{U}_1$ and the (q,p) cable of $\mathcal{U}_2$, because the boundaries of V_1 and V_2 are endowed with opposite orientations.

In addition to the standard coordinate system on ∂V_1 where the meridian of V_1 has slope 0 and the longitude has slope ∞, we will have one other coordinate system on these unknotted tori which will be denoted by $\mathcal{C}^{(p,q)}$. Under this coordinate system the (p,q) torus knot has slope ∞. To determine what corresponds to slope 0 in these coordinates, choose a transformation $M \in SL(2,\mathbb{Z})$ which sends vectors in the coordinates $\mathcal{C}^{(p,q)}$ to vectors in the coordinates $\mathcal{C}_{\mathcal{U}_1}$. Since $(0,1)^t$ in $\mathcal{C}^{(p,q)}$ must be sent to $(p,q)^t$ in $\mathcal{C}_{\mathcal{U}_1}$ we have

$$M = \begin{bmatrix} x & p \\ y & q \end{bmatrix}$$

where x, y are chosen such that $xq - yp = 1$. Then the vector $(1,0)^t$ (slope 0) in coordinates $\mathcal{C}^{(p,q)}$ is given by $(x,y)^t$ (slope $\frac{y}{x}$) in coordinates $\mathcal{C}_{\mathcal{U}_1}$.

Note this is different notation from $\mathcal{C}_{\mathcal{U}_i}^{(p,q)}$ which is a coordinate system for *neighborhoods of the (p,q) cable of $\mathcal{U}_i$*, while $\mathcal{C}^{(p,q)}$ is a coordinate system for *neighborhoods of $\mathcal{U}_i$*.

The transformations between $(\mathbb{R}^2/\mathbb{Z}^2, \mathcal{C}^{(p,q)})$ and $(\mathbb{R}^2/\mathbb{Z}^2, \mathcal{C}_{\mathcal{U}_1})$ are given by:

$$(5) \qquad \begin{bmatrix} x & p \\ y & q \end{bmatrix} : (\mathbb{R}^2/\mathbb{Z}^2, \mathcal{C}^{(p,q)}) \to (\mathbb{R}^2/\mathbb{Z}^2, \mathcal{C}_{\mathcal{U}_1})$$

$$(6) \qquad \begin{bmatrix} q & -p \\ -y & x \end{bmatrix} : (\mathbb{R}^2/\mathbb{Z}^2, \mathcal{C}_{\mathcal{U}_1}) \to (\mathbb{R}^2/\mathbb{Z}^2, \mathcal{C}^{(p,q)})$$

Note that the transformation between $(\mathbb{R}^2/\mathbb{Z}^2, \mathcal{C}_{\mathcal{U}_1})$ and $(\mathbb{R}^2/Z^2, \mathcal{C}_{\mathcal{U}_2})$ is

$$\begin{bmatrix} 0 & 1 \\ 1 & 0 \end{bmatrix} : (\mathbb{R}^2/\mathbb{Z}^2, \mathcal{C}_{\mathcal{U}_2}) \to (\mathbb{R}^2/Z^2, \mathcal{C}_{\mathcal{U}_1})$$

This matrix has determinant -1 and is thus not in $SL(2,\mathbb{Z})$ because the orientation on a neighborhood of $\mathcal{U}_2$ is the opposite of the orientation on a neighborhood of $\mathcal{U}_2$. (Recall U_1 and U_2 are the core curves of V_1 and V_2 where $V_1 \cup V_2 = S^3$ and $V_1 \cap V_2 = \partial V_1 = -\partial V_2$.) Then to change coordinates from $\mathcal{C}_{\mathcal{U}_2}$ to $\mathcal{C}^{(p,q)}$ we have the transformation

$$(7) \qquad \begin{bmatrix} -p & q \\ x & -y \end{bmatrix} = \begin{bmatrix} q & -p \\ -y & x \end{bmatrix} \begin{bmatrix} 0 & 1 \\ 1 & 0 \end{bmatrix} : (\mathbb{R}^2/\mathbb{Z}^2, \mathcal{C}_{\mathcal{U}_2}) \to (\mathbb{R}^2/\mathbb{Z}^2, \mathcal{C}_{\mathcal{U}_1}) \to (\mathbb{R}^2/\mathbb{Z}^2, \mathcal{C}^{(p,q)})$$

We summarize these coordinate systems in the following table:

∂N	N neighborhood of:	slope ∞ is given by	slope 0 given by
$\mathcal{C}_{\mathcal{U}_i}$	$\mathcal{U}_i$ for $i \in \{1,2\}$	Longitude of N (bounds a disk outside N)	Meridian of N
$\mathcal{C}^{(p,q)}$	$\mathcal{U}_1$	The slope of the (p,q) torus knot on ∂N	slope $\frac{y}{x}$ in $\mathcal{C}_{\mathcal{U}_1}$
$\mathcal{C}_{\mathcal{U}_{(p,q)}}$	$\mathcal{U}_{1(p,q)}$	Longitude (bounds a Seifert surface for $\mathcal{K}$)	Meridian of N
$\mathcal{C}_{\mathcal{U}}^{(p,q)}$	$\mathcal{U}_{1(p,q)}$	$N \cap A$, s.t. $\exists\, S$ nbhd of $\mathcal{U}$, $\partial N^+ \cup A \cong \partial S \cong \partial N^- \cup A$, $\partial N^+ \sqcup \partial N^- \sqcup (\partial N \cap A) = \partial N$	Meridian of N
$\mathcal{C}_{\mathcal{K}_{(p,q)}}$	(p,q) cable of $\mathcal{K}$	Longitude (bounds Seifert surface for $\mathcal{K}_{(p,q)}$)	Meridian of N
$\mathcal{C}_{\mathcal{K}}^{(p,q)}$	(p,q) cable of $\mathcal{K}$	$N \cap A$, s.t. $\exists\, S$ nbhd of $\mathcal{K}$, $\partial N^+ \cup A \cong \partial S \cong \partial N^- \cup A$, $\partial N^+ \sqcup \partial N^- \sqcup (\partial N \cap A) = \partial N$	Meridian of N

4.4. **Knots with the UTP.** Although it seems that the UTP is an interesting property since it is a sufficient condition on a knot to ensure that all cables of a Legendrian simple knot are Legendrian simple, it is only useful if there are many knots that satisfy the UTP. The following results establish this.

Theorem 13 (Etnyre, Honda [10])**.** *Negative torus knots satsify the UTP.*

We also have a more general theorem, that certain cables of knots that satisfy the UTP, also satisfy the UTP.

Theorem 14 (Etnyre, Honda [10])**.** *If a knot type $\mathcal{K}$ satisfies the UTP, then for all pairs (p, q) such that $\frac{p}{q} < w(\mathcal{K})$, the (p, q) cable of $\mathcal{K}$ also satisfies the UTP.*

Note that although negative torus knots are cables of the unknot satisfying the inequality above, the unknot $\mathcal{U}$ does not satisfy the UTP ($\overline{tb}(\mathcal{U}) = -1$ while $w(\mathcal{U}) = 0$) so theorem 13 does not follow from theorem 14, however they can be proved using similar techniques. We will prove theorem 14 following the lines of Etnyre and Honda and omit a proof of theorem 13.

Proof. Suppose $\mathcal{K}$ is a knot satisfying the UTP and $\frac{p}{q} < w(\mathcal{K})$. Let $\mathcal{K}_{(p,q)}$ be the (p, q) cable of $\mathcal{K}$. In order to prove that $\mathcal{K}_{(p,q)}$ satisfies the UTP, we must show each of the two properties in the definition of the UTP are satisfied.

Property 1: $w(\mathcal{K}_{(p,q)}) = \overline{tb}(\mathcal{K})$.

By lemma 11 this is equivalent to showing that the maximal twisting of $\mathcal{K}_{(p,q)}$ with respect to the framing $\mathcal{C}_{\mathcal{K}}^{(p,q)}$, denoted $\bar{t}(\mathcal{K}_{(p,q)}, C_{\mathcal{K}}^{(p,q)})$, is 0.

First we will show that $t(K_{(p,q)}, C_{\mathcal{K}}^{(p,q)}) = 0$ can be attained by a Legendrian knot $K_{(p,q)} \in \mathcal{K}_{(p,q)}$ and thus

$$\bar{t}(\mathcal{K}_{(p,q)}, \mathcal{C}_{\mathcal{K}}^{(p,q)}) \geq 0$$

Since $\frac{p}{q} < w(\mathcal{K})$, if we take a neighborhood $N(\mathcal{K})$ of maximal thickness, then we can thin it (lemma 9) to find a convex torus whose dividing curves have slope $\frac{q}{p}$. A Legendrian divide on such a torus L satisfies $t(L, C_{\mathcal{K}}^{(p,q)}) = 0$ and is a (p, q) cable of $\mathcal{K}$.

Next we show that there are no neighborhoods of any $K_{(p,q)} \in \mathcal{K}_{(p,q)}$ whose boundary has dividing curves of strictly positive slope.

Suppose $N_{(p,q)}$ is a neighborhood of $K_{(p,q)} \in \mathcal{K}_{(p,q)}$ with convex boundary, and there are two dividing curves of slope $s > 0$. We can shrink $\frac{1}{s}$ as much as we want by thinning the torus. Therefore we may assume that s is a large positive integer. Also we may isotope $N_{(p,q)}$ so that it has Legendrian rulings of slope ∞ (with respect to $C_{\mathcal{K}}^{(p,q)}$) by the Giroux flexibility theorem.

Now choose an annulus A such that $R = N_{(p,q)} \cup A \times [-\varepsilon, \varepsilon]$ is diffeomorphic to $T^2 \times I$ where each boundary component is parallel to the boundary of a neighborhood of $\mathcal{K}$ (here $A \times [-\varepsilon, \varepsilon]$ is $[-\varepsilon, \varepsilon]$ invariant). Let $N(\mathcal{K})$ be this solid torus neighborhood and suppose $\partial R = T_1 \cup T_2$ where T_1 is inside $N(\mathcal{K})$ and T_2 is outside $N(\mathcal{K})$. Let $\partial N(\mathcal{K}) = T_{1.5}$.

If the dividing curves on A have any boundary parallel curves then we can find a bypass to thicken $N_{(p,q)}$. Using lemma reffareylemma we compute that after the bypass the slope of the dividing curves will be ∞ (with respect to $C_{\mathcal{K}}^{(p,q)}$), since there is a jump from s which is a positive integer to ∞ and the ruling curves have slope ∞. In this case we can find a convex annulus bounded by these Legendrian divides which lies inside $N_{(p,q)}$. We can choose two Legendrian curves C_1, C_2 on the annulus which divide it into two disks D_1, D_2 glued together along these curves. Then $tb(\partial D_1) + tb(\partial D_2) = 0$ since the twisting along C_1 and C_2 cancels out in the sum, and the annulus is bounded by curves which

have twisting 0. However this means that $tb(\partial D_i) \geq 0$ for $i \in \{1, 2\}$, which means that there is an overtwisted disk in $N_{(p,q)}$. Therefore A has two dividing curves, each of which begins on one boundary component and ends on the other.

We can compare the slopes of the dividing curves T_1 and T_2, by computing the difference in the slopes of the boundary curves when attaching the top half of $\partial N_{(p,q)}$ to A versus attaching the bottom half of $\partial N_{(p,q)}$ to A. Because the slope on $\partial N_{(p,q)}$ is measured with respect to the meridional curve of $N_{(p,q)}$, the slope on the top appears to be opposite the slope on the bottom because counterclockwise around the meridional curve points to the left on the top and to the right on the bottom. Therefore the dividing curves on T_1 and T_2 near each component of $N_{(p,q)}$ appear as in figure 28. When the slope of the dividing curves on $\partial N_{(p,q)}$ is a positive integer s, the slope of T_2 is obtained by performing $s + 1$ negative Dehn twists to the dividing curves of T_1. Therefore we may recoordinatize $\partial N(\mathcal{K})$ so that $\mathrm{slope}(\Gamma_{T_1}) = -s$, $\mathrm{slope}(\Gamma_{T_2}) = 1$.
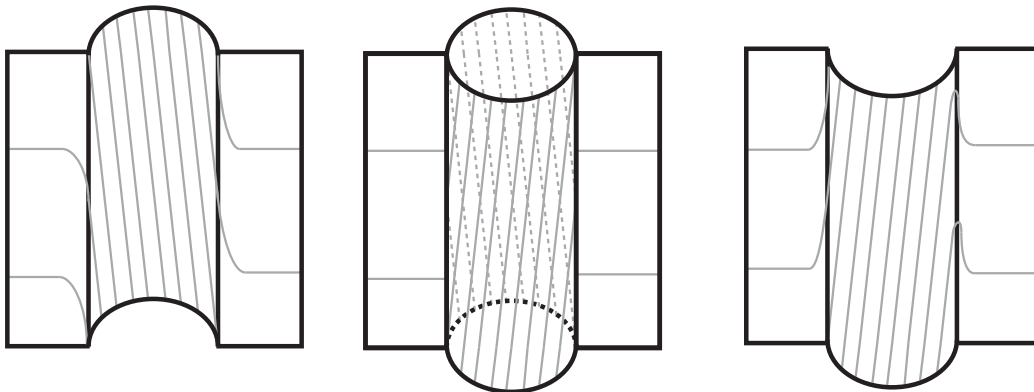
FIGURE 28. Attaching the two halves of $\partial N_{(p,q)}$ to the annulus A to obtain T_1 (left) and T_2 (right). When the slope of the dividing curves on $\partial N_{(p,q)}$ is a positive integer s, the slope of T_2 is obtained by performing $s + 1$ negative Dehn twists to the dividing curves of T_1.

Given $T^2 \times [1, 2]$ with $\mathrm{slope}(\Gamma_{T_1}) = -s$ and $\mathrm{slope}(\Gamma_{T_2}) = 1$, we can split $T^2 \times [1, 2]$ into two basic slices: $T^2 \times [1, 1.5]$ and $T^2 \times [1.5, 2]$, where $\mathrm{slope}(\Gamma_{T_{1.5}}) = \infty$. This splitting exists because ∞ is the point on the Farey tessellation which has a jump to $-s$ and 1.

The Poincaré duals of the relative half-Euler classes of the possible tight contact structures on $T^2 \times [1, 1.5]$ are $\pm((0, 1) - (-1, s)) = \pm(1, 1 - s)$. On $T^2 \times [1.5, 2]$ they are $\pm((1, 1) - (0, 1)) = \pm(1, 0)$. Therefore there are four possible values of $PD(e(\xi))$ for $T^2 \times [1, 2]$ which are $\pm(1, 0) \pm (1, 1 - s)$. If one of the signs is $+$ and the other is $-$, there is a mixing of signs at $T_{1.5}$.

Let γ be a Legendrian ruling curve on A of slope ∞. Let $A' = \gamma \times [-\varepsilon, \varepsilon]$. We find out which combination of basic slices is on our solid torus by computing $\langle e(\xi), A' \rangle = \chi(A'_+) - \chi(A'_-)$. Because A' is $[-\varepsilon, \varepsilon]$ invariant, its dividing set is $\{p_1, \cdots, p_n\} \times [-\varepsilon, \varepsilon]$ where n is even, and A'_+

and A'_- are the disks between the dividing curves (alternating between $+$ and $-$). Therefore $\langle e(\xi), A' \rangle = \chi(A'_+) - \chi(A'_-) = 0$. This tells us that $PD(e(\xi)) = (0, \pm(1-s))$ which means that there is mixing of sign. Such a mixing of signs cannot happen when the slope is not a negative integer or the reciprocal of a negative integer (lemma 10). This provides a contradiction to the fact that there is a neighborhood of $\mathcal{K}_{(p,q)}$ whose boundary has dividing curves of positive slope.

Property 2: Every neighborhood $N_{(p,q)}$ of a Legendrian knot of type $\mathcal{K}_{(p,q)}$ can be thickened to a standard neighborhood (in the sense of 16) of a Legendrian knot $K_{(p,q)}$ with $t(K_{(p,q)}, C_{\mathcal{K}}^{(p,q)})$.

Suppose $N_{(p,q)}$ is a neighborhood of $K_{(p,q)} \in \mathcal{K}_{(p,q)}$, with convex boundary such that slope$(\Gamma_{\partial N_{(p,q)}}) = s$ where $-\infty < s < 0$ (since we have eliminated the possibility that $s > 0$ in step 1). Isotope $N_{(p,q)}$ so that it has Legendrian rulings of slope ∞. Let $R = A \times [-\varepsilon, \varepsilon] \cup N_{(p,q)} \cong T^2 \times I$ and $T_i = T^2 \times \{i\} \subset \partial R$ as in step 1. If A has any boundary parallel curves, then there is a bypass for $N_{(p,q)}$ to a new solid torus $N'_{(p,q)}$ with dividing curves of slope s' where $-\infty < s' < 0$, which is the same situation we started with. Therefore we can assume that A has dividing curves which are parallel arcs that begin and end on different boundary components. Since $A \times [-\varepsilon, \varepsilon]$ is $[-\varepsilon, \varepsilon]$ invariant, the dividing curves on $A \times \{\pm\varepsilon\}$ are the same as those on A. After smoothing the edges on R the dividing curves on the boundary can have a wide range of slopes, but they cannot have slope $\frac{q}{p}$ with respect to $C_{\mathcal{K}}$. Furthermore, the slope of T_1 (the lower boundary component) will be less than the slope of T_2 (the upper boundary component). See figure 29 and its caption for a detailed explanation.
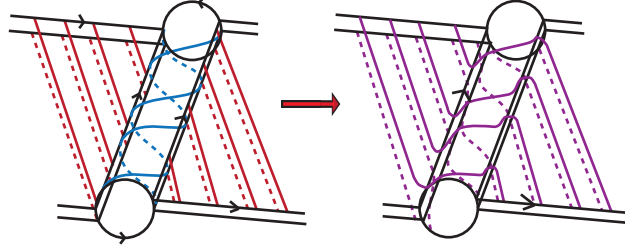
FIGURE 29. One piece of $R = N_{(p,q)} \cup A \times [-\varepsilon, \varepsilon]$ with dividing curves and smoothing of edges. The front and back faces are identified. The arrows indicate the positive directions when each surface is identified with $\mathbb{R}^2/\mathbb{Z}^2$ so that the slope can be determined. No matter what slope you choose for the dividing curves of A, the dividing curves after smoothing will never be parallel to $A \times \{\pm\varepsilon\} \cap N_{(p,q)}$ (slope ∞). After smoothing, the dividing curves on the lower boundary component (T_1) have a more negative slope than those on the upper boundary component (T_2). This is because the counterclockwise direction around the meridian of $N_{(p,q)}$ opposes the orientation of the meridian of T_2 (subtracts a negative slope) and agrees with the orientation of the meridian of T_1 (adds a negative slope).

Recall that T_1 and T_2 are parallel to the boundary of a neighborhood of $\mathcal{K}$, $N(\mathcal{K})$ and $T_1 \subset N(\mathcal{K})$ and $T_2 \subset S^3 \setminus N(\mathcal{K})$. Because the interval between the slopes of the dividing curves on T_1 and T_2
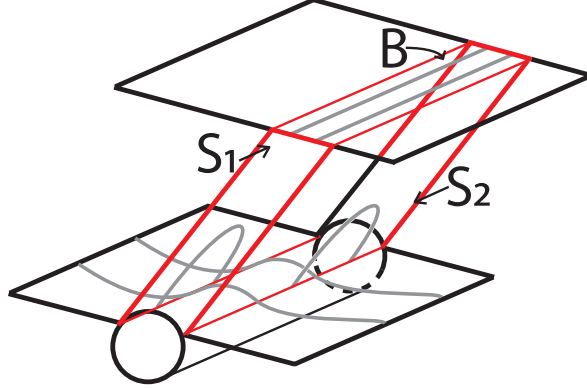
FIGURE 30. The red box is the thickened annulus (identify front and back sides). After attaching this thickened annulus to the torus $N_{(p,q)}$ (here represented by the cylinder), we obtain a thickening of $N_{(p,q)}$ with dividing curves of slope ∞ with respect to $\mathcal{C}_{\mathcal{K}}^{(p,q)}$.

does not contain $\frac{q}{p}$, there are no tori isotopic to T_i in R whose dividing curves have slope $\frac{q}{p}$. Since $\mathcal{K}$ satisfies the UTP, and $\frac{p}{q} < w(\mathcal{K}) = \overline{tb}(\mathcal{K})$, $N(\mathcal{K})$ can be thickened to a solid torus $N'(\mathcal{K})$, whose boundary has dividing curves of slope IIp with respect to $C_{\mathcal{K}}$. This allows us to find a thickening for $N_{(p,q)}$ to a neighborhood of $K_{(p,q)}$ with dividing curves of slope ∞ with respect to $C_{\mathcal{K}}^{(p,q)}$ by adding a thickened annulus as in figure 30. The top part of the thickened annulus is an annulus B cut out of $\partial N'(\mathcal{K})$ which has dividing curves of slope $\frac{q}{p}$ in coordinates $\mathcal{C}_{\mathcal{K}}$ which is paralle to curves of slope ∞ on on $N_{(p,q)}$ in coordinates $\mathcal{C}_{\mathcal{K}}^{(p,q)}$. We attach the sides of the thickened annulus S_1, S_2, to B along its boundary which is made up of two Legendrian divides in parallel to the dividing curves of B. We attach S_1, S_2 to $\partial N_{(p,q)}$ along $\partial N_{(p,q)} \cap A \times \{\varepsilon\}$. Since the dividing curves on B do not intersect the boundary of B, any dividing curves on S_1 or S_2 must be boundary parallel to $S_i \cap N_{(p,q)}$. After smoothing the edges where $\partial N_{(p,q)}$ meets S_1 and S_2, the boundary parallel disks must attach to the dividing curves of $\partial N_{(p,q)}$ so that they are parallel to the dividing curves on B of slope ∞ based on the classification of dividing curves on convex tori in tight contact structures. Therefore attaching the thickened annulus to $N_{(p,q)}$ gives a thickening of $N_{(p,q)}$ whose boundary has dividing curves of slope ∞ in $\mathcal{C}_{\mathcal{K}}^{(p,q)}$.

Finally, to show that $K_{(p,q)}$ satisfies the UTP, we need to show $N_{(p,q)}$ thickens to a standard neighborhood, namely one with exactly 2 dividing curves of slope $\overline{tb}(K)$ (which is slope ∞ with respect to $C_{\mathcal{K}}^{(p,q)}$). This follows from Honda's classification of tight contact structures on solid tori, which finds a non-rotative thickening to a torus with only 2 dividing curves.

$\square$

4.5. **Sufficiently Positive Cables.** The proof of theorem 11 is split into two parts. We will first prove that (p, q) cables of $\mathcal{K}$ with $\frac{p}{q} > w(\mathcal{K})$ are Legendrian simple (such cables will be called *sufficiently positive cables*), and then show that cables where $\frac{p}{q} < w(\mathcal{K})$ are Legendrian simple (such cables will be called *sufficiently negative cables*). Now we look at the former case.

Lemma 12. *Suppose $\mathcal{K}$ satisfies the UTP. If $K_{(p,q)}$ is a sufficiently positive cable of $\mathcal{K}$ with maximal tb then it lies on the boundary of a standard neighborhood of $K \in \mathcal{K}$ with maximal tb.*

Proof. The key to this proof relies on the following theorem from Kanda:

Theorem 15 (Kanda [17])**.** *Let C be a Legendrian curve on a convex surface F. Then*

$$tb(C) = lk(C, C') - \frac{1}{2}\#(C \cap \Gamma_F)$$

where C' is a curve obtained by pushing C slightly in the positive normal direction of F, and $\#(C \cap \Gamma_F)$ is the number of times C intersects Γ_F.

This tells us that $tb(K_{(p,q)})$ is maximal when the number of intersection points of $K_{(p,q)}$ with the dividing set on T is minimized. Because $K_{(p,q)}$ intersects Γ_T efficiently, we can compute the number of intersections from their slopes. Let $\mathrm{slope}(\Gamma_T) = \frac{m}{n}$ in coordinates $\mathcal{C}_\mathcal{K}$. Under these coordinates, the slope of $\mathcal{K}_{(p,q)}$ is $\frac{q}{p}$ so

$$\#(K_{(p,q)} \cap \Gamma_T) = (\#\Gamma_T) \det \begin{bmatrix} n & m \\ q & p \end{bmatrix} = (\#\Gamma_T)|np - qm|$$

I claim that this is minimized over all possible slopes of the dividing curves on T when

$$\frac{m}{n} = \frac{1}{w(\mathcal{K})} = \frac{1}{\overline{tb}(\mathcal{K})}$$

This is because $|np - mq|$ is minimized when the $\mathrm{slope}(\Gamma_T) = \frac{m}{n}$ is chosen such that $np - mq$ is as close as possible to 0. This happens when $\frac{n}{m}$ is as close as possible to $\frac{q}{p}$. Because we are looking at the sufficiently positive case, $\frac{p}{q} > w(\mathcal{K}) > \frac{1}{s}$ for any possible $s = \mathrm{slope}(\Gamma_T)$. Therefore $|np - mq|$ is minimized when $\frac{m}{n} = \frac{1}{w(\mathcal{K})}$. $\qquad\square$

Step 1: Maximal tb Legendrian knots are determined by their rotation number, and the set of rotation numbers of maximal tb Legendrian knots is

$$\{q \cdot r(L) | L \in \mathcal{K}, \ \ tb(L) = w(\mathcal{K})\}$$

Suppose $K_{(p,q)}$ has maximal tb. Using the previous lemma, $K_{(p,q)}$ lies on the boundary of a standard neighborhood of $K \in \mathcal{K}$ of maximal tb. This allows us to compute the possible rotation numbers for $K_{(p,q)}$ using the following formula:

Lemma 13 (Etnyre, Honda [10])**.** *Let D be a convex meridonal disk of $N(\mathcal{K})$ with Legendrian boundary on $\partial N(\mathcal{K})$ and Σ a convex Seifert surface with Legendrian boundary $K \in \mathcal{K}$, $K \subset \partial N(\mathcal{K})$. Then*

$$r(K_{(p,q)}) = p \cdot r(\partial D) + q \cdot r(\partial \Sigma)$$
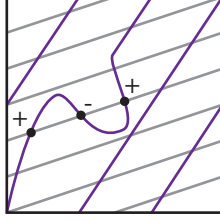
FIGURE 31. A case where $K_{(p,q)}$ (purple) does not intersect the dividing curves (grey) of T efficiently. The $+$ and $-$ signs indicate the oriented intersection numbers of $K_{(p,q)}$ with Γ_T.

Since $N(K)$ is a standard neighborhood of K whose boundary has dividing curves of slope $\frac{1}{n}$, ∂D intersects each of the two dividing curves once. Therefore D can have only one dividing curve which has its endpoints on ∂D. Then D is contactomorphic to the standard Seifert surface of the standard unknot which has rotation number 0. Therefore $r(\partial D) = 0$. The lemma then implies $r(K_{(p,q)}) = q \cdot r(K)$ so the rotational number of $K_{(p,q)}$ is determined by the rotation number of K, the Legendrian knot at the core of the torus that $K_{(p,q)}$ lies on. Now suppose we have two Legendrian knots $K_{(p,q)}, K'_{(p,q)} \in \mathcal{K}_{(p,q)}$ with maximal tb and the same rotation number. Then they lie on the boundaries of solid tori N, N' whose core curves are Legendrian knots $K, K' \in \mathcal{K}$ respectively each with convex boundary and slope$(\Gamma_{\partial N})$ =slope$(\Gamma_{\partial N'}) = \frac{1}{w(\mathcal{K})}$. Since $K_{(p,q)}$ and $K'_{(p,q)}$ have the same rotation numbers the above implies K and K' have the same rotation numbers. Since $\mathcal{K}$ is assumed to be Legendrian simple this means that K and K' are Legendrian isotopic. Thus we can assume that $K = K'$ and $V = N \cap N'$ is another solid torus with convex boundary and slope$(\Gamma_{\partial V}) = \frac{1}{w(\mathcal{K})}$. ∂V has ruling curves of slope $\frac{q}{p}$. $N \setminus V$ and $N' \setminus V$ are isotopic to $T^2 \times I$ with an I-invariant contact structure, therefore we can Legendrian isotope $K_{(p,q)}$ and $K'_{(p,q)}$ onto ∂V. Then they are Legendrian isotopic on ∂V through other ruling curves.

Step 2: Knots with less than maximal tb destabilize.

Suppose $K_{(p,q)} \in \mathcal{K}_{(p,q)}$ has $tb(K_{(p,q)}) < \overline{tb}(\mathcal{K}_{(p,q)})$. Find a neighborhood $N(\mathcal{K})$ whose boundary is a convex torus T such that $K_{(p,q)} \subset T$. Because $\frac{p}{q} > w(\mathcal{K}) = \sup \frac{1}{\text{slope}(\Gamma_T)}$, we can choose a dividing set on T that intersects all curves of slope $\frac{q}{p}$ transversely. By Giroux's Flexibility Theorem (Theorem 8) we may assume that the Legendrian rulings of T are the curves of slope $\frac{q}{p}$.

If $K_{(p,q)}$ does not intersect Γ_T efficiently (the geometric intersection number is equal to the actual intersection number), then we can destabilize it. This is because the only way $K_{(p,q)}$ could intersect Γ_T first with one sign and then with a different sign, is if $K_{(p,q)}$ bounds a disk with Γ_T between these two intersections points of opposite intersection sign (Figure 31). This means we have a part of the dividing set that is parallel to $K_{(p,q)}$, indicating there is a bypass along $K_{(p,q)}$ which gives a destabilization of $K_{(p,q)}$.

Now suppose $K_{(p,q)}$ intersects Γ_T efficiently. Because $tb(K_{(p,q)}) \neq \overline{tb}(\mathcal{K}_{(p,q)})$, we know that slope$\Gamma_T \neq \frac{1}{w(\mathcal{K})}$ because otherwise the argument in step 1 using theorem 15 would indicate that $K_{(p,q)}$ has maximal tb. Since $\mathcal{K}$ satisfies the UTP, $N(\mathcal{K})$ can be thickened to a solid torus with boundary T' such that slope$(\Gamma_{T'}) = \frac{1}{w(\mathcal{K})}$. This thickening of $N(\mathcal{K})$ is done by attaching a bypass disk along the Legendrian rulings of T. Since the Legendrian rulings are Legendrian isotopic to
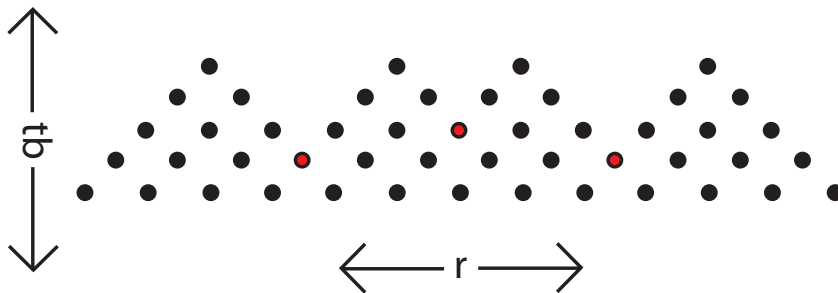
FIGURE 32. A "mountain range" representing the values of (r, tb) which are realized by Legendrian knots of a given knot type. A stabilization of a knot changes (r, tb) so that the dot moves diagonally down. The valleys (dots with red centers) are the first places where knots with distinct (r, tb) values stabilize in different ways to produce two knots with the same value of (r, tb). We need to check whether or not these knots are Legendrian isotopic to determine Legendrian simplicity.

$K_{(p,q)}$ (we assumed the Legendrian rulings have slope $\frac{q}{p}$), this bypass provides a destabilization of $K_{(p,q)}$.

Step 3: For each value of (r, tb), there is at most one Legendrian knot of type $\mathcal{K}_{(p,q)}$ up to Legendrian isotopy.

Steps 1 and 2 tell us that all Legendrian knots of type $\mathcal{K}_{(p,q)}$ are stabilizations of those with maximal tb, and the rotation numbers of these knots with maximal tb are multiples of q. Recall that stabilizations decrease tb by 1, and change the rotation number by ± 1. Therefore we simply need to check when two knots of maximal tb but different rotation numbers, have stabilizations which share the same values for tb and r.

Because of the distribution of the rotation numbers of the maximal tb Legendrian knots, this amounts to showing the following. If two Legendrian knots, $K_{(p,q)}, K'_{(p,q)}$ with maximal tb, have $r(K_{(p,q)}) - r(K'_{(p,q)}) = 2qn$ for some $n \in \mathbb{Z}$ then $S_-^{qn}(K_{(p,q)})$ is Legendrian isotopic to $S_+^{qn}(K'_{(p,q)})$.

These are all the "valleys" in a diagram like figure 32, which indicate with a dot, the (r, tb) coordinates that are realized by Legendrian knots of a given knot type. The valleys correspond to the places where stabilizations of distinct knots first meet. The peaks are given by the knots which do not destabilize.

The key point here is that if $K_{(p,q)}$ lies on a standard neighborhood of K then $S_-^q(K_{(p,q)})$ lies on a standard neighborhood of $S_-(K)$. Suppose $K_{(p,q)}$ and $K'_{(p,q)}$ lie on standard neighborhoods of K and K' respectively where K, K' have maximal tb. Then

$$qr(K) - qr(K') = r(K_{(p,q)}) - r(K_{(p,q)}) = 2qn$$

so

$$r(K) - r(K') = 2n$$

Also $S_-^{qn}(K_{(p,q)})$ lies on a standard neighborhood of $S_-^n(K)$ and $S_+^{qn}(K'_{(p,q)})$ lies on a standard neighborhood of $S_+^n(K')$. Since $K, K' \in \mathcal{K}$ which is Legendrian simple and $S_+^n(K)$ and $S_+(K')$ have the same tb and rotation number, $S_-^n(K)$ is Legendrian isotopic to $S_+(K')$. Then we can use the

method from the end of Step 1 to show that $K_{(p,q)}$ is Legendrian isotopic to $K'_{(p,q)}$. Thus completing the proof for sufficiently positive cables.

4.6. **Sufficiently Negative Cables.** The proof for cables where sufficiently negative has the same structure as the proof for sufficiently positive cables, but differs in details.

Step 1: Maximal tb Legendrian knots are determined by their rotation number, and the set of rotation numbers for Legendrian knots in $\mathcal{K}_{(p,q)}$ with maximal tb is

$$\{\pm(p + q(n + r(L)))|L \in \mathcal{K}, \ tb(L) = -n\}$$

where n is the integer such that

$$-n - 1 < \frac{p}{q} < -n$$

We want to use the formula for the rotation number of a cable in lemma 13. Let $N(\mathcal{K})$ be a neighborhood of $\mathcal{K}$ such that $K_{(p,q)} \subset \partial N(\mathcal{K})$ where $\partial N(\mathcal{K})$ is convex. We need to compute the rotation numbers of the boundary of a meridional disk D of $N(\mathcal{K})$ and the boundary of a Seifert surface Σ for a Legendrian curve of slope ∞ with respect to $\mathcal{C}_\mathcal{K}$ on $\partial N(\mathcal{K})$. Since slope ∞ is defined by the longitude of $N(\mathcal{K})$, Σ can be extended to a Seifert surface for the core of $N(\mathcal{K})$.

In order to simplify the computations for $r(\partial D)$ and $r(\partial \Sigma)$, we decompose D and Σ into components we understand well. The idea is to find a smaller solid torus N_1, inside $N(\mathcal{K})$ which has dividing curves of slope $\frac{1}{k}$ for some integer k. Then let $D = D' \cup A$ where D' is a meridional disk of N' whose boundary is Legendrian and intersects the dividing curves of N' efficiently. In this situation $r(\partial D') = 0$ via the argument given in Step 1 in the case of sufficiently positive cables. Similarly we choose a thicker solid torus N_2 containing $N(\mathcal{K})$ which has dividing curves on its convex boundary of slope $\frac{1}{\ell}$ for an integer ℓ. We decompose $\Sigma = \Sigma' \cup B$ where Σ' is a Seifert surface for a Legendrian curve on ∂N_2 of slope ∞ with respect to $\mathcal{C}_\mathcal{K}$ and such that $\partial \Sigma$ intersects the dividing curves of ∂N_2 efficiently. Then

$$r(\partial \Sigma) = r(\partial \Sigma') + \chi(B_+) - \chi(B_-) = r(\partial \Sigma') + \langle e(\xi), B \rangle$$

and

$$r(\partial D) = r(\partial D') + \langle e(\xi), A \rangle = \langle e(\xi), A \rangle$$

Therefore we need to know the relative half-Euler class $e(\xi)$ for $T^2 \times [1, 2]$ and understand its relation to A and B. To do this we choose N_1 and N_2 carefully. Identify $N_2 \setminus N_1$ with $T^2 \times I$ so $\partial N_i = T_i = T^2 \times \{i\}$. We want the slopes of the dividing curves on T_1 and T_2 to be $-\frac{1}{n}$ and $-\frac{1}{n+1}$ respectively, where

$$-n - 1 < \frac{p}{q} < -n$$

We choose these particular slopes so that $T^2 \times [1, 2]$ is a basic slice. Then Honda's classification [14] describes all the possible tight contact structures on $T^2 \times [1, 2]$. From this classification, we know that the Poincaré dual of the relative half-Euler class of this $T^2 \times [1, 2]$ is either $(-n, 1) - (-n-1, 1) = (1, 0)$ or its negation. This allows for two possible combinations of relative half-Euler classes on $T^2 \times [1, 1.5]$ and $T^2 \times [1.5, 2]$. The first is that

$$PD(e(\xi), T^2 \times [1, 1.5]) = (p, q) - (-n - 1, 1) \ \text{ and } \ PD(e(\xi), T^2 \times [1.5, 2]) = (-n, 1) - (p, q)$$

The second is that

$$PD(e(\xi), T^2 \times [1, 1.5]) = -(p, q) + (-n - 1, 1) \ \text{ and } \ PD(e(\xi), T^2 \times [1.5, 2]) = -(-n, 1) + (p, q)$$

B is an annulus in $T^2 \times [1.5, 2]$ with boundary going along the longitudes of $T^2 \times \{1.5, 2\}$ (which are parallel to the $(1, 0)$ in these coordinates) so $\langle e(\xi), B \rangle = \pm(p + n)$ and

$$r(\Sigma) = r(K) \pm (p + n)$$

where $K = \partial \Sigma'$ is a Legendrian knot of type $\mathcal{K}$ on $T^2 \times \{2\}$ which intersects the dividing curves on $T^2 \times \{2\}$ (which have slope $-\frac{1}{n}$) efficiently and thus has $tb(K) = -n$. Similarly A is an annulus in $T^2 \times [1, 1.5]$ with boundary going along the meridians of $T^2 \times \{1, 1.5\}$ (which are parallel to $(0,1)$), so $\langle e(\xi), A \rangle = \pm(1 - q)$ and

$$r(\partial D) = r(\partial D') \pm (1 - q) = \pm(1 - q)$$

This gives us either

$$r(K_{(p,q)}) = p(1 - q) + q(r(K) + p + n) = p + q(r(K) + n)$$

or

$$r(K_{(p,q)}) = -p(1 - q) + q(r(K) - p - n) = -p + q(r(K) - n)$$

Because the possible rotation numbers of a Legendrian knot with a specfied tb are symmetric around 0, for every value $r(K)$ there is another Legendrian knot $K' \in \mathcal{K}$ with $tb(K') = tb(K)$ and $r(K') = -r(K)$. Thus we can replace $r(K)$ in the second equation above with $-r(K)$. Then we get that the set of rotation numbers of $K_{p,q} \in \mathcal{K}_{(p,q)}$ with maximal tb is

$$\{\pm(p + q(r(K) + n)) : K \in \mathcal{K}, tb(K) = -n\}$$

Step 2: Knots with less than maximal tb destabilize.

Since $\frac{p}{q} < w(\mathcal{K})$, $\mathcal{K}_{(p,q)}$ satisfies the UTP by theorem 14. Therefore if $K_{(p,q)}$ has less than maximal tb, its standard neighborhood (for which the slope of the dividing curves on the boundary is $\frac{q}{p}$) can be thickened to a solid torus such that the slope of the dividing curves is $1/\overline{tb}(\mathcal{K}_{(p,q)})$. Thickening corresponds to a sequence of bypass disks which provide destabilizations for $K_{(p,q)}$.

Step 3: For pairs (tb, r) which can be obtained through stabilizations from multiple different maximal tb Legendrian knots, there is a unique Legendrian knot with that tb and r.

Using the distribution of rotation numbers for maximal tb cables given in step 1, we can find the first places where two sequences of stabilizations of two distinct Legendrian knots $K_{(p,q)}, K'_{(p,q)} \in \mathcal{K}_{(p,q)}$ result in Legendrian knots of the same (r, tb) pair. This happens when two maximal tb Legendrian knots of type $\mathcal{K}_{(p,q)}$ are next to each other, and they stabilize in opposite r directions to meet in a valley as in figure 32. This occurs in two situations.

Situation 1: We have two maximal tb Legendrian knots, $K_{(p,q)}$ and $K'_{(p,q)}$ with $r(K_{(p,q)}) = p + qn + qr(K)$ and $r(K'_{(p,q)}) = -p - qn + qr(K)$ for some $K \in \mathcal{K}$ with $tb(K) = -n$. Then

$$r(S_+^{-p-qn}(K_{(p,q)})) = r(S_-^{-p-qn}(K'_{(p,q)})) = qr(K)$$

and

$$tb(S_+^{-p-qn}(K_{(p,q)})) = tb(S_-^{-p-qn}(K'_{(p,q)})) = \overline{tb}(\mathcal{K}_{(p,q)}) + p + qn$$

(Note that $-p - qn > 0$ because $\frac{p}{q} < -n$.)

Suppose we have any Legendrian knot $L_{(p,q)} \in \mathcal{K}_{(p,q)}$ with the values $r(L_{(p,q)}) = qr(K)$ and $tb(L_{(p,q)}) = \overline{tb}(\mathcal{K}_{(p,q)}) + p + qn$. Then $L_{(p,q)}$ lies on the boundary of a standard neighborhood $N(K)$ of K where $tb(K) = -n$ as above, and $L_{(p,q)}$ is a Legendrian ruling curve of slope $\frac{q}{p}$ on $\partial N(K)$. It is also true that $S_-^{-p-qn}(K'_{(p,q)})$ and $S_+^{-p-qn}(K_{(p,q)})$ are Legendrian ruling curves of the same slope on $N(K)$. Therefore $L_{(p,q)}$ is Legendrian isotopic to $S_-^{-p-qn}(K'_{(p,q)})$ and $S_+^{-p-qn}(K_{(p,q)})$ through the Legendrian realization principle. This shows that any Legendrian knot with (r, tb) in a valley from this situation destabilizes in two ways.

Situation 2: We have two maximal tb Legendrian knots, $K_{(p,q)}$ and $K'_{(p,q)}$ with $r(K_{(p,q)}) = p + qn + qr(K)$ and $r(K'_{(p,q)}) = -p - qn + qr(K')$ for two Legendrian knots $K, K' \in \mathcal{K}$ with $tb(K) = tb(K') = -n$ such that there does not exist any other Legendrian knot $K'' \in \mathcal{K}$ with $tb(K'') = -n$ and $r(K) < r(K'') < r(K')$. Then

$$r(S_-^{p+qn+qm}(K_{(p,q)})) = r(S_+^{p+qn+kqm}(K'_{(p,q)})) = q(r(K) - m) = q(r(K') + m)$$

for some $m \in \mathbb{Z}^+$, and these knots have the same tb since they are $p+qn+qm$ stabilizations of maximal tb knots. Then for any Legendrian $L_{(p,q)} \in \mathcal{K}_{(p,q)}$ with these values $(r(L_{(p,q)}) = q(r(K) - m) = q(r(K') + m)$ and $tb(L_{(p,q)}) = \overline{tb}(\mathcal{K}_{(p,q)} - p - qn - qm)$. Then $L_{(p,q)}$ lies on the boundary of a standard neighborhood of $S_+^k(K) = S_-^k(K')$ as a Legendrian ruling curve of slope $\frac{q}{p}$. Then $L_{(p,q)}$ is Legendrian isotopic to $S_-^{p+qn+qm}(K_{(p,q)})$ and $S_+^{p+qn+qm}(K'_{(p,q)})$, so it destabilizes in two ways as desired.

5. Transversely Nonsimple Knots

5.1. **Transverse Simplicity.** We have so far been discussing knots which are Legendrian simple. It turns out that it is significantly more difficult to find knots which are transversely simple. A knot can be transversely simple without being Legendrian simple. However, we can understand transverse simplicity entirely through a classification of the Legendrian knots. To do this we must understand the following notion.

Definition 17. *A knot $\mathcal{K}$ is* stably simple *if for every pair of Legendrian knots, K, K' which have the same values for (r, tb), there exists some $n \geq 0$ such that $S_-^n(K) = S_-^n(K')$.*

One reason for using negative stabilizations only is because we obtain the following *stable invariant* of Legendrian knots,
$$s(K) = tb(K) - r(K)$$
Because this is invariant under positive stabilizations, we have the following equivalent definition of stably simple:

Definition 18. *A knot $\mathcal{K}$ is* stably simple *if and only if for any Legendrian knots, $K, K' \in \mathcal{K}$ such that $s(K) = s(K')$ there are positive integers n, m such that $S_+^n(K) = S_+^m(K')$.*

$s(K)$ is a particularly useful invariant because if $T_+(K)$ is the positive transverse pushoff of K then $sl(T_+(K)) = s(K)$. We can use this to understand transverse simplicity, due to the following theorem:

Theorem 16 (Etnyre, Honda [9])**.** *A knot is transversely simple if and only if it is stably simple.*

In the proof of this theorem we will use the following lemma, which can be proved in a similar manner to the Legendrian standard neighborhood theorem.

Lemma 14. *Every transverse knot has a neighborhood contactomorphic to*
$$N_\varepsilon = \{r, \theta, z) \in \mathbb{R}^2 \times S^1 : r < \varepsilon\}$$
where the contact structure on $\mathbb{R}^2 \times S^1$ is $ker(dz + r^2 d\theta)$.

Proof of theorem 16. Suppose $\mathcal{K}$ is stably simple. Let τ_1 and τ_2 be transverse knots of type $\mathcal{K}$ with $sl(\tau_1) = sl(\tau_2)$. There are standard transverse neighborhoods N_{ε_i} of τ_i as in lemma 14. For $m \in \mathbb{Z}_+$ sufficiently large, (we need $\frac{1}{\sqrt{m}} < \varepsilon_i$) define
$$T_m^i = \left\{(r, \theta, z) \in \mathbb{R}^2 \times S^1 : r = \frac{1}{\sqrt{m}}\right\} \subset N_{\varepsilon_i} \quad (i = 1, 2)$$
Since the tangent space to T_m^i at any point is $\{a\frac{\partial}{\partial\theta} + b\frac{\partial}{\partial z}\}$ and the contact structure on N_{ε_i} is $ker(dz + r^2 d\theta)$, the intersection of the tangent planes with the contact planes occurs when
$$dz\left(a\frac{\partial}{\partial\theta} + b\frac{\partial}{\partial z}\right) + \left(\frac{1}{\sqrt{m}}\right)^2 d\theta\left(a\frac{\partial}{\partial\theta} + b\frac{\partial}{\partial z}\right) = 0$$
$$b + \frac{1}{m}a = 0$$

So the the characteristic foliation is given by curves of slope $-\frac{1}{m}$ corresponding to the vector $m\frac{\partial}{\partial\theta} - \frac{\partial}{\partial z}$ on T_m^i. Now look at a leaf L_m^i of the characteristic foliation on T_m^i (any curve of slope $-\frac{1}{m}$). Note
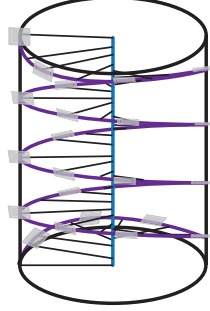
FIGURE 33. Annulus which shows that the core of N_ε is the positive transverse pushoff of the Legendrian curves L_m.

that a negative stabilization on L_m^i adds in a negative Dehn twist, so $S_-(L_m^i) = L_{m+1}^i$. This gives us two families, $\mathcal{F}_1 = \{L_m^1 : m \geq \frac{1}{\varepsilon_1^2}\}$ and $\mathcal{F}_2 = \{L_m^2 : m \geq \frac{1}{\varepsilon_2^2}\}$ of Legendrian knots where all knots in a given family are related by negative stabilization. Furthermore, we can find an annulus in N_{ε_i} with one boundary component along the core curve τ_i and the other boundary component along L_m^i such that the tangent planes to the annulus coincide with the contact planes along L_m^i (see figure 33), which shows that τ_i is the positive transverse pushoff of L_m^i for all m.

Since L_m^i and L_n^i are related by negative stabilizations, their stable invariants are equal, $s(L_m^i) = s(L_n^i)$ for all $n, m \geq \frac{1}{\varepsilon_i^2}$, for $i = 1$ or 2. Then since $\tau_1, \tau_2 \in \mathcal{K}$, we also have $L_m^i \in \mathcal{K}$ for $i = 1, 2$, $m \geq \frac{1}{\varepsilon_i^2}$. Furthermore $s(L_m^1) = sl(\tau_1) = sl(\tau_2) = s(L_n^2)$ for sufficiently large m, n. Because $\mathcal{K}$ is stably simple, this means that there exist m_1, m_2 such that $L_{m_1}^1$ is Legendrian isotopic to $L_{m_2}^2$. Since τ_1 is the positive transverse pushoff of $L_{m_1}^1$ and τ_2 is the positive transverse pushoff of $L_{m_2}^2$, this tells us that τ_1 is transversely isotopic to τ_2 since the positive transverse pushoff is well-defined.

Now we show the other direction. Suppose $\mathcal{K}$ is transversely simple, and let $K, K' \in \mathcal{K}$ be Legendrian knots where $s(K) = s(K')$. Take the annulus $A = S^1 \times [-\varepsilon, \varepsilon]$ where $S^1 \times \{0\} = K$ whose tangent planes along K coincide with the contact planes. The positive transverse pushoff of K is the curve $T_+(K) = S^1 \times \{\frac{\varepsilon}{2}\}$. Now thicken A to get a neighborhood N of $T_+(K)$ such that copies of K are Legendrian divides on ∂N. By recoordinatizing we may assume $T_+(K)$ is the core of N and K has slope $-\frac{1}{n}$ on ∂N.

We can do the same for K' to get a neighborhood N' of $T_+(K')$. Because $s(K) = s(K')$, $sl(T_+(K)) = sl(T_+(K'))$. Since $\mathcal{K}$ is transversely simple $T_+(K)$ is transversely isotopic to $T_+(K')$. Therefore via a contactomorphism we may assume that the core curves of N and N' are the same. Furthermore there is a standard transverse neighborhood N_ε inside N and N' as in lemma 14. As before we have tori T_m inside N_ε whose characteristic foliations are composed of Legendrian curves L_m of slope $-\frac{1}{m}$.

We will show that K can be negatively stabilized to obtain L_m for some m. The same will hold for K' and thus we will have shown that $\mathcal{K}$ is stably simple. We may isotope T_m such that it is a convex surface with L_m as a Legendrian divide, and ruling curves of slope $-\frac{1}{n}$ which is the slope of K on ∂N. Then take an annulus in $N \setminus N_\varepsilon$ with one boundary component being K on ∂N and the other being a Legendrian ruling curve on T_m. Since K is a Legendrian divide, the dividing curves of the annulus do not intersect K, so any dividing curves on the annulus are boundary parallel to L_m. This shows that through a sequence of destabilizations we can get from L_m to K. We need to know these are all negative stabilizations. If some were positive stabilizations then the value of $s(K)$ would differ from $s(L_m)$. However both K and L_m share the same positive transverse pushoff, so they must have the same value for their stable invariants. This shows that L_m is a negative stabilization of K. Repeating for K' completes the proof.

5.2. **Finding neighborhoods that do not thicken.**

While cables of Legendrian simple knots that do satisfy the UTP are Legendrian simple and thus are transversely simple, cables of Legendrian simple knots that do not satisfy the UTP need not be. We will prove that in fact, the $(2,3)$ torus knot does not satisfy the UTP and none of its positive cables are transversely simple. The idea of the proof is to find numerous solid tori representing $\mathcal{K}$ which do not thicken. This shows that $\mathcal{K}$ does not satisfy the UTP. We use these tori to find cables which do not have maximal tb but do not destabilize. It turns out that a stabilization of the maximal tb representatives of that cable provides a knot of the same type and values of (r, tb) as the knot which does not destabilize. This will show that such cables are not Legendrian simple. We then make a further argument to show that the knot is not stably simple. By theorem 16, this will show that the cable is not transversely simple. While it seems likely that this argument extends to cables of a general (p,q) torus knot where $p, q > 0$, extending the proof to this more general setting would require a better understanding of certain properties of the twisting of the contact structures on S^1 bundles over a general genus g surface than what is so far known. While there is a classification of tight contact structures on S^1-bundles, it does not describe the maximal twisting of the fibers, as in the classification on T^3. We will work in the general setting for the first part of this proof and will discuss exactly what is needed to extend the rest of the argument to the general case.

5.2.1. *Necessary condition on maximally thickened neighborhoods.* Let $\mathcal{K}$ be the (p,q) torus knot. First we will look at how a solid neighborhood N of $K \in \mathcal{K}$ sits in relation to standard neighborhoods N_1 and N_2 in $S^3 \setminus N$ of Legendrian knots $U_1 \in \mathcal{U}_1$ and $U_2 \in \mathcal{U}_2$ respectively. Recall that $\mathcal{U}_1$ and $\mathcal{U}_2$ are the core curves of unknotted solid tori which provide a Heegaard splitting of S^3. Suppose

$$tb(U_1) = -m_1 \text{ and } tb(U_2) = -m_2$$

We know $\overline{tb}(\mathcal{U}) = -1$ so m_1 and m_2 will always be positive integers. Because N_1 and N_2 are standard neighborhoods of U_1 and U_2, slope$(\Gamma_{\partial N_1} = -\frac{1}{m_1}$ and slope$(\Gamma_{\partial N_2}) = -m_2$ with respect to the coordinate system $\mathcal{C}_{\mathcal{U}_1}$.

We will switch to the coordinates $\mathcal{C}^{(p,q)}$ on ∂N_1 and ∂N_2 to make it more convenient to compare slopes on ∂N_1 and ∂N_2 with the (p,q) torus knot. We can find the slopes of the dividing curves on

∂N_i in these coordinates using the transformations in equations 6 and 7.

$$\begin{bmatrix} q & -p \\ -y & x \end{bmatrix} \begin{bmatrix} -m_1 \\ 1 \end{bmatrix} = \begin{bmatrix} -qm_1 - p \\ ym_1 + x \end{bmatrix}$$

$$\begin{bmatrix} -p & q \\ x & -y \end{bmatrix} \begin{bmatrix} -m_2 \\ 1 \end{bmatrix} = \begin{bmatrix} pm_2 + q \\ -xm_2 - y \end{bmatrix}$$

So

(8)
$$\text{slope}(\Gamma_{\partial N_1}) = -\frac{ym_1 + x}{qm_1 + p}$$

and

(9)
$$\text{slope}(\Gamma_{\partial N_2}) = -\frac{xm_2 + y}{pm_2 + q}$$

In this coordinate system $S^3 \setminus (N_1 \cup N_2) \cong T^2 \times [1, 2]$ where $T_1 = \partial N_1$ and $T_2 = \partial N_2$. We will think of K as sitting on $T_{1.5}$. K has slope ∞ on $T_{1.5}$ under the coordinates $\mathcal{C}^{(p,q)}$. The neighborhood N of K (a (p,q) torus knot) has coordinates on its boundary given by $\mathcal{C}_{\mathcal{U}}^{(p,q)}$. In this situation, the lines of slope ∞ on ∂N are parallel to the lines of slope ∞ on T.

Now choose an annulus A' whose interior is in $S^3 \setminus (N \cup N_1 \cup N_2)$ where $\partial A' = \gamma_1 \cup \gamma_2$ where γ_i is a curve of slope ∞ on ∂N_i. Let $A' \times [-\varepsilon', \varepsilon']$ be a $[-\varepsilon', \varepsilon']$ invariant neighborhood of $A' = A' \times \{0\}$. Then $\partial(N_1 \cup A' \times [-\varepsilon', \varepsilon'] \cup N_2)$ is isotopic to ∂N. See figure 34.
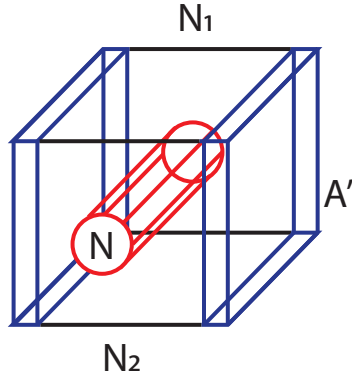
FIGURE 34. The front and back sides are identified and the left and right sides are identified. The square on the top face is ∂N_1 and N_1 lies above the top face. Similarly the bottom face is ∂N_2 where N_2 lies below. N (red) lies in between and runs parallel to the curves of slope ∞ on ∂N_1 and ∂N_2 with respect to the coordinates $\mathcal{C}^{(p,q)}$. A' is the annulus on the left (identified with the right) side of the box. $A' \times [-\varepsilon', \varepsilon']$ is highlighted in blue. Note that $\partial(N_1 \cup N_2 \cup A' \times [-\varepsilon', \varepsilon'])$ is isotopic to ∂N.

If we chose an N that cannot be thickened any further, and we thicken N_1 and N_2 as much as possible in the complement of N, then the space between N and $N_1 \cup N_2 \cup A' \times [-\varepsilon', \varepsilon']$ will simply

be an I-invariant neighborhood of ∂N (i.e. N essentially is $S^3 \setminus (N_1 \cup N_2 \cup A' \times [-\varepsilon', \varepsilon'])$. Thus we can determine the dividing sets for N that do not thicken by determining the dividing set of $\partial(N_1 \cup N_2 \cup A' \times [-\varepsilon, \varepsilon])$ when N_1 and N_2 are maximally thickened in the complement of N. We will determine conditions on the dividing sets of N_2, N_2, and A'.

If any of the dividing curves on A' are boundary parallel, they would provide a bypass along N_1 or N_2. Suppose we have thickened N_1 and N_2 as much as possible in the complement of N (or equivalently chosen U_1 and U_2 to have the maximal possible tb in the complement of N). Then we may assume that A' has no boundary parallel curves so the number of intersections of the dividing curves with each boundary component is the same.

Lemma 1 shows that when two convex surfaces S_1 and S_2 intersect at a curve γ, the points in $\Gamma_{S_1} \cap \gamma$ alternate with the points in $\Gamma_{S_2} \cap \gamma$ and thus $|\Gamma_{S_1} \cap \gamma| = |\Gamma_{S_2} \cap \gamma|$ (where $|\cdot|$ indicates number of points in the intersection). Let α be the number of times the dividing curves on A' intersect each boundary component. Then the dividing curves on ∂N_i intersect $A' \cap \partial N_i$ α times for $i = 1, 2$.

On the other hand we know that $\partial N_i \cap A'$ is a curve of slope ∞ on ∂N_i ($i = 1, 2$). Since we have computed the slopes of the dividing curves on ∂N_i, we can compute how many times each of the two dividing curves on ∂N_i intersects $A' \cap \partial N_i$ by taking the denominator of slope($\Gamma_{\partial N_i}$) (this gives the dot product of the vector representing slope ∞ with the vector representing slope($\Gamma_{\partial N_i}$)). Therefore $\alpha = 2(qm_1 + p)$ and $\alpha = 2(pm_2 + q)$. This tells us that when we take maximally destabilized U_1 and U_2, $qm_1 + p = pm_2 + q$. We can find all solutions to this equation by setting

(10)
$$m_1 = 1 + pk \quad \text{and} \quad m_2 = 1 + qk$$

and taking all $k \in \mathbb{Z}$, $k \geq 0$. Then

(11)
$$\alpha = 2(q(1 + pk) + p) = 2qpk + 2q + 2p$$

Now we want to determine the possible slopes of a maximally thickened ∂N or equivalently the slope of $\partial(N_1 \cup N_2 \cup (A' \times [-\varepsilon, \varepsilon]))$. We do not know the slope on the dividing curves on $A' \times \{-\varepsilon\}$ or $A' \times \{\varepsilon\}$ but we know that they have the same slope. Because the orientation on $A' \times \{-\varepsilon\}$ will be opposite the orientation on $A' \times \{\varepsilon\}$ when they are considered as parts of a torus as in figures 34 and 35, the two slopes will cancel each other out. Thus, we can assume that the dividing curves of A' are simply $\alpha = 2qpk + 2q + 2p$ vertical lines. The orientation of ∂N_1 is the opposite of the orientation inherited on the section of ∂N_1 as part of $\partial(N_1 \cup N_2 \cup (A' \times [-\varepsilon, \varepsilon]))$. Therefore the slope of the dividing curves on $\partial(N_1 \cup N_2 \cup A' \times [-\varepsilon', \varepsilon'])$ is given by the equation:

$$-\text{slope}(\Gamma_{\partial N_1}) + \text{slope}(\Gamma_{\partial N_2}) + \frac{2}{\alpha}$$

where $\frac{2}{\alpha}$ is a correction term which comes from smoothing the edges (see figure 35).
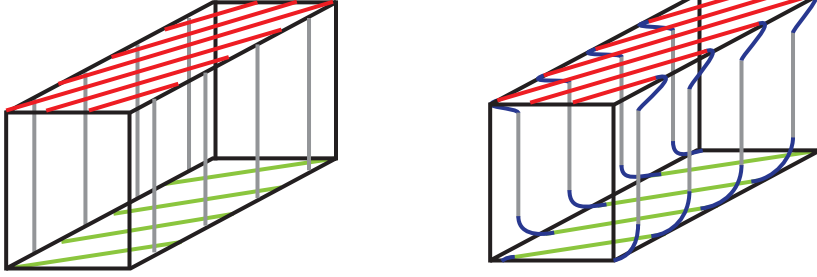
FIGURE 35. The dividing curves on $\partial(N_1 \cup N_2 \cup (A' \times [-\varepsilon, \varepsilon]))$ or equivalently on ∂N. The edges are smoothed on the right.

Plugging in the values we computed for the slopes of ∂N_1 and ∂N_2 (equations 8, 9), the values for m_1, m_2, and α (equations 10, 11), and using the fact that $xq - yp = 1$, we get

$$
\begin{aligned}
\text{slope}(\Gamma_{\partial N}) &= \text{slope}(\Gamma_{\partial(N_1 \cup N_2 \cup (A' \times [-\varepsilon, \varepsilon]))}) \\
&= -\text{slope}(\Gamma_{\partial N_1}) + \text{slope}(\Gamma_{\partial N_2}) + \frac{2}{\alpha} \\
&= \frac{ym_1 + x}{qm_1 + p} - \frac{xm_2 + y}{pm_2 + q} + \frac{2}{2pqk + 2q + 2p} \\
&= \frac{y(1 + pk) + x - x(1 + qk) + y + 1}{pqk + p + q} \\
&= \frac{k(yp - xq) + 1}{pqk + p + q} \\
&= \frac{-k - 1}{pqk + p + q}
\end{aligned}
$$

where $k \in \mathbb{Z}$, $k \geq 0$. Note that if we view this as a slope for N, the coordinate system we are using is actually $\mathcal{C}_{\mathcal{U}}^{(p,q)}$ because slope ∞ is given by lines parallel to the standard (p,q) cable of the unknot on the standard torus (since we were using coordinates $\mathcal{C}^{(p,q)}$ on ∂N_1 and ∂N_2), and slope 0 is given by a meridian. See figure 36.

This shows that if N is a neighborhood of $\mathcal{K}$, the $(2,3)$ torus knot, which does not thicken, then its dividing curves have slope $-\frac{k+1}{pqk+p+q}$ for some $k \in \mathbb{Z}$, $k \geq 0$.

5.2.2. *Existence of candidate neighborhoods in* (S^3, ξ_{std}). Now we must check whether all values of k give slopes of dividing curves on N which can be realized in (S^3, ξ_{std}). Note that $k = 0$ gives slope $-\frac{1}{p+q}$ which is the slope of the standard neighborhood of the maximal tb (p,q) torus knot, so at least for $k = 0$, the neighborhood is realized and does not thicken.
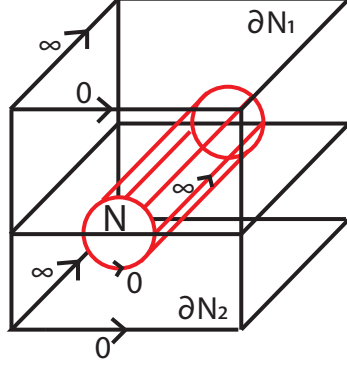
FIGURE 36. Coordinates $\mathcal{C}^{(p,q)}$ on ∂N_1 and ∂N_2. Coordinates $\mathcal{C}_{\mathcal{U}}^{(p,q)}$ on ∂N.

Let N_k be a solid torus representing $\mathcal{K}$ with dividing curves of slope $-\frac{k+1}{pqk+p+q}$ in coordinates $\mathcal{C}_{\mathcal{U}}^{(p,q)}$. Changing to coordinates $\mathcal{C}_{\mathcal{K}}$,

$$\begin{bmatrix} 1 & pq \\ 0 & 1 \end{bmatrix} \begin{bmatrix} -pqk - p - q \\ k + 1 \end{bmatrix} = \begin{bmatrix} -p - q + pq \\ k + 1 \end{bmatrix}$$

the slope of the dividing curves on N_k is

$$\frac{k+1}{pq - p - q}$$

To determine whether we actually find a tight contact structure on N_k with this dividing set, such that N_k glues to its complement in S^3 to give the unique tight contact structure on S^3, we need to classify the possible tight contact structures on N_k. The classification of tight contact structures on solid tori is given by the following theorem:

Theorem 17 (Honda [14]). *Suppose $S^1 \times D^2$ has convex boundary T^2, where $\#\Gamma_{T^2} = 2$.*
(a) Suppose $slope(\Gamma_{T^2}) = -\frac{m}{n}$, $m > n > 0$, $(m, n) = 1$. Suppose

$$-\frac{m}{n} = r_0 - \cfrac{1}{r_1 - \cfrac{1}{r_2 - \cdots - \frac{1}{r_k}}}$$

where $r_i < -1$ for $0 \leq i \leq k$. Then there are exactly $|(r_0 + 1)(r_1 + 1) \cdots (r_{k-1} + 1)(r_k)|$ tight contact structures on $S^1 \times D^2$ with the given boundary condition (up to isotopy relative the boundary). Of these tight contact structures, exactly 2 of them are universally tight.

(b) If $slope(\Gamma_{T^2}) = -1$ then there is a unique tight contact structure on $S^1 \times D^2$ which is contactomorphic to a standard neighborhood of a Legendrian core curve of $S^1 \times D^2$ of twisting number -1. This tight contact structure is universally tight.

(c) If $slope(\Gamma_{T^2}) = \frac{k}{\ell}$ where $\frac{k}{\ell} > -1$ then apply a change of coordinates corresponding to Dehn

twists through multiplication by

$$C = \begin{bmatrix} 1 & m \\ 0 & 1 \end{bmatrix} \in SL(2, \mathbb{Z})$$

where $m \in \mathbb{Z}$ is chosen so that $C \begin{bmatrix} \ell \\ k \end{bmatrix} = \begin{bmatrix} -n \\ m \end{bmatrix}$ such that $-\frac{m}{n} \le -1$. Then apply case (a).

In the case where $\mathcal{K}$ is the $(2,3)$ torus knot, we have a particularly simple situation. In this case the slope of the dividing curves on N_k with respect to $\mathcal{C}_{\mathcal{K}}$ is $k+1$. We apply a transformation of Dehn twists so that we can use theorem 17. In the case $k > 0$ we are in case 1 (above) so we get

$$\begin{bmatrix} 1 & -1 \\ 0 & 1 \end{bmatrix} \begin{bmatrix} 1 \\ k+1 \end{bmatrix} = \begin{bmatrix} -k \\ k+1 \end{bmatrix}$$

we get a slope of

$$-\frac{k}{k+1}$$

These slopes have a simple continued fraction of the form

$$\frac{k+1}{pq - p - q - k - 1} = -\frac{k+1}{k} = -2 - \cfrac{1}{-2 - \cfrac{1}{-2 - \cdots \frac{1}{-2}}}$$

where the number of -2's is equal to k. In the notation of theorem 17 we get $(r_0, r_1, \cdots, r_{k-1}) = (-2, -2, \cdots, -2)$ so the number of tight contact structures on N_k is

$$|(r_0 + 1)(r_1 + 1) \cdots (r_{k-2} + 1)(r_{k-1})| = |(-1)(-1) \cdots (-1)(-2)| = 2$$

When $k = 0$ we are in case 3 so we get

$$\begin{bmatrix} 1 & -2 \\ 0 & 1 \end{bmatrix} \begin{bmatrix} 1 \\ 1 \end{bmatrix} = \begin{bmatrix} -1 \\ 1 \end{bmatrix}$$

so the slope is -1 which is the special case of theorem 17 which says there is a unique tight contact structure on N_0.

The idea behind the classification of solid tori, is that $S^1 \times D^2$ can be decomposed into $S^1 \times D^2 = N \cup T^2 \times I$. N is a standard neighborhood of a core Legendrian curve of $S^1 \times D^2$ with twisting number -1. $T^2 \times I$ is given by $(S^1 \times D^2) \setminus N$ so its two boundary components match up with ∂N and $\partial(S^2 \times D^2)$. There are exactly two dividing curves on $\partial(S^1 \times D^2)$ and they have slope $-\frac{m}{n}$, and two dividing curves on ∂N of slope -1. Since the tight contact structure on a standard neighborhood is unique, the number of tight contact structures on $S^1 \times D^2$ is the same as the number of tight contact structures on $T^2 \times I$ (note this also relies on a gluing theorem that allows us to glue any $T^2 \times I$ with a tight contact structure to a standard neighborhood providing the slopes of the dividing curves on the boundaries match up). In the case of the $(2,3)$ torus knot, there are exactly two tight contact structures on $T^2 \times I$ with boundary slopes -1 and $-\frac{k}{k+1}$ which are distinguished by the sign of the Poincaré dual of the Euler class.

We now show each of these tight contact structures exists in (S^3, ξ_{std}). Let N_k have one of its two universally tight contact structures, and let $R = N_k \cup A \times [-\varepsilon, \varepsilon]$, where A is an annulus from N_k to

itself, $A \times [-\varepsilon, \varepsilon]$ is its $[-\varepsilon, \varepsilon]$ invariant neighborhood, and ∂R has two parallel components, T_1 and T_2 each of which is an unknotted torus. Note that A meets A' transversely, along a curve which is parallel to ∂A and to $\partial A'$. Because A' has no boundary parallel curves, we can find a contact isotopy of $A \times [-\varepsilon, \varepsilon]$ that contains $A' \times [-\varepsilon', \varepsilon']$. We know from section 5.2.1, that this means that the complement of $R = N_k \cup A \times [-\varepsilon, \varepsilon]$ is two standard neighborhoods of unknots, and the boundary of R has dividing curves which match the dividing curves on these standard neighborhoods. The contact structure on R is obtained by extending the chosen tight contact structure on N_k. The closed curves which run parallel to the core curve of A' provide an S^1 fibration of R. For all universally tight contact structures on N_k, the contact planes are transverse to these fibers. If we choose a contact structure for R such that A has no boundary parallel curves then the contact planes throughout R will be transverse to the fibers. Such a contact manifold which has S^1 fibers everywhere transverse to the contact planes is called a *horizontal* contact structure. This is useful because of the following lemma:

Lemma 15 (Honda [15]). *Let ξ be a contact structure that is everywhere transverse to the fibers of a circle bundle M over a closed oriented surface Σ with $g(\Sigma) \geq 1$. Then ξ is (weakly) symplectically fillable and universally tight.*

Therefore the contact structure on R is tight. Then we can glue a standard neighborhood N_1 of $U_1 \in \mathcal{U}_1$, $tb(U_1) = -n_1$ to R to get a solid torus with a tight contact structure, because of the correspondence between the classification of tight contact structures on solid tori with the those on $T^2 \times I$. Then $R \cup N_1$ is a neighborhood of the unknot. Note that S^3 decomposes into two standard neighborhoods of unknots with $tb = -1$. By thinning one of these neighborhoods and looking at the complement in S^3 we find that any standard neighborhood of an unknot thickens to a solid torus such that the slope of the dividing curves on the boundary is $-n_2$ for any $n_2 \in \mathbb{Z}_+$. Therefore we can thicken $R \cup N_1$ in S^3 to such a solid torus which will glue to a standard neighborhood of $U_2 \in \mathcal{U}_2$ where $tb(U_2) = -n_2$ to give the standard contact structure on S^3.

5.2.3. *The complement of N_k.* The S^1 bundle on R described above, extends to a Seifert fibration of S^3 in the following way. S^3 can be decomposed into two solid tori, each of which can be foliated by tori together with the core curve at the center of each solid torus. On one of these tori we have K, a (p, q) torus knot. By taking curves parallel to K, we can foliate this torus by (p, q) torus knots. We can repeat this foliation continuously in each of the other tori in the foliation of $S^3 \setminus \{$core curves$\}$. The fibers in the Seifert fibration are these closed curves together with the two core curves. Since K is one of these fibers, $S^3 \setminus N_k \cong S^3 \setminus K$ is a Seifert fibered space. The base space of this fibration is a punctured S^2 with two orbifold points, of degrees p and q. One can see this by thinking of $S^3 \setminus \{$core curves$\}$ as $T^2 \times (0, 1)$. In each $T^2 \times \{t\}$, there is an S^1 worth of fibers, this gives us an open cylinder worth of fibers. The puncture corresponds to K. The two core curves are the two remaining fibers. These are the two orbifold points which attach to the two boundary components of the open cylinder in the base space. The degree of these orbifold points, comes from the degree of the covering of the core curve by the generic Seifert fibers as they collapse towards the core curve. See figure 37.
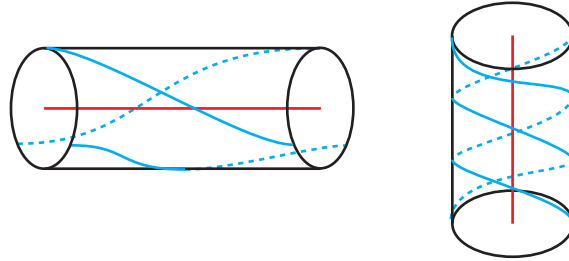
FIGURE 37. The two solid tori which decompose S^3, fibered by $(2,3)$ torus knots, which collapse towards the core curve creating orbifold points in the base space of degrees 2 and 3. (Identify ends of the cylinders to get tori.)

We use some basic results about 2-dimensional orbifolds to get a manifold which is a pq cover of the punctured sphere with orbifold points of order p and q. For a detailed introduction to orbifolds and Seifert fibered spaces, see [26]. In fact we will find a cover for S^2 with three orbifold points of degrees p, q, pq. The orbifold-Euler characteristic of this orbifold is

$$\chi(S^2) - \left(1 - \frac{1}{p}\right) - \left(1 - \frac{1}{q}\right) - \left(1 - \frac{1}{pq}\right) = \frac{-pq + q + p + 1}{pq}$$

There is a manifold which is a pq-fold cover of this orbifold which necessarily has Euler characteristic $-pq + q + p + 1$. We will show this explicitly in the case of $(p,q) = (2,3)$. In this case the cover has Euler characteristic 0 and is thus a torus. In general the cover will be a genus $g = (2 + pq - q - p - 1)/2$ surface, which will be greater than 1 in cases other than $(p,q) = (2,3)$.

Let X be S^2 with three orbifold points of degrees $2, 3, 6$. We obtain the covering map $f' : T^2 \to X$ as the composition of two maps. The first is $g : T^2 \to X'$ where X' is the sphere with four orbifold points, each of degree 2. g is the quotient map which quotients by the relation $x \sim Ax$ where $A = \begin{bmatrix} -1 & 0 \\ 0 & -1 \end{bmatrix}$ (here we identify T^2 with $\mathbb{R}^2/\mathbb{Z}^2$). $Ax = x$ if and only if $(-a, -b) \cong (a, b)$ (mod 1) if and only if $2a = 2b = 0$ which happens if and only if a and b are 0 or $\frac{1}{2}$. Therefore $A : T^2 \to T^2$ has four fixed points, and every other point has order 2. Therefore q is a two-fold covering map, where the four fixed points of A map onto the orbifold points of order 2. We see that the image of q is a sphere with 4 orbifold points in figure 38.

Then we take another map $h : X' \to X$, which takes X' (S^2 with 4 orbifold points of order 2). Start with X' so that one of the orbifold points is at the north pole, and the other three are evenly spaced around the equator. Let $B : S^2 \to S^2$ rotate the sphere by $2\pi/3$ around the north-south axis. h is the quotient map by the relation $x \sim Bx$. Note that r has 2 fixed points, the north and south pole. Therefore h is a 3-fold covering map where these fixed points become orbifold points. Since the north pole was already an orbifold point of degree 2 it becomes an orbifold point of degree 6. The south pole becomes an orbifold point of degree 3. The other 3 orbifold points of X' are identified into one orbifold point of degree 2. See figure 39.
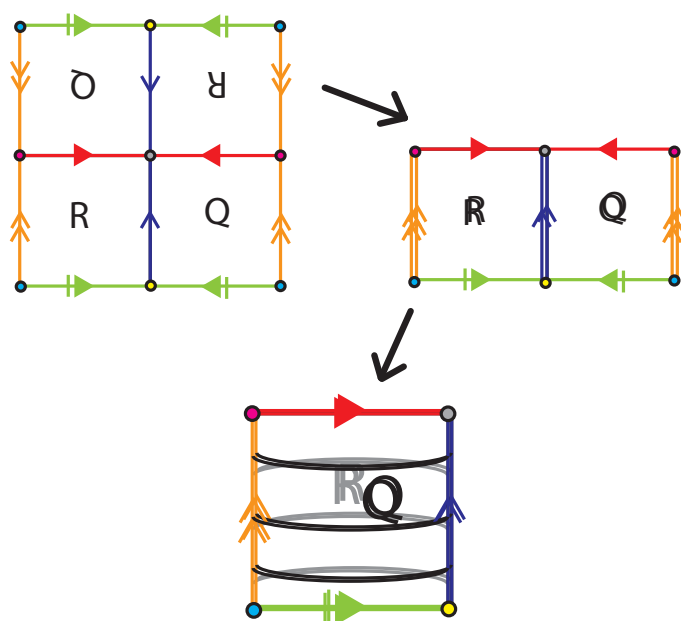
FIGURE 38. Quotienting $T^2 = \mathbb{R}^2/\mathbb{Z}^2$ by $A = -I$. In the first picture the identifications are indicated by identical symbols and colors. The fixed points are marked by dots. In the second picture, some of the identifications have been made. The points which have been covered by two points of T^2 are so indicated by double lines and symbols. The final picture completes the identifications by gluing the edges of the rectangle of the second picture. This results in a pillow shape where the four points which have only been covered once are at the corners and every other point has been covered exactly twice. This is the 2-sphere with 4 orbifold points of order 2.
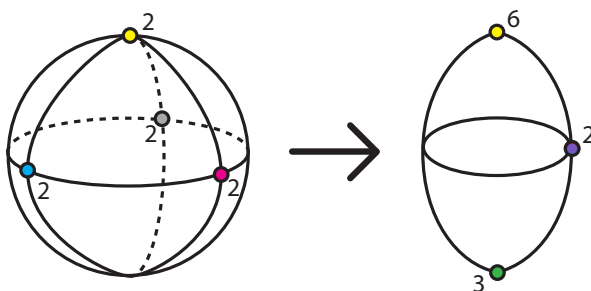
FIGURE 39. Quotienting S^2 with four orbifold points of degree 2, to S^2 with three orbifold points of degrees $2, 3, 6$.

Therefore $f' = h \circ g$ is a 6-fold covering map from T^2 to X. The orbifold point of degree 6 in X which has a single point in its preimage under f, therefore we may remove this point and its preimage to get a 6-fold covering map $f : T^2 \setminus \{*\} \to Y$ where Y is the punctured sphere with two orbifold points of degrees 2 and 3. Recall that $S^3 \setminus N_k$ is a Seifert fibered space over Y. Therefore f induces a 6-fold covering map $F : (T^2 \setminus \{*\}) \times S^1 \to S^3 \setminus N_k$ sending S^1 fibers of $(T^2 \setminus \{*\}) \times S^1$ injectively onto S^1 fibers.

Now we want to find a contact structure on $(T^2 \setminus \{*\}) \times S^1$ which is the pullback of the contact structure on $S^3 \setminus N_k$ (the restriction of the standard contact structure on S^3). The tight contact structures on T^3 were completely classified by Kanda in [16]. The restriction of the tight contact structures on T^3 give tight contact structures on $(T^2 \setminus \{*\}) \times S^1$. Kanda's classification states:

Theorem 18 (Kanda [16])**.** *Every tight contact structure on T^3 is contactomorphic to*

$$\xi_n = \ker(\cos(2\pi nt)dx + \sin(2\pi nt)dy)$$

for some $n \in \mathbb{Z}_+$ where (x,y) are coordinates on $T^2 = \mathbb{R}^2/\mathbb{Z}^2$ and t is a coordinate on S^1 so (t,x,y) are coordinates on $S^1 \times T^2 = T^3$.

Furthermore, the maximal twisting with respect to the fibration of any S^1 which is smoothly isotopic to a fiber in (T^3, ξ_n), is $-n$, and so (T^3, ξ_n) is contactomorphic to (T^3, ξ_m) if and only if $n = m$.

Notice that the S^1 fibers in the t direction in (T^3, ξ_n) have twisting $-n$ with respect to the fibration over T^2.

We know that the twisting of the fibers on the boundary of $S^3 \setminus N_k$ is $-(6k+5)$ with respect to ∂N_k, or equivalently with respect to the Seifert fibration. I claim that the pullback of $(S^3 \setminus N_k, \xi_{std})$ under F is $((T^2 \setminus \{*\}) \times S^1, \xi_{6k+5})$ (where ξ_n and ξ_{std} are understood to be restrictions of the tight contact structures on T^3 and S^3 respectively). Suppose ξ' is the contact structure on $(T^2 \setminus \{*\}) \times S^1$ which is the image under F of $(S^3 \setminus N_k, \xi_{std})$. We know that the fibers in $A \times [-\varepsilon, \varepsilon] \subset S^3 \setminus N_k$ have twisting $-(6k+5)$ with respect to the Seifert fibration, therefore ξ' agrees with ξ_{6k+5} on the preimage of $A \times [-\varepsilon, \varepsilon]$. Note that ξ' also agrees (up to isotopy) with ξ_{6k+5} on the preimage of a neighborhood of ∂N_k for the same reason, since the fibers in ∂N_k have twisting $-(6k+5)$ and contact structures are determined in a neighborhood of a surface by the characteristic foliation of the surface. Putting together these preimages we see that we have removed a neighborhood of the puncture $\times S^1$. Then we simply need to know that ξ' agrees with ξ_{6k+5} on the remainder. Here we utilize Kanda's classification results 18. This implies that we have a 6-fold covering map of contact manifolds:

$$F : ((T^2 \setminus \{*\}) \times S^1, \xi_{6k+5}) \to (S^3 \setminus N_k, \xi_{std})$$

This covering map will be important in showing that we cannot thicken N_k, because the contact structures on $(T^2 \setminus \{*\}) \times S^1$ are well-understood. When (p,q) are not $(2,3)$, the situation becomes more complicated because the corresponding covering map would be from $(\Sigma_g \setminus \{*\}) \times S^1$ where Σ_g is the orientable genus g surface. The classification of tight contact structures on such manifolds is more complicated. We will complete the argument below in the case of $(p,q) = (2,3)$, and note what would be required to generalize.

5.2.4. *Proving N_k does not thicken.* First note that it suffices to show that N_k does not thicken to $N_{k'}$ for $k' < k$. Because the slope of the dividing curves on N_k is $-\frac{k+1}{6k+5}$, all thickenings will be to slopes which are strictly more negative. This means that if N_k thickens to $N_{k'}$, then $k' < k$ (otherwise we would simply be thinning). If N_k thickens to some other solid torus which does not have a slope of the form $-\frac{k'+1}{6k'+5}$ then that torus will further thicken to a solid torus which does have the form of an $N_{k'}$.

Now suppose N_k thickens to $N_{k'}$, $k' < k$. Then a ruling curve γ of slope ∞ (with respect to $\mathcal{C}_{\mathcal{U}_1}^{(p,q)}$, on $N_{k'}$ has twisting number $-(6k'+5) > -(6k+5)$. Note that since $N_{k'}$ is assumed to be a thickening of N_k, γ is in $S^3 \setminus N_k$. Recall the 6-fold covering map $F : (T^2 \setminus \{*\}) \times S^1 \to S^3 \setminus N_k$. Since γ is a fiber in $S^3 \setminus N_k$, $F^{-1}(\gamma) = \{x\} \times S^1 \in (T^2 \setminus \{*\}) \times S^1$. Because F preserves the twisting of the fibers, this implies that $F^{-1}(\gamma)$ is a fiber in $((T^2 \setminus \{*\}) \times S^1, \xi_{6k+5})$ of twisting $-(6k'+5) > -(6k+5)$. However Kanda's theorem (18) implies that the maximal twisting of an S^1 in (T^3, ξ_{6k+5}) is $-(6k+5)$, so this is a contradiction. This completes the proof that N_k does not thicken.

5.3. **Transverse knots not distinguished by classical invariants.** We have an example of a knot which we know does not satisfy the UTP. Furthermore we have classified the neighborhoods of this knot which do not thicken. Now we want to use these neighborhoods to find Legendrian knots which share the same classical invariants, but there is no number of positive stabilizations one can apply to make these knots Legendrian isotopic. Then we will have a knot type which is not stably simple and is thus not transversely simple.

5.3.1. *Identifying potential cables.* The fact that we have neighborhoods of $\mathcal{K}$, the $(2,3)$ torus knot, which do not thicken, tells us that we should be able to find a knot that lies on the boundary of such neighborhoods which does not destabilize. This correspondence comes from the fact that both thickening of solid tori and destabilization of knots result from finding a bypass along the boundary of the solid torus. To ensure that the cable we choose will not destabilize, we need to choose a cable which intersects the dividing curves on ∂N_k fewer times than it intersects the boundary curves on any parallel torus inside N_k. The range of slopes of dividing curves on parallel tori inside N_k is $[-\frac{k+1}{6k+5}, 0)$. If the slope of our curve is $-\frac{a}{b}$ then we want

$$\left| \det \begin{bmatrix} -k+1 & -a \\ 6k+1 & b \end{bmatrix} \right| > \left| \det \begin{bmatrix} -c & -a \\ d & b \end{bmatrix} \right|$$

whenever c and d are relatively prime and $-\frac{k+1}{6k+5} < -\frac{c}{d} < 0$. There is a trick we can use that makes use of the Farey tesselation to determine slopes that satisfy this condition. The idea is that a shorter sequence of jumps along the Farey tesselation corresponds to a smaller number of intersections between a curve of the slope at the starting point of the sequence of jumps and a curve of the slope at the ending point. Therefore if we choose a slope $-\frac{a}{b}$ such that every sequence of jumps to a slope $-\frac{c}{d}$ where $-\frac{k+1}{6k+5} < -\frac{c}{d} < 0$ necessarily includes a jump to $-\frac{k+1}{6k+5}$, we will satisfy the necessary condition. This happens if we choose $-\frac{(k-1)+1}{6(k-1)+5} < -\frac{a}{b} < -\frac{k+1}{6k+5}$ (see figure 40).
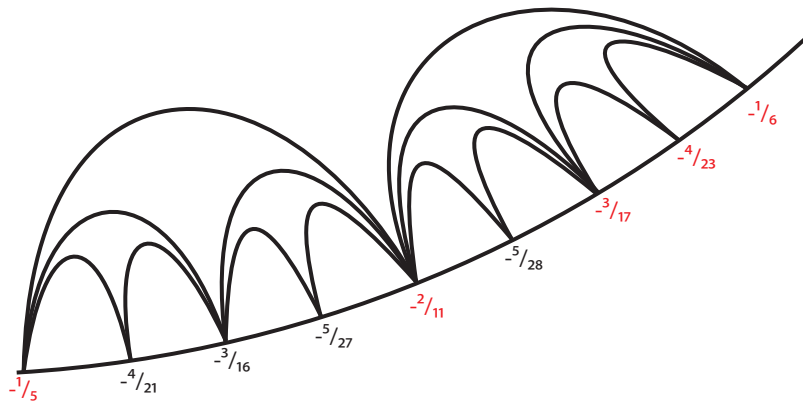
FIGURE 40. A segment of the Farey tesselation. Slopes corresponding to $-\frac{k+1}{6k+5}$ $0 \leq k \leq \infty$ are in red. Arcs between any two adjacent red slopes separate all the slopes in between from slopes which are larger.

Such slopes have the form

$$(12) \qquad -\frac{((k-1)+1)m+(k+1)n}{(6(k-1)+5)m+(6k+5)n} = -\frac{(m+n)k+n}{6(m+n)k+5n-m}$$

For $m \geq 0$, $n, k > 0$, $m, n \in \mathbb{Z}$. Recall that we are using the coordinates $\mathcal{C}_{\mathcal{U}_1}^{(p,q)}$. Changing to longitudinal coordinates $\mathcal{C}_{\mathcal{K}}$:

$$\begin{bmatrix} 1 & 6 \\ 0 & 1 \end{bmatrix} \begin{bmatrix} -6(m+n)-5n+m \\ (m+n)k+n \end{bmatrix} = \begin{bmatrix} n+m \\ (m+n)k+n \end{bmatrix}$$

So we get an $((m + n)k + n, m + n)$ cable of the $(2, 3)$ torus knot lying on the surface of N_k. By the Legendrian Realization Principle 9 we may assume that this cable is a Legendrian knot. Furthermore, these knots do not destabilize. The proof of this relies on an understanding of generally useful techniques [13] called state traversal and isotopy discretization.

5.3.2. *State traversal and Isotopy Discretization.* The idea of state traversal is that you can cut up a 3-manifold along convex surfaces and look at all the pieces to get information about the possible tight contact structures on each piece, which will glue together to give a tight contact structure on the entire 3-manifold.

More specifically, suppose M is a compact oriented 3-manifold whose boundary (if nonempty) has a dividing set which can extend to a tight contact structure on all of M. Cut M along an incompressible surface N where $\partial N \cap \Gamma_{\partial M} \neq \emptyset$ whenever $\partial M \neq \emptyset$ to get a sutured manifold decomposition, M' whose boundary consists of two copies of N together with ∂M. Now we can look at different possibilities for the dividing set on N. Suppose Γ_N^i extends to a contact structure ξ^i on M'. We say there is an *allowable state transition from* (Γ_N^1, ξ^1) *to* (Γ_N^2, ξ^2) if:

(1) ξ^1 is tight on M'
(2) (Γ_N^2, ξ^2) is obtained from (Γ_N^1, ξ^1) by a nontrivial bypass along N.

(3) ξ^2 is obtained from ξ^1 by peeling off the $N \times I$ layer corresponding to the bypass and reattaching this layer to the other copy of N in M'.

Let G be a graph with vertices all possible (Γ_N, ξ), where there is an edge between vertices exactly when there is a state transition from one vertex to the other. Using this notation, we have the following gluing theorem:

Theorem 19 (Honda [13]). *Suppose M' is endowed with the contact structure given by (Γ_N, ξ). We obtain a tight contact structure on M by identifying the two copies of N in M' if and only if every other vertex (Γ'_N, ξ') which is path connected to (Γ_N, ξ) in G induces a tight contact structure on M'.*

In order to classify distinct contact structures, Honda uses *isotopy discretization*. Here we will use it to determine the possible convex surfaces with a fixed Legendrian boundary. The relevant theorem is the following:

Theorem 20 (Honda [13]). *If ξ is a tight contact structure on M and N and N' are two (topologically) isotopic convex surfaces with the same Legendrian boundary, then there is a sequence of allowable state transitions from $(\Gamma_N, \xi_{M\setminus N})$ to $(\Gamma_{N'}, \xi_{M\setminus N'})$.*

We are trying to show that the Legendrian curve of slope $\frac{(n+m)k+n}{n+m}$ (in coordinates $\mathcal{C}_\mathcal{K}$ on the surface of N_k does not destabilize, which will give us candidates for transversely nonsimple knots. Let $L_{n,m,k}$ be this knot. If $L_{n,m,k}$ destabilizes then there is a bypass along $L_{n,m,k}$ for ∂N_k. In other words, there is a torus T, parallel to ∂N_k which contains $L_{n,m,k}$ and the bypass disk that gives the destabilization. Then $T \setminus L_{n,m,k}$ is an annulus isotopic to $\partial N_k \setminus L_{n,m,k}$ with the same Legendrian boundary, so we can use isotopy discretization to say that $L_{n,m,k}$ only destabilizes if there is a nontrivial bypass along ∂N_k. We know there is no nontrivial bypass on the outside of N_k because N_k does not thicken. If there were a nontrivial bypass inside N_k then we would obtain a torus parallel to ∂N_k with slope $s \geq -\frac{k+1}{6k+5}$ (in coordinates $\mathcal{C}_{\mathcal{U}_1}^{(p,q)}$) where s could be found one jump away from the slope of $L_{n,m,k}$ on the Farey tesselation. However we choose the slope so that the only slope on the Farey tesselation with these properties is the slope of the dividing curves on ∂N_k itself. Therefore the only bypasses on the inside of N_k are trivial. This shows that $L_{n,m,k}$ does not destabilize.

5.3.3. *Thurston Bennequin and Rotation Numbers.* I claim that $tb(L_{n,m,k})$ is strictly less than the maximal tb for $((m+n)k+n, m+n)$ cables of the $(2,3)$ torus knot. We can compute $tb(L_{n,m,k})$ using theorem 15 since (in coordinates $\mathcal{C}_{\mathcal{U}_1}^{(p,q)}$) it is a curve of slope $-\frac{(m+n)k+n}{6(m+n)k+5n-m}$ on a convex torus with dividing curves of slope $-\frac{k+1}{6k+5}$:

$$
\begin{aligned}
tb(L_{n,m,k}) &= lk(L_{n,m,k}, L'_{n,m,k}) - \frac{1}{2}|L_{n,m,k} \cap \Gamma_{\partial N_k}| \\
&= lk(L_{n,m,k}, L'_{n,m,k}) - |(6(m+n)k+5n-m)(k+1) - ((m+n)k+n)(6k+5)| \\
&= lk(L_{n,m,k}, L'_{n,m,k}) - m
\end{aligned}
$$

where $L'_{n,m,k}$ is obtained from $L_{n,m,k}$ by pushing off slightly in the direction normal to N_k. The linking number of a (p,q) cable lying on a torus with its pushoff in the direction normal to the torus

is pq, so in this case $lk(L_{n,m,k}, L'_{n,m,k}) = (n+m)((n+m)k+n)$. Let $\mathcal{L}_{n,m,k}$ be the knot type of the $(n+m, (n+m)k+n)$ cable of $\mathcal{K}$. Then the Legendrian knot of type $\mathcal{L}_{n,m,k}$ with maximal tb must lie on a torus representing $\mathcal{K}$ whose dividing curves are parallel to the knot so that they do not intersect. This is possible because, in coordinates $\mathcal{C}_{\mathcal{U}_1}^{(p,q)}$, the thickest solid torus representing $\mathcal{K}$ has dividing curves of slope $-\frac{1}{5}$. By lemma 9 there is a solid torus representing $\mathcal{K}$ with dividing curves on the boundary of any slope s where $-\frac{1}{5} < s < 0$. In these coordinates, $\mathcal{L}_{n,m,k}$ has slope $-\frac{(m+n)k+n}{6(m+n)k+5n-m}$ (equation 12), where $m \geq 0$ and $n, k > 0$. These are all of the slopes on the Farey tessellation between $-\frac{(k-1)+1}{6(k-1)+5}$ and $-\frac{k+1}{6k+5}$. When $k = 1$, $-\frac{(k-1)+1}{6(k-1)+5} = -\frac{1}{5}$. The sequence $-\frac{k+1}{6k+5}$ is monotonically increasing so every cable we are considering can be realized as the Legendrian divides on a torus representing $\mathcal{K}$. Suppose that N is the torus with dividing curves parallel to this $L \in \mathcal{L}_{n,m,k}$. Then

$$
\begin{aligned}
\overline{tb}(\mathcal{L}_{n,m,k}) &= lk(L, L') - \frac{1}{2}|L \cap \Gamma_{\partial N}| \\
&= lk(L, L') \\
&= (n+m)((n+m)k+n)
\end{aligned}
$$

This tells us that for $m > 0$, $L_{n,m,k}$ is a knot which does not destabilize but does not have maximal tb. To determine that the knot is not stably simple, we first need to compute the rotation numbers of the knots with maximal tb and the knots like $L_{n,m,k}$ with less than maximal tb, which do not destabilize. As we did when we were looking at cables of knots that do satisfy the UTP, we want to use lemma 13.

First we compute the rotation number for a knot of maximal tb which is the Legendrian divide on a solid torus N_{max} representing $\mathcal{K}$ whose boundary has dividing curves of slope $\frac{(n+m)k+n}{n+m}$ in coordinates $\mathcal{C}_{\mathcal{K}}$ ($-\frac{(m+n)k+n}{6(m+n)k+5n-m}$ in coordinates $\mathcal{C}_{\mathcal{U}_1}^{(p,q)}$). We want to compute the rotation number of a Legendrian meridian of N_{max} and a Legendrian longitude of N_{max} to use lemma **??**. By our results above, we know that we can thicken N_{max} of $\mathcal{K}$ to N_{k-1}, a solid torus whose boundary has dividing curves of slope k in coordinates $\mathcal{C}_{\mathcal{K}}$ ($-\frac{k}{6(k-1)+5}$ in coordinates $\mathcal{C}_{\mathcal{U}_1}^{(p,q)}$). Let D be a meridional disk of N_{max} with Legendrian boundary and Σ a Seifert surface for $\mathcal{K}$ whose boundary is a Legendrian longitudinal curve on N_{max}. Correspondingly let D' be a meridional disk of N_{k-1} with Legendrian boundary on ∂N_{k-1} which contains D, and let Σ' be a Seifert surface for $\mathcal{K}$ with Legendrian boundary on N_{k-1} which is contained in Σ. Let $R = N_{k-1} \setminus N_{max}$. Then

$$
r(\partial D') = r(\partial D) + \langle e(\xi, R), D' \setminus D \rangle
$$

$$
r(\partial \Sigma) = r(\partial \Sigma') + \langle e(\xi, R), \Sigma \setminus \Sigma' \rangle
$$

R is contactomorphic to $T^2 \times [0, 1]$ where $\text{slope}(\Gamma_{T_0}) = \text{slope}(\Gamma_{N_{max}}) = \frac{(n+m)k+n}{n+m}$ and $\text{slope}(\Gamma_{T_1}) = \text{slope}(\Gamma_{N_{k-1}}) = k$ with respect to $\mathcal{C}_{\mathcal{K}}$. Therefore, by the classification of tight contact structures on $T^2 \times [0, 1]$,

$$
PD(e(\xi, R)) = \pm((1, k) - (n+m, (n+m)k+n)) = \pm(1-n-m, k-(n+m)k-n)
$$

Furthermore $r(\partial D') = \pm(k-1)$. This is because N_{k-1} has dividing curves of slope k can be decomposed into layers divided by tori of decreasing integer slopes. The meridional disk of the layer

with slope 1 has rotational number 1, and then the Euler class can be used to compute the difference. The sign depends on which of the two contact structures we take for N_{k-1} and necessarily agrees with the sign of $PD(e(\xi, R))$.

We also have $r(\partial \Sigma') = 0$. This is because the longitude on N_{k-1} intersects each of the two dividing curve exactly once, which implies that there is a single dividing curve on Σ', and exactly two singularities on $\partial \Sigma'$ of opposite signs. We may perturb Σ' so that it contains no other singularities and then it is not difficult to find a section of $\xi|_{\Sigma'}$ that agrees with $T(\partial \Sigma')$ on the boundary which has no zeroes.

Therefore if $L^{max}_{n,m,k}$ is a Legendrian knot which is a $(n+m, (n+m)k+n)$ cable of $\mathcal{K}$ of maximal tb, then

$$
\begin{aligned}
r(L^{max}_{n,m,k}) &= (n+m)(r(\partial D)) + ((n+m)k+n)(r(\partial \Sigma)) \\
&= (n+m)(r(\partial D') - \langle e(\xi, R), D' \setminus D \rangle) + ((n+m)k+n)(r(\partial \Sigma') + \langle e(\xi, R), \Sigma \setminus \Sigma' \rangle) \\
&= (n+m)(\pm(k-1) - (\pm(k-(n+m)k-n))) + ((n+m)k+n)(0 \pm (1-n-m)) \\
&= \pm((n+m)k-m)
\end{aligned}
$$

Similarly we can compute the rotation number for $L_{n,m,k}$ which lies on N_k. Let D'' be a meridional disk for N_k and Σ'' be a Seifert surface for $\mathcal{K}$ with boundary being a longitudinal curve on ∂N_k. We know $r(\partial D'') = \pm k$, and $r(\partial \Sigma'') = 0$. Then lemma 13 gives us

$$
\begin{aligned}
r(L_{m,n,k}) &= (n+m)(r(\partial D'')) + ((n+m)k+n)(r(\partial \Sigma'')) \\
&= \pm(n+m)k
\end{aligned}
$$

Notice that if we take the knot $L^{max}_{n,m,k}$ where $r(L^{max}_{n,m,k}) = ((n+m)k-m)$, it has $tb(L^{max}_{n,m,k}) = \overline{tb}(\mathcal{L}_{n,m,k})$ so the values of (r, tb) for $S^m_+(L^{max}_{n,m,k})$ are $((n+m)k, \overline{tb}(\mathcal{L}_{n,m,k}) - m)$ which are exactly the values of (r, tb) for $L_{m,n,k}$ when we take the $L_{m,n,k}$ with rotation number $(n+m)k$. However we know that $L_{m,n,k}$ does not destabilize and $S^m_+(L^{max}_{n,m,k})$ clearly does destabilize. This shows that $\mathcal{L}_{n,m,k}$ is not Legendrian simple. We would like to prove further that $\mathcal{L}_{n,m,k}$ is not stably simple (and is thus not transversely simple). Thus our next goal is to show that $S^j_-(L_{n,m,k})$ is not Legendrian isotopic to $S^j_-(S^m_+(L^{max}_{n,m,k}))$ for any positive integer j.

To simplify notation, let $\mathbf{L} = L_{m,n,k}$, $\mathbf{L}_j = S^j_-(\mathbf{L})$, $\mathbf{K} = S^m_+(L^{max}_{n,m,k})$, and $\mathbf{K}_j = S^j_-(\mathbf{K})$. We want to show that $\mathbf{L}_j$ is not Legendrian isotopic to $\mathbf{K}_j$ for any $j \in \mathbb{Z}_+$. We know that $\mathbf{L}$ lies on the boundary of a solid torus N_k whose dividing curves have slope $-\frac{k+1}{6k+5}$ in coordinates $\mathcal{C}^{(p,q)}_{\mathcal{K}}$ which are the coordinates we will use for the rest of this proof. $\mathbf{L}_j$ is related to $\mathbf{L}$ by a sequence of j negative stabilizations. Therefore through a sequence of j destabilizations (equivalently bypass disks), we can get from $\mathbf{L}_j$ to $\mathbf{L}$. Therefore we can place $\mathbf{L}_j$ on ∂N_k such that the annulus $A_0 = \partial N_k \setminus \mathbf{L}_j$ has j boundary parallel dividing curves on each side as in figure 41.

Lemma 16. *Every torus isotopic to $\Sigma_0 = \partial N_k$ containing $\mathbf{L}_j$ has slope $-\frac{k+1}{6k+5}$.*

This will indicate that $\mathbf{L}_j$ is never Legendrian isotopic to $\mathbf{K}_j$ because a torus of slope $-\frac{k+1}{6k+5}$ cannot thicken to the torus on which $L^{max}_{m,n,k}$ is a Legendrian divide, but any torus containing $\mathbf{K}_j$ can thicken to the torus containing $L^{max}_{m,n,k}$.
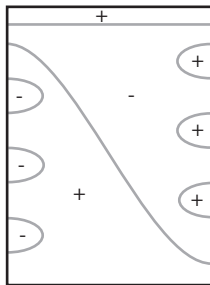
FIGURE 41. The annulus $A_0 = \partial N_k \setminus \mathbf{L}_j$ with dividing curves. The top and bottom are identified. ∂A_0 consists of two copies of $\mathbf{L}_j$. The $+$ and $-$ signs indicate the regions in R_+ and R_- respectively.

Proving that every torus isotopic to Σ_0 containing $\mathbf{L}_j$ has dividing curves of slope $-\frac{k+1}{6k+5}$ is equivalent to proving that every torus isotopic to Σ_0 relative to $\mathbf{L}_j$ has dividing curves of slope $-\frac{k+1}{6k+5}$. We can do this using the state traversal technique. First look at a $[0,1]$ invariant neighborhood of Σ_0. This is a $T^2 \times [0,1]$ on which we will perform the state traversal technique. We will let $T_{0.5} = \Sigma_0$ and cut this $T^2 \times [0,1]$ along $T_{0.5}$. Then state traversal dictates that the possible states (dividing sets on $T_{0.5}$) can be obtained by a sequence of allowable state transitions (see section 5.3.2). We will describe these allowable state transitions to show is that the slope of the dividing curves on $T_{0.5}$ in all possible states is $-\frac{k+1}{6k+5}$. In order to ensure that we can still glue $T^2 \times [0,1]$ in to S^3 after performing a state transition, we need to find a contactomorphism $\phi : S^3 \to S^3$ which sends the $[0,1]$ invariant neighborhood of Σ_0 to $T^2 \times [0,1]$ with the tight contact structure it inherits after the state transition, and matches up their complements. Since state transitions are discrete steps, we are basically proving lemma 16 by induction where the inductive hypothesis is:

(1) $T_{0.5}$ is a convex torus containing $\mathbf{L}_j$ with dividing curves of slope $-\frac{k+1}{6k+5}$.
(2) $T_{0.5}$ lies in a $[0,1]$ invariant $T^2 \times [0,1]$ where slope(Γ_{T_0}) =slope$(\Gamma_{T_1}) = -\frac{k+1}{6k+5}$ and $\#\Gamma_{T_0} = \#\Gamma_{T_1} = 2$.
(3) There is a contactomorphism $\phi : S^3 \to S^3$ sending $T^2 \times [0,1]$ to the $[0,1]$ invariant neighborhood of Σ_0 and matching up the complements.

We will first show that the first condition is preserved by an allowable state transition in the following two steps.

Allowable state transitions are obtained by attaching a bypass to $T_{0.5}$. $T_{0.5}$ bounds a solid torus N isotopic to N_k which cannot thicken to a solid torus with dividing curves of different slope since its dividing curves have slope $-\frac{k+1}{6k+5}$. Therefore if the slope of the dividing curves of $T_{0.5}$ changes it is because of a bypass attached on the interior of N. Therefore all possible slopes obtained by allowable state transitions are $[-\frac{k+1}{6k+5}, 0)$. We show that of these, the only one which can actually be obtained is $-\frac{k+1}{6k+5}$ in the following two steps.

Claim 1. $\mathbf{L}_j$ cannot lie on a convex torus Σ inside N_k that is isotopic to Σ_0 with 2 dividing curves of slope $-\frac{1}{6}$.

Proof. A convex torus with 2 dividing curves of slope $-\frac{1}{6}$ isotopic to Σ_0 inside N_k, bounds a standard neighborhood of the Legendrian $(2,3)$ torus knot $K \in \mathcal{K}$ where $tb(K) = 0$ and $r(K) = -1$. A curve of slope $-\frac{(m+n)k+n}{6(m+n)k+5n-m}$ (which corresponds to the cable $\mathcal{L}_{m,n,k}$ pulled tight onto the torus) is $S_+(\mathbf{L})$. This is because we can attach a bypass to a torus with 2 dividing curves of slope $-\frac{1}{6}$ along a curve of slope $-\frac{(m+n)k+n}{6(n+m)k+5n-m}$ yielding a torus of slope $-\frac{k+1}{6k+5}$ by lemma 5. Therefore if $\mathbf{L}_j$ lies on a convex torus with 2 dividing curves of slope $-\frac{1}{6}$ it is a stabilization of $S_-(\mathbf{L})$. However stabilizations of $S_-(\mathbf{L})$ can never have the same (r, tb) values as $S_-^j(\mathbf{L}) = \mathbf{L}_j$, thus proving step 1. $\qquad \square$

Claim 2. *If there were a convex torus containing $\mathbf{L}_j$ with dividing curves of slope $s \in (-\frac{k+1}{6k+5}, 0)$, then there is a sequence of bypasses disjoint from $\mathbf{L}_j$ which after attached give a convex torus containing $\mathbf{L}_j$ with 2 dividing curves of slope $-\frac{1}{6}$.*

Proof. Suppose after we attach the bypass we obtain a convex torus Σ containing $\mathbf{L}_j$ with dividing curves of slope $s \in (-\frac{k+1}{6k+5}, -\frac{1}{6})$. Then Σ bounds a solid torus which contains another torus Σ' which has 2 dividing curves of slope $-\frac{1}{6}$ by the classification of tight contact structures on solid tori. Now take an annulus A with one boundary curve parallel but disjoint from $\mathbf{L}_j$ on Σ and the other boundary curve of the same slope on Σ'. Then A intersects the dividing curves on Σ' fewer times than the dividing curves on Σ so there are boundary parallel curves to $A \cap \Sigma$ which provide a sequence of bypass disks disjoint from $\mathbf{L}_j$ to a torus with 2 dividing curves of slope $-\frac{1}{6}$.

If after we attach the bypass we obtain a convex torus Σ of slope $s \in (-\frac{1}{6}, 0)$ then the solid torus bounded by Σ can be thickened (via a sequence of bypasses along Legendrian ruling curves parallel to $\mathbf{L}_j$ to a solid torus whose boundary has dividing curves of slope $-\frac{1}{6}$. $\qquad \square$

This shows that every state transition can only change the number of dividing curves, not the slope. Finally, we show that the second and third conditions in the inductive hypothesis are preserved by allowable state transitions.

Suppose we start out with a surface Σ bounding a solid torus N and satisfying the inductive hypothesis, and then we attach a bypass to obtain Σ', where the dividing curves on both surfaces have slope $-\frac{k+1}{6k+5}$. Then there is a $T^2 \times [0,1]$ containing Σ as $T_{0.5}$ where T_0 and T_1 each have exactly two dividing curves of slope $-\frac{k+1}{6k+5}$. Suppose first that the bypass is on the inside of N, so Σ' is inside N. Let $P = T^2 \times [0.5, 1]$, so $\partial P = \Sigma \cup T_1$. There is a thickened torus Q between Σ and Σ' inside N. Furthermore Σ' bounds a solid torus N'. Honda's classification of tight contact structures on solid tori proves that if Σ' has more than 2 dividing curves then there is a nonrotative outer layer $Q \cong T^2 \times [0,1]$ of N' such that $\partial R = \Sigma' \cup T'$ where T' is a torus parallel to Σ' with two dividing curves of slope $-\frac{k+1}{6k+5}$, and every torus parallel to Σ' and T' inside of Q has slope $-\frac{k+1}{6k+5}$. Then $P \cup Q \cup R$ is a thickened torus with boundary $T_1 \cup T'$, both of which have exactly 2 dividing curves of the correct slope. Furthermore $P \cup Q \cup R$ is non-rotative and thus the contactomorphism in condition 3 exists.

In the case that the bypass is attached to Σ on the outside of N, we let $P = T^2 \times [0, 0.5]$ which has $\partial P = T_0 \cup \Sigma$. Let R be the thickened torus such that $\partial R = \Sigma \cup \Sigma'$. Now we want to find a non-rotative thickened torus $\mathbb{Q}$ on the other side of Σ' from R such that $\partial Q = \Sigma' \cup T'$ where T' has exactly 2 dividing curves of slope $-\frac{k+1}{6k+5}$. This is slightly more difficult than in the previous

case because the complement of $N' = N \cup R$ is not a solid torus. However, we can decompose $S^3 \setminus N'$ into two unknotted solid tori V_1, V_2, which are standard neighborhoods of core unknotted Legendrian curves, connected by a thickened annulus that runs parallel to N'. This is the same technique used in section 5.2. Essentially we choose the core Legendrian curves of V_1 and V_2 to have maximal possible tb such that their standard neighborhoods lie in $S^3 \setminus N'$. After we choose V_1 and V_2 as thick as possible and then attach the thickened annulus $A' \cap [-\varepsilon, \varepsilon]$ in between and rounding the edges as in figures 34 and 35, the boundary has exactly 2 dividing curves of slope $-\frac{k+1}{6k+5}$ and the space between N' and $V_1 \cup V_2 \cup A' \cap [-\varepsilon, \varepsilon]$ is a non-rotative solid torus, which will be our Q. Then $P \cup R \cup Q$ gives the $T^2 \times [0, 1]$ containing Σ' that satisfies conditions 2 and 3.

$\square$
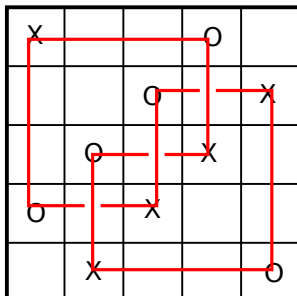
FIGURE 42. A grid diagram for the trefoil knot

6. ALGEBRAIC TOOLS IN CONTACT TOPOLOGY

6.1. **Grid Diagrams.** Grid diagrams provide a way of presenting a knot diagram in a way that is accessible to combinatorial manipulations. They have come up in many different contexts, in studying knots. A grid diagram is simply an $n \times n$ grid of squares (n is called the *grid number*), where each row and column contains exactly one X and one O. To obtain a knot from such a diagram, draw an oriented horizontal segment from each O to the X in the same row and an oriented vertical segment from each X to the O in the same column. At each intersection, let the horizontal segment pass under the vertical segment. This produces a knot diagram. See figure 42 for an example.

Grid diagrams are a natural way to study Legendrian knots, because the mirror image of any Legendrian front projection can be placed on a grid diagram.

Note: While it is a rather annoying convention to always look at the mirror image of the knot instead of the knot itself, this convention is standard in the literature so we keep it here. We will always implicitly assume we are looking at the mirror image of the Legendrian front in these sections using grid diagrams.

Given a Legendrian front projection, Legendrian isotope the segments between consecutive cusps and/or horizontal tangencies so that they are straight diagonal line segments except for the slight curve for the cusp or horizontal tangency. Then Legendrian isotope to raise or lower the cusps and horizontal tangencies so that all the diagonal lines with positive slope are parallel to $y = z$ and disjoint and all the diagonal lines with negative slope are parallel to $y = -z$ and disjoint. Now turn the diagram 45° counterclockwise. Now each straight segment is either horizontal or vertical. Create a row for each horizontal segment and a column for each vertical segment, and place the X's and O's on the cusps and (previously horizontal) tangencies) according to the orientation of the Legendrian knot. (See figure 43). In the other direction, we can turn a grid diagram into a
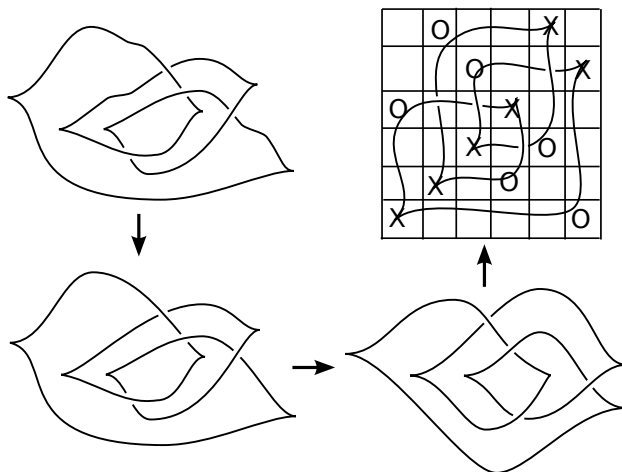
FIGURE 43. Changing a Legendrian front projection to a grid diagram
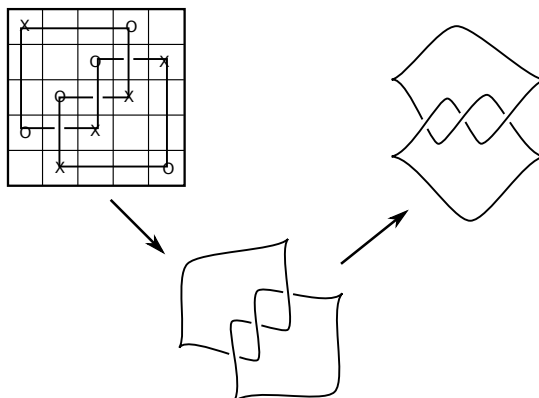
FIGURE 44. Changing a grid diagram into a Legendrian front projection

Legendrian front projection by smoothing out the southwest and northeast corners, turning the northwest and southeast corners into cusps, and rotating the diagram 45° clockwise. (See figure 44).

There are three types of moves (and their inverses) one can perform on a grid diagram to obtain a topologically equivalent knot. These are *cyclic permutation*, *commutation*, and *(de)stabilization*.

- Cyclic permutation: Permutes the rows (or columns) of the grid cyclically. (Figure 45)
- Commutation: Suppose there are two adjacent rows (or columns) such that the markings do not alternate between the two rows (or columns), and each marking in the two rows (columns) is in a different column (row). The commutation move switches two such rows (columns). (Figure **??**)
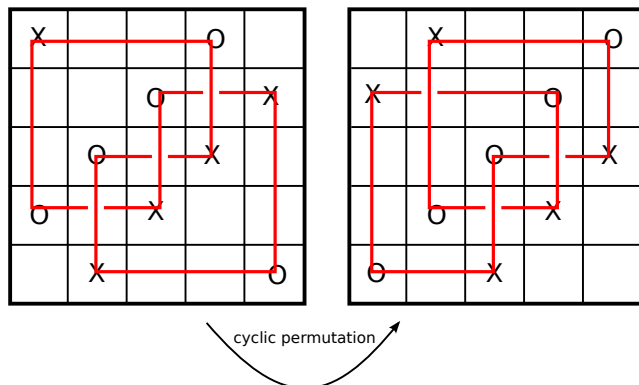
FIGURE 45. Cyclic Permutation of a grid diagram

- Stabilization: Split one row into two adjacent rows, one containing the X and the other containing the O (without changing the columns the X and O occupy), then add in an additional column adjacent to the column with the X or the column with the O. In this column introduce a new X and O to ensure that there is exactly one X and one O in the two rows resulting from the splitting. To invert stabilization (destabilization) we must find a 2×2 square in the grid which has exactly three markings, delete the column containing two markings in the 2×2 square, and merge together the two rows in the 2×2 square. (Figure 47)

Any two grid diagrams which represent the same topological knot type can be obtained from one another through these moves. This is proven in Cromwell [4]. To be more specific, we need to further classify (de)stabilizations. We do this by specifying which of the four squares in the 2×2 square is empty and whether there are more X's or O's in the 2×2 square. This results in 8 types of destabilizations. The empty square can be in one of four compass directions: NW, NE, SW, SE so the 8 types of (de)stabilization moves are $X\colon NW, X\colon NE, X\colon SW, X\colon SE, O\colon NW, O\colon NE, O\colon SW, O\colon SE$ (figure 48). It turns out that some of these moves are repetitive once we include commutation and cyclic permutation. We will first reduce the number of moves we need in the following two lemmas.

Lemma 17. *A stabilization of type $O\colon SE$ (respectively $O\colon NE$, $O\colon NW$, or $O\colon SW$) is equivalent to a stabilization of type $X\colon NW$ (respectively $X\colon SW$, $X\colon SE$, or $X\colon NE$) followed by a sequence of commutation and cyclic permutation moves.*

Proof. Perform the X stabilization so that after stabilizing, the X is in row i, and a new column is introduced adjacent to the X in row i. The new column introduced has an X in row $i \pm 1$ and one O in row i. Therefore the new column will commute with every adjacent row on the other side of the X in row i until the adjacent column contains an O in row $i \pm 1$. (If commutation pushes the new column to the end of the grid, use a cyclic permutation to bring it to the other side.) Then we
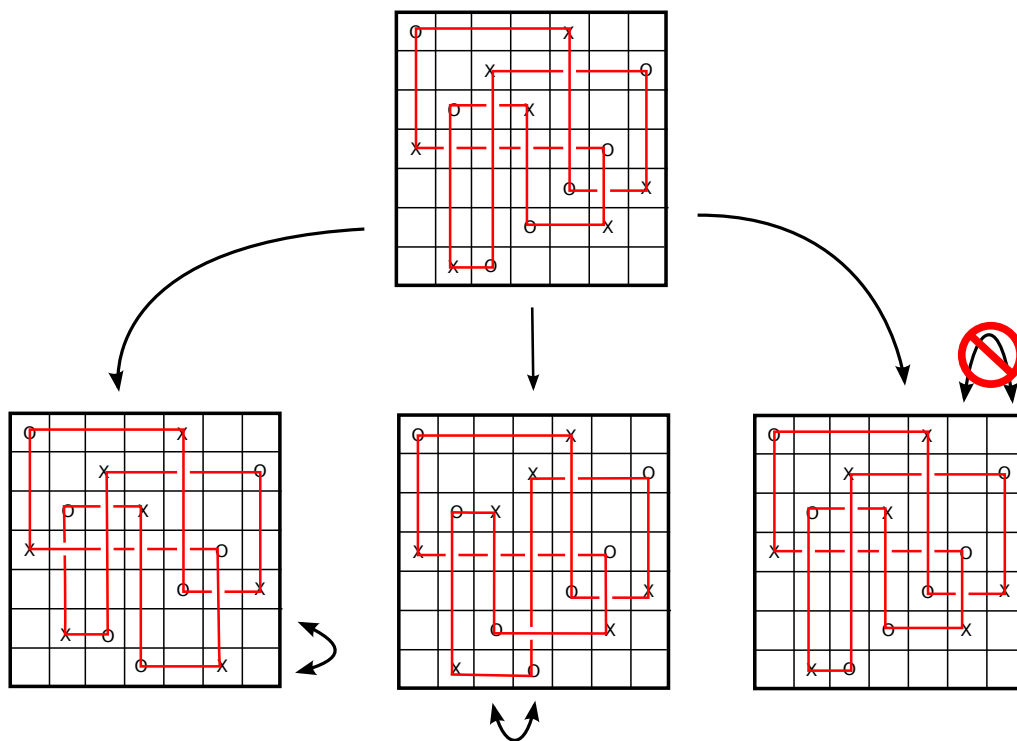
FIGURE 46. Commutation on a grid diagram
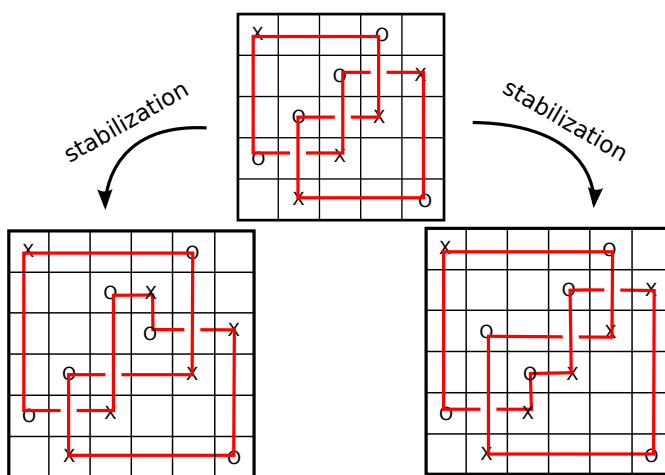
FIGURE 47. Stabilizations of a grid diagram
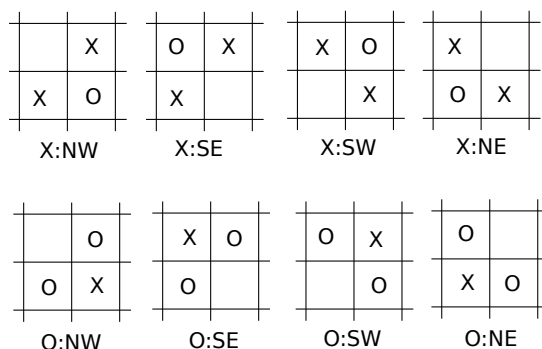
FIGURE 48. The different types of stabilization.

will have a new 2×2 square in rows i and $i \pm 1$ which contains two O's and an X where the missing square is as in the statement of the lemma. □

Lemma 18. *A cyclic permutation can be achieved through a sequence of commutations and (de)stabilizations of types* $X \colon NW$, $X \colon SE$, $O \colon NW$, *and* $O \colon SE$.

Proof. We will discuss the case where we want to move a row from the bottom to the top. Symmetric moves apply to the other cases. We provide two examples: one moving a row from bottom to top (figure 49) and the other moving a column from left to right (figure 50). It may be useful to go through a couple examples to convince oneself this method works. Follow figure 49 for this proof.

Suppose we want to move the bottom row to the top. Without loss of generality, suppose the X in the bottom row is on the left of the O (otherwise do the same process with X's and O's switched). We will call the X in the bottom row X_1, the O in the same column as X_1, will be called O_1. The O in the bottom column will be O_2 and the X in the same column as O_2 will be X_2.

Since we want to move X_1 to the top above O_1, we would like to switch the order from top to bottom of X_1 and O_1, but we cannot commute them past each other since they are in the same column. We instead perform a $O \colon SE$ stabilization to create a new column containing the symbols X' and O' in the order we want (O' is above X'). O' will now hold the position of O_1, and we will move O_1 to the top to represent the cyclically permuted O_2. We chose the stabilization such that there is nothing above the segment from X' to O_1. This is possible since X_1 is below O_1. This allows us to commute the row containing $\widetilde{X}$ and O_1 up to the top of the diagram, since X' and O_1 are directly next to each other. We will leave X' at the top here directly above O' which has taken the place of O_1. Therefore X' is in the position that we want the cyclically permuted original X_1 to be.

Since X_1 is on the bottom row and O_1 is in the top row of the same column, we can commute this column to the right until X_1 is directly next to O_2. Recall that X' is the only other symbol in the row with O_1 and it is on the left of O_1 and thus does not get in the way of this commutation.
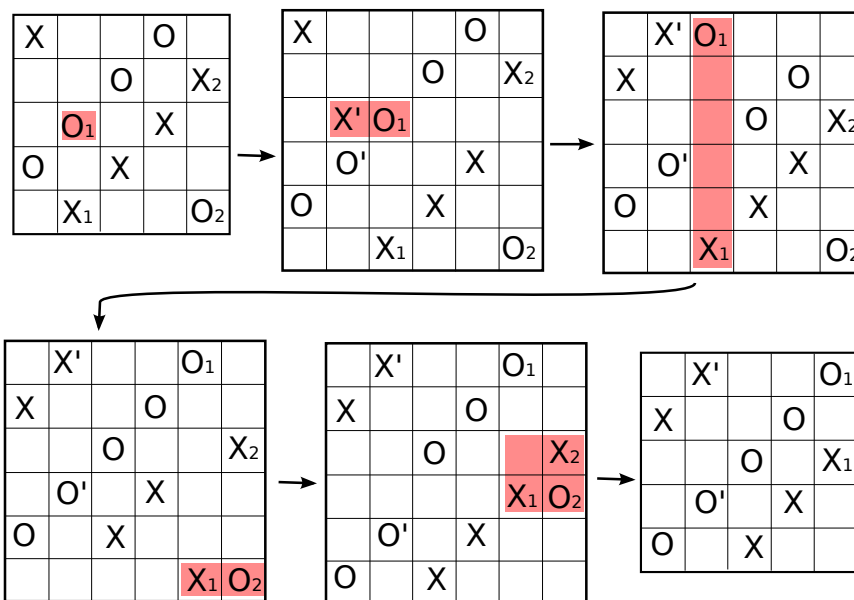
FIGURE 49. Moving a row from bottom to top using only commutation and (de)stabilizations of types NW and SE. Step 1: $O\colon SE$ stabilization. Steps 2-4: Commutation. Step 5: $X\colon NW$ destabilization. The area where the (de)stabilization/commutation will occur is highlighted in red.

This places O_1 in almost the position that we would like the cyclic permutation of O_2 to be, but in a larger grid due to the stabilization.

Now we essentially have the X's and O's in the positions we want them on the top row and we simply need to destabilize to eliminate the extra positions and symbols in the grid. Since X_1 and O_2 are directly next to each other in the bottom row, we can commute the bottom row up until O_2 is directly next to X_2. This allows us to perform a $X\colon NW$ destabilization which sets the grid back to its original size and has created a grid diagram which is one cyclic permutation away from the original.

$\square$

Now we would like to know which of these moves preserves the Legendrian isotopy type of the knot. It is not difficult to see that commutation corresponds to a combination of planar isotopy and Legendrian Reidemeister II and III moves (see figure 51 for examples). Analysis of the stabilization moves shows that $X\colon NW$ and $X\colon SE$ preserve the Legendrian knot type, but $X\colon NE$ and $X\colon SW$ do not, and in fact correspond to positive and negative stabilizations of the Legendrian knot. See figures 52, 53, 54, and 55.
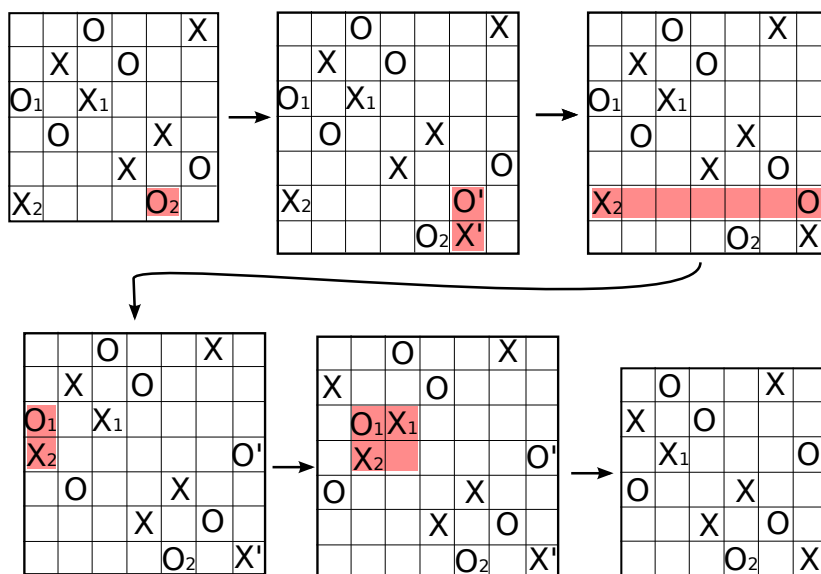
FIGURE 50. Moving a column from left to right using only commutation and (de)stabilizations of types NW and SE. Step 1: $O\colon NW$ stabilization. Steps 2-4: Commutation. Step 5: $X\colon SE$ destabilization. The area where the (de)stabilization/commutation will occur is highlighted in red.

This allows us to only consider commutations and (de)stabilizations of types $X\colon NW$, $O\colon NW$, $X\colon SE$ and $O\colon SE$. Now we need to check which of these moves corresponds to Legendrian isotopy. It is not difficult to see that

6.2. Combinatorial Knot Floer Homology.
Knot Floer homology is an invariant of knots that is defined in terms of Heegaard Floer homology, an invariant of 3-manifolds. Typically, computing Heegaard Floer homology involves counting holomorphic disks. Recently, Manolescu, Ozsváth, and Sarkar developed a combinatorial description of knot Floer homology for knots in S^3 in [19]. In [20] it was shown that knot Floer homology is an invariant of topological knot types in S^3 through the purely combinatorial description. The data used to compute combinatorial knot Floer homology comes from a grid diagram. Because of the correspondence between grid diagrams and Legendrian and transverse knots in (S^3, ξ_{std}), this combinatorial description provided an indication of a link between knot Floer homology and Legendrian and transverse knots.

Although the isomorphism type of the knot Floer homology is an invariant of topological knot type, we get more refined invariants by tracking particular elements from the chain complex, and look at their image in the homology. In this manner, Ozsváth, Szabó, and Thurston, defined invariants of Legendrian and transverse knots. They pick out a particular element of the chain complex for a given grid diagram, and look at its image in the knot Floer homology. To prove that this is actually
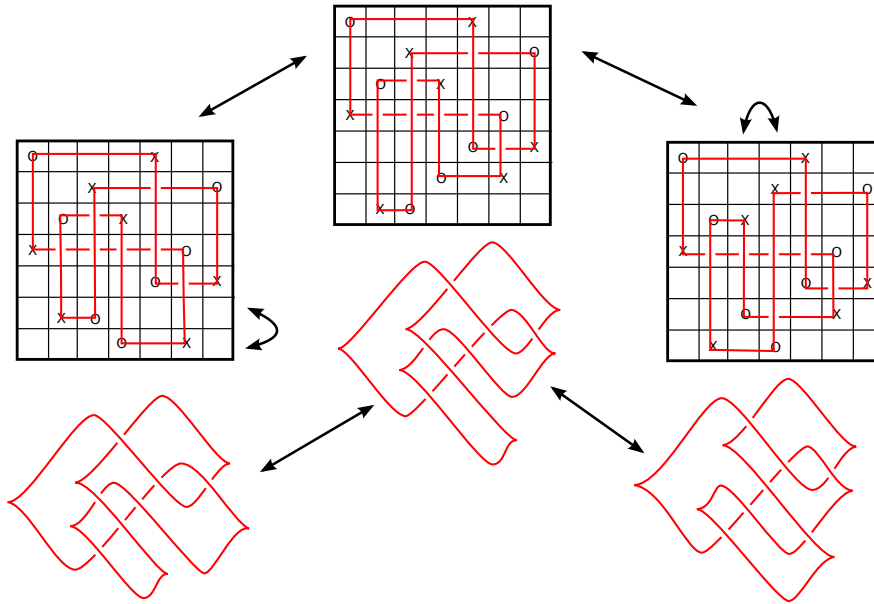
FIGURE 51. Commutation of grid diagrams corresponds to Legendrian Reidemeister II and III moves and planar isotopy
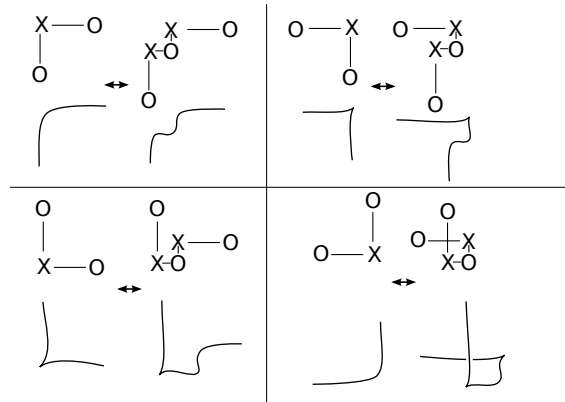
FIGURE 52. Results of an $X\colon NW$ stabilization on Legendrian fronts

an invariant of Legendrian knots (or their transverse pushoffs), they simply need to check that they are invariant under commutation, cyclic permutation, and $X\colon NW$ and $X\colon SE$ (de)stabilizations (and $X\colon SW$ (de)stabilization in the case of the transverse invariant).

We will describe these invariants, after going through a description of the combinatorial construction of knot Floer homology.

We begin with a grid diagram G, with grid number n. We denote the set of O's by $\mathbb{O} = \{O_i\}_{i=1}^n$ and the set of X's by $\mathbb{X} = \{X_i\}_{i=1}^n$. The generators of the chain complex are sets of n dots on the
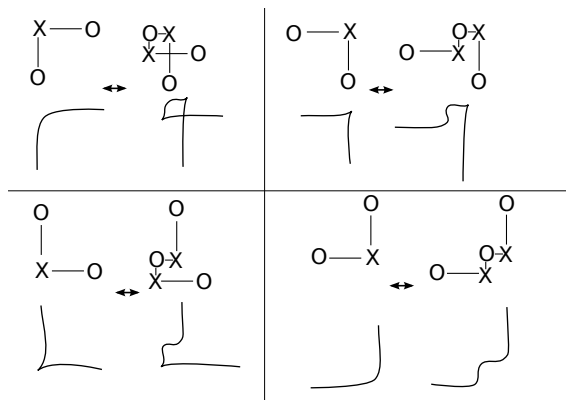
FIGURE 53. Results of an $X\colon SE$ stabilization on Legendrian fronts
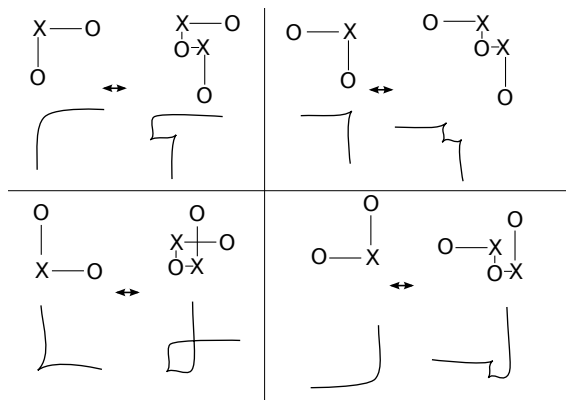
FIGURE 54. Results of an $X\colon NE$ stabilization on Legendrian fronts. With orientations specified by X's and O's this is a positive stabilization.
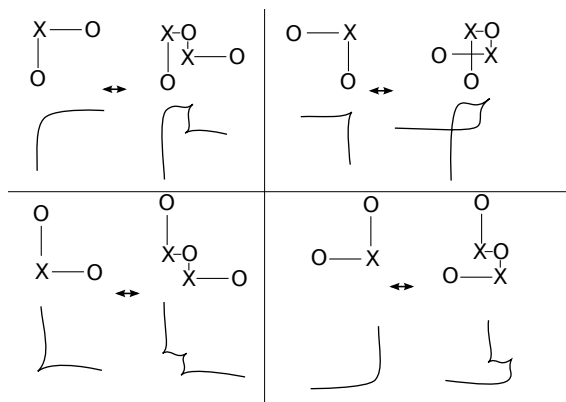
FIGURE 55. Results of an $X\colon SW$ stabilization on Legendrian fronts. With orientations this is a negative stabilization.

corners where horizontal grid lines meet vertical grid lines, such that there is exactly one dot on each horizontal and vertical line. Let this generating set be called $\mathbf{S}(G)$. Let $R = \mathbb{F}_2[U_1, \cdots, U_n]$, where the $\mathbb{F}_2 = \mathbb{Z}/2\mathbb{Z}$ and the U_i are transcendental variables. The chain complex $C^-(G)$ is the free module generated by $\mathbf{S}(G)$ over R.

Knot Floer homology is a bigraded homology theory. The two gradings are called the *Maslov* and *Alexander* gradings. To compute these gradings, we must define a way of counting generators, X's, and O's and their certain relations to each other. Suppose A and B are sets of points in $\mathbb{R}^2$. Then $\mathcal{I}(A, B)$ is the number of pairs $((a_1, a_2), (b_1, b_2)) \in A \times B$ such that $a_1 < b_1$ and $a_2 < b_2$. Let $\mathcal{J}(A, B) = \frac{1}{2}(\mathcal{I}(A, B) + \mathcal{I}(B, A))$. (Note that $\mathcal{J}$ is symmetric but $\mathcal{I}$ is not.

Now place the grid diagram in $\mathbb{R}^2$ in the natural way with the lower left corner at the origin and grid lines on successive integers. We compute the Maslov grading of a generator $\mathbf{x} \in \mathbf{S}$ by

$$M(\mathbf{x}) = \mathcal{J}(\mathbf{x}, \mathbf{x}) - 2\mathcal{J}(\mathbf{x}, \mathbb{O}) + \mathcal{J}(\mathbb{O}, \mathbb{O}) + 1 = \mathcal{J}(\mathbf{x} - \mathbb{O}, \mathbf{x} - \mathbb{O}) + 1$$

where we view $\mathbf{x}$ and $\mathbb{O}$ as sets of points in the grid diagram. The last equality is simply a formal shorthand for writing out the expanded form as if $\mathcal{J}$ were bilinear over formal sums and differences. Similarly the Alexander grading of a generator is defined by

$$A(\mathbf{x}) = \mathcal{J}(\mathbf{x} - \frac{1}{2}(\mathbb{X} + \mathbb{O}), \mathbb{X} - \mathbb{O}) - \frac{n-1}{2}$$

where n is the number of components in the link. We extend these gradings to all of $C^-(G)$ by saying multiplication by U_i reduces the Maslov grading by 2 and the Alexander grading by 1.

Now we define the differential on $C^-(G)$. View G as lying on the oriented torus $\mathbb{R}^2/(\mathbb{Z}/n\mathbb{Z})^2$. Suppose $\mathbf{x}, \mathbf{y} \in \mathbf{S}$. If all but two of the points of $\mathbf{x}$ agree with the points of $\mathbf{y}$, then there are two rectangles in $\mathbb{R}^2/(\mathbb{Z}/n\mathbb{Z})^2$ whose lower left and upper right corners are points of $\mathbf{x}$ and whose lower right and upper left corners are points of $\mathbf{y}$ (note that upper/lower and left/right are determined by the orientation on $\mathbb{R}^2/(\mathbb{Z}/n\mathbb{Z})^2$). We say such rectangles connect $\mathbf{x}$ to $\mathbf{y}$, and denote the collection of such rectangles by $\mathrm{Rect}(\mathbf{x}, \mathbf{y})$. Note that here we are viewing the grid as being on a torus with opposite edges identified so a rectangle may push through one edge to continue on the opposite side. We say that $r \in \mathrm{Rect}(\mathbf{x}, \mathbf{y})$ is *empty* if the interior of r does not contain any points of $\mathbf{x}$ (or equivalently of $\mathbf{y}$) and denote the set of empty rectangles from $\mathbf{x}$ to $\mathbf{y}$ by $\mathrm{Rect}^\circ(\mathbf{x}, \mathbf{y})$. Then

$$\partial^-(\mathbf{x}) = \sum_{\mathbf{y} \in \mathbf{S}} \sum_{r \in \mathrm{Rect}^\circ(\mathbf{x}, \mathbf{y})} U_1^{O_1(r)} \cdots U_n^{O_n(r)} \cdot \mathbf{y}$$

where $O_i(r)$ is 0 if O_i is not in r and 1 if O_i is in r.

We now check that ∂^- is actually a differential:

Lemma 19.

$$\partial^- \circ \partial^-(\mathbf{x}) = 0$$

for all generators $\mathbf{x}$ of $C^-(G)$, and thus $\partial^- \circ \partial^- = 0$.

Proof. The key to the argument is understanding $\partial^- \circ \partial^-(\mathbf{x})$ as a way of counting pairs of rectangles: one in $\mathrm{Rect}^\circ(\mathbf{x}, \mathbf{y})$ and the other in $\mathrm{Rect}^\circ(\mathbf{y}, \mathbf{z})$ over all possible generators $\mathbf{y}$ and $\mathbf{z}$. Since we are
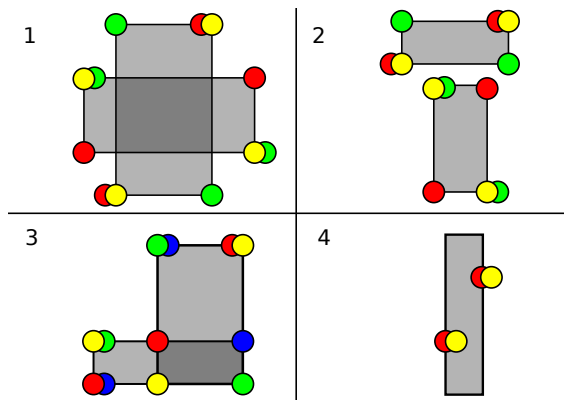
FIGURE 56. Distinct generators are represented by different colored dots. It is assumed that all pictured generators agree outside of the specified corners. Case 4 represents a degenerate rectangle which is actually an annulus.
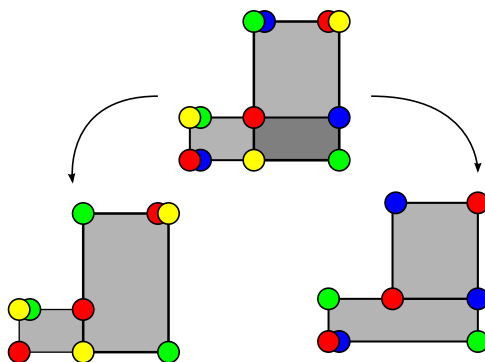
FIGURE 57. The two pairs of rectangles coming from case 3.

working with coefficients in $\mathbb{F}_2$, we simply need to ensure that such pairs of rectangles come in cancelling pairs. There are four ways that such rectangles can appear, which are shown in figure 56.

In cases 1 and 2 in figure 56, one can count the rectangles in either order. There is a pair of rectangles from red to yellow and then yellow to green, and there is another pair from red to green and then green to yellow (in these cases the rectangle from green to yellow wraps around the other direction).

The two pairs of rectangles coming from case 3 are pictured in figure 57.

In case 4 the rectangle is actually an annulus from a generator to itself. There are an even number of such annuli (of width 1 in the grid so as to not contain any other points of the generator) since there is one for each column and each row. The number of columns equals the number of rows so these cancel out as well. $\qquad\square$
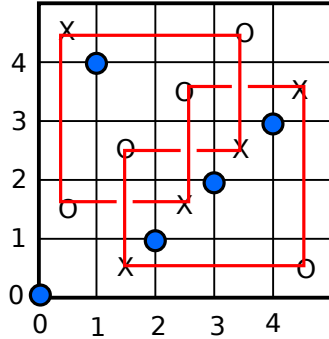
FIGURE 58. Grid diagram for the trefoil knot with a generator $\mathbf{x}$ indicated by the collection of blue dots.

The differential reduces the Maslov grading by 1. Each term in the image of the ∂^- reduces the Alexander grading, though not necessarily by the same amount. Thus, the Alexander grading is actually only a filtration, not a grading on (C^-, ∂^-).

The reason for the naming of the Alexander filtration comes from the relation of knot Floer homology to the Alexander polynomial. When we take the homology of the complex (C^-, ∂^-) and then look at the Euler characteristic of that bigraded homology (i.e. the alternating sum over the Maslov grading) we obtain the coefficients of the Alexander polynomial.

The proof that M and A are independent of grid moves is in [20]. We will omit the proofs here because they are basic counting arguments, and are not necessary to define the invariants of Legendrian and transverse knots.

The Alexander filtration counts the winding number of the knot around the points of a generator. This comes from the term

$$\mathcal{J}(\mathbf{x} - \frac{1}{2}(\mathbb{X} + \mathbb{O}), \mathbb{X} - \mathbb{O})$$

This comes from an analysis of examining which segments of the knot contribute to the winding number. The term $\mathcal{J}(\mathbf{x}, \mathbb{X} - \mathbb{O})$ counts the number of horizontal segments above the points of $\mathbf{x}$ which go partly counterclockwise around the points of $\mathbf{x}$ (and negatively counts those that go clockwise). The term $\frac{1}{2}\mathcal{J}(\mathbb{X} + \mathbb{O}, \mathbb{X} - \mathbb{O}) = \frac{1}{2}\mathcal{J}(\mathbb{X}, \mathbb{X}) - \frac{1}{2}\mathcal{J}(\mathbb{O}, \mathbb{O})$ accounts for which of these strands continue sufficiently far down and around to wind around the points of $\mathbf{x}$ and adds on a constant in terms of the positions of the X's and O's.

It may be useful to go through a brief example to compute the Maslov and Alexander gradings of a generator of $C^-(K)$ where K is the trefoil in figure 58 and $\mathbf{x}$ is the collection of dots on the integral lattice points on the grid.

We recall that $M(\mathbf{x}) = \mathcal{J}(\mathbf{x} - \mathbb{O}, \mathbf{x} - \mathbb{O}) + 1$. To compute $\mathcal{J}(\mathbf{x}, \mathbf{x})$ we count the number of pairs of points where one has both coordinates greater than the other. There are 4 points strictly "greater"

than $(0,0)$, 0 greater than $(1,4)$, 2 greater than $(2,1)$, 1 greater than $(3,2)$, and 0 greater than $(4,1)$. Therefore $\mathcal{J}(\mathbf{x},\mathbf{x}) = 4 + 0 + 2 + 1 + 0 = 7$. To compute $2\mathcal{J}(\mathbf{x},\mathbb{O})$ we need to count the number of O's greater than each point in $\mathbf{x}$ and the number of point in $\mathbf{x}$ greater than each O. Counting the number of O's greater than each point of $\mathbf{x}$ from left to right, and then the number of points of $\mathbf{x}$ greater than each O from left to right we get:

$$2\mathcal{J}(\mathbf{x},\mathbb{O}) = (5 + 1 + 2 + 1 + 0) + (3 + 1 + 0 + 0 + 0) = 13$$

Similarly to $\mathbf{J}(\mathbf{x},\mathbf{x})$, we compute $\mathbf{J}(\mathbb{O},\mathbb{O}) = 3 + 2 + 1 + 0 + 0 = 6$. Therefore

$$M(\mathbf{x}) = 7 - 13 + 6 + 1 = 1$$

The Alexander grading can be computed similarly.

We can look at the associated graded chain complex to (C^-, ∂^-) where the differential decreases the Alexander grading uniformly by 1. We will call the associated graded complex (CK^-, ∂). $CK^- = C^-$ but in computing the differential, we only sum over rectangles $r \in \text{Rect}^\circ(\mathbf{x},\mathbf{y})$ which do not contain any X's:

$$\partial(x) = \sum_{\mathbf{y} \in \mathbf{S}} \sum_{\substack{r \in \text{Rect}^\circ(\mathbf{x},\mathbf{y}) \\ r \cap \mathbb{X} = \emptyset}} U_1^{O_1(r)} \cdots U_n^{O_n(r)} \cdot \mathbf{y}$$

One can verify that if there are any X's in a rectangle, the term coming from that rectangle will have Alexander grading reduced by more than 1.

There is one other variation of knot Floer homology that we will use besides the homology of $(C^-(G), \partial^-)$. The chain complex is simply

$$\widetilde{CK}(G), \widetilde{\partial}) = (CK^-(G)/(U_1 = \cdots = U_n = 0), \partial)$$

This version makes computations more reasonable, and frequently carries enough information to be useful in distinguishing knots. Note that we can compute the differential $\widetilde{\partial}$ by only counting rectangles with no X's or O's.

One can show, using only this combinatorial description, that the homology of any of these chain complexes is independent of the grid diagram (i.e. is invariant under grid moves). These arguments can be found in [20]. They use similar techniques as in the proof that ∂^- is a differential. We will also use similar techniques in the upcoming section to define an invariant of Legendrian and transverse knots.

7. Legendrian and transverse invariants from knot Floer homology

7.1. **The Legendrian and transverse invariants.** We construct two invariants of Legendrian knots by choosing a particular element of $CK^-(G)$ (recall this is the associated graded object whose differential does not count rectangles containing X's) and looking at their images in the homology $HFK^-(G)$. We will show that the value of these elements in the homology is invariant under commutation, cyclic permutation, and (de)stabilizations of type $X\colon NW$ and $X\colon SE$. The image in the homology of one of these elements will also be invariant under $X\colon SW$ which corresponds to negative stabilization, so this will be a stable invariant and can thus be used to generate a transverse invariant of the transverse pushoffs.

Let $\mathbf{z}^+ \in \mathbf{S}(G)$ be the generator which has one dot in the upper right corner of each square containing an X, and let $\mathbf{z}^-$ be the generator with one dot in the lower left corner of each square containing an X. These are in $\mathbf{S}(G)$ because of the way the X's are required to be placed in the grid (one in each row and column). First we need to check that $\mathbf{z}^+$ and $\mathbf{z}^-$ are cycles, in the graded complex (CK^-, ∂), i.e.

$$\partial(\mathbf{z}^+) = \partial(\mathbf{z}^+) = 0$$

so that they are not always trivial in the homology. Because every rectangle from $\mathbf{z}^\pm$ to some other generator $\mathbf{y}$ has a point from $\mathbf{z}^\pm$ in the lower left corner and the upper right corner, there will always be an X in a rectangle from $\mathbf{z}^\pm$ to any $\mathbf{y}$. Therefore $\partial(\mathbf{z}^\pm) = 0$. Let $\lambda^\pm$ be the image of $\mathbf{z}^\pm$ in the homology.

Now we need to check that $\lambda^\pm$ are invariant under the grid moves corresponding to Legendrian isotopy. We will show that λ^+ is also invariant under the grid moves corresponding to negative stabilization and thus λ^+ is an invariant of the transverse pushoff. Any transverse knot can be approximated by a Legendrian knot, such that the transverse pushoff of the Legendrian knot is transversely isotopic to the knot we started with. Therefore to get the invariant of a transverse knot, find one such Legendrian approximation and then compute λ^+. This is well defined because λ_+ is invariant under negative stabilization.

To prove the homology $HFK^-(G)$ is invariant under grid moves, the authors of [**?**, MOST]onstructed chain maps which are quasi-isomorphisms (induce isomorphisms on homology) between the chain complexes $CK^-(G)$ and $CK^-(G')$ where G' is the grid obtained by G by performing a grid move. Therefore, to show that $\lambda^\pm$ are Legendrian/transverse invariants, we simply need to show that $\mathbf{z}^\pm$ are preserved under these chain maps. Since we reduced the grid moves to commutation and certain (de)stabilizations, we need only check preservation under these chain maps.

7.1.1. *Commutation.* To understand the chain map for commutation, we need to first depict both the commuted and uncommuted diagram on a single diagram as in figure 59

On this combined diagram, we see the grid line β coming from G and the grid line γ coming from the commuted diagram G'. They intersect at two points a and b. We say there is a pentagon, $p \in \text{Pent}_{\beta\gamma}(\mathbf{x}, \mathbf{y})$, if $\mathbf{x}$ agrees with $\mathbf{y}$ at all but 2 of its points, and there is an embedded disk p in the combined diagram whose boundary is 5 arcs each of which is a horizontal or vertical grid line (including β, γ), such that going counterclockwise around the boundary one starts at a point in
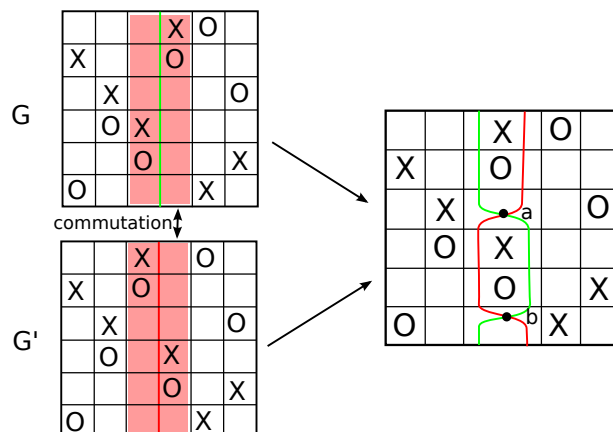
FIGURE 59. Placing a grid diagram G and its commuted grid diagram G' on a single diagram. β is the green strand corresponding to a grid line in G and γ is the red strand corresponding to a grid line in G'.
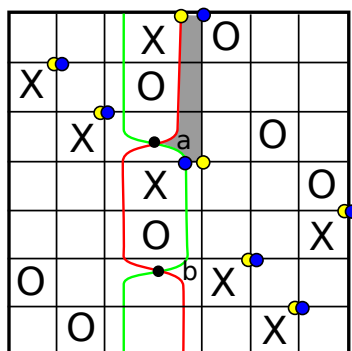
FIGURE 60. The shaded part is a pentagon in $\text{Pent}_{\beta\gamma}(\mathbf{x}, \mathbf{y})$. Here $\mathbf{x}$ is denoted by the blue dots and $\mathbf{y}$ is denoted by the yellow dots. Notice that $\mathbf{x}$ is a generator in the grid with the green line (β) and $\mathbf{y}$ is a generator in the grid with the red line (γ).

$\mathbf{x} \cap \beta$, follows a horizontal circle to a point of $\mathbf{y}$, follows a vertical circle to another point of $\mathbf{x}$, follows a horizontal circle to a point of $\mathbf{y} \cap \gamma$, follows γ to a point in $\gamma \cap \beta$, and then follows β to the starting point. See figure 60. The angles of the pentagon cannot exceed 180°, so the point of intersection of β and γ is determined by the orientation given to p. Thus all pentagons in $\text{Pent}_{\beta\gamma}(\mathbf{x}, \mathbf{y})$ contain one point of intersection and all pentagons in $\text{Pent}_{\gamma\beta}(\mathbf{y}, \mathbf{x})$ contain the other point of intersection.
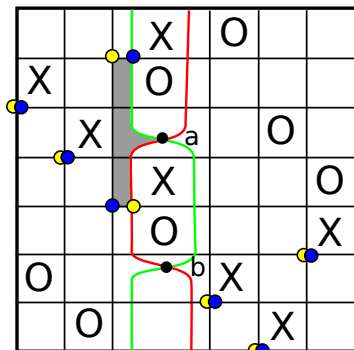
FIGURE 61. The pentagon from $\mathbf{z}^-$ to $\mathbf{z}^{-'}$.

We define the $\mathrm{Pent}^\circ_{\beta\gamma}(\mathbf{x}, \mathbf{y})$ to be the set of pentagons in $\mathrm{Pent}_{\beta\gamma}(\mathbf{x}, \mathbf{y})$ containing no point of $\mathbf{x}$ or $\mathbf{y}$. We can now define a chain map $\Phi_{\beta\gamma} : CK^-(G) \to CK^-(G')$:

$$\Phi_{\beta\gamma}(\mathbf{x}) = \sum_{y \in \mathbf{S}(G')} \sum_{\substack{p \in \mathrm{Pent}^\circ(\mathbf{x}, \mathbf{y}) \\ p \cap \mathbb{X} = \emptyset}} U_1^{O_1(p)} \cdots U_n^{O_n(p)} \cdot \mathbf{y}$$

The proof that $\Phi_{\beta\gamma}$ is actually a chain map (i.e. $\Phi_{\beta\gamma} \circ \partial = \partial \circ \Phi_{\beta\gamma}$) involves counting rectangle, pentagon pairs and comparing them to pentagon, rectangle pairs, similar to the argument counting rectangle, rectangle pairs in the proof that $\partial^- \circ \partial^-$ is a differential. The details are in [20]. Furthermore, they show that it is a chain homotopy equivalence explicitly. Therefore, we only need to show that $\Phi_{\beta\gamma}(\mathbf{z}^\pm) = \mathbf{z}^\pm$, where $\mathbf{z}^{\pm'}$ are the selected elements for G and $\mathbf{z}^{\pm'}$ for G'.

Figure 60 shows $\mathbf{z}^+$ (blue) and $\mathbf{z}^{+'}$ (yellow), and a single pentagon between them. Notice that any other pentagon from $\mathbf{z}^+$ must have boundary along β between the point a and the blue point of $\mathbf{z}^+$ which lies on β. If the other blue point of $\mathbf{z}^+$ on the boundary of a pentagon is not the one shown, then the pentagon will necessarily contain an X since every other point of $\mathbf{z}^+$ is in the upper right corner of a box with an X. Therefore the only pentagon we need to count is the one shown. Since it cannot contain any O's, we find that $\Phi_{\beta\gamma}(\mathbf{z}^+) = \mathbf{z}^{+'}$ as desired.

The argument is similar for $\mathbf{z}^-$. The single pentagon from $\mathbf{z}^-$ to $\mathbf{z}^{-'}$ is shown in figure 61. All other pentagons will contain an X in the lower left corner, so $\Phi_{\beta\gamma}(\mathbf{z}^-) = \mathbf{z}^{-'}$. This completes the proof that $\mathbf{z}^\pm$ are invariant under commutation moves.

7.1.2. *(De)stabilization.* To prove the equivalence of a stabilized and destabilized grid diagram, we find another chain complex that is quasi-isomorphic to the chain complexes of both the stabilized and destabilized grid diagrams. Let G be a grid diagram, and H be a grid diagram of a stabilization.

We will first define the map for $X \colon S*$ stabilization. The maps for $X \colon N*$ can be obtained by rotating all diagrams in the definition by $180°$.

We will denote the X and O in the added column by X_1 and O_1 respectively, Let m be the vertical grid line in H just left of X_1 and O_1 (it will be on the right for stabilizations of type $X \colon N*$). Let n
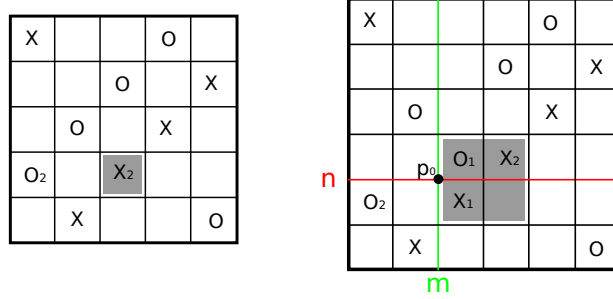
FIGURE 62. Grid G and its stabilized grid H

be the horizontal circle separating X_1 and O_1. Let p_0 be the point of intersection of m and n. See figure 62.

Let $C_G = CK^-(G)$ and $C_H = CK^-(H)$. Note that C_G is over $\mathbb{F}_2[U_2, \cdots, U_n]$ and C_H is over $\mathbb{F}_2[U_1, \cdots, U_n]$. Let C' be the mapping cone of

$$U_2 - U_1 : C_G[U_1] \to C_G[U_1]$$

i.e. C' is the chain complex $(C_G[U_1] \oplus C_G[U_1], \partial')$ where $\partial'(a, b) = (\partial a, (U_2 - U_1) \cdot a - \partial b)$, where ∂ is the differential of C_G.

To get a quasi-isomorphism from C_H to C' and then to C_G, we need more notation. Let $\mathbf{I} \subset \mathbf{S}(H)$ denote the subset of generators of C_H which contain the point p_0. This is in natural bijection with the generators of C_G since if we remove the lines m and n, and the decorations X_1 and O_1, we get exactly the grid C_G. Choosing generators with p_0 ensures that no other point lies on m or n.

We now define a generalization of rectangles between a generator in G and a generator in H.

Definition 19. *Suppose $\mathbf{x} \in \mathbf{S}(G)$ and $\mathbf{y} \in \mathbf{I} \subset \mathbf{S}(H)$. A domain $d \in \pi(\mathbf{x}, \mathbf{y})$ is a 2-chain whose boundary ∂d lies in the vertical and horizontal grid lines whose intersection with the vertices where the grid lines meet is exactly $\mathbf{y} - \mathbf{x}$. This means that the vertices along the boundary alternate between point of $\mathbf{x}$ and points of $\mathbf{y}$ and the boundary contains exactly the points of $\mathbf{x}$ and $\mathbf{y}$ where $\mathbf{x}$ and $\mathbf{y}$ disagree.*

A domain is said to be of type L or type R if it satisfies the following conditions:

(1) The local multiplicity of p is everywhere non-negative

(2) At each point in $\mathbf{x} \cup \mathbf{y}$ there are four adjacent rectangles (see figure 63). If $p \in \mathbf{x} \cup \mathbf{y}$, $p \neq p_0$ then the local multiplicity of at least 3 of these adjacent rectangles must be 0. At p_0 3 of the adjacent rectangles must have local multiplicity k. If d is a domain of type L then the lower left rectangle must have local multiplicity $k - 1$. If d is a domain of type R then the lower right rectangle must have local multiplicity $k + 1$. Examples are shown in figure 64.
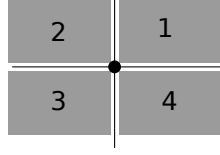
FIGURE 63. Adjacent rectangles to a point in a generator
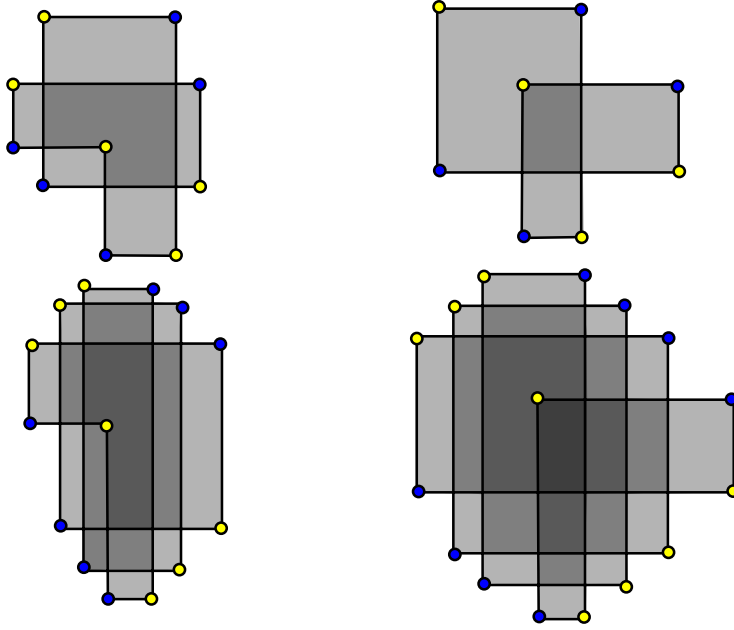
FIGURE 64. L domains from $\mathbf{x}$ (blue) to $\mathbf{y}$ (yellow) (left), and R domains from $\mathbf{x}$ (blue) to $\mathbf{y}$ (yellow) (right). The local multiplicity is indicated by the level of darkness of the shading.

Note: when defining the map for $X\colon N*$ stabilizations, these definitions will be rotated $180°$.

Using the notation $\pi^L(\mathbf{x}, \mathbf{y})$ for domains of type L and $\pi^R(\mathbf{x}, \mathbf{y})$ for domains of type R, we define for $\mathbf{x} \in CK^-(G)$:

$$F^L(\mathbf{x}) = \sum_{y \in \mathbf{I}} \sum_{\substack{d \in \pi^L(\mathbf{x},\mathbf{y}) \\ d \cap (\mathbb{X} \backslash X_1) = \emptyset}} U_2^{O_2(d)} \cdots U_n^{O_n(d)} \cdot \mathbf{y}$$

$$F^R(\mathbf{x}) = \sum_{y \in \mathbf{I}} \sum_{\substack{d \in \pi^R(\mathbf{x},\mathbf{y}) \\ d \cap (\mathbb{X} \backslash X_1) = \emptyset}} U_2^{O_2(d)} \cdots U_n^{O_n(d)} \cdot \mathbf{y}$$

The chain map which gives the quasi-isomorphism between C_H and C' is then $F : C_H \to C'$, defined by $F(a) = (F^L(a), F^R(a))$.

We want to show that $\mathbf{z}^{\pm}$ is invariant under the (de)stabilizations that preserve Legendrian isotopy type: $X\colon NW$ and $X\colon SE$. The relevant chain map that we need to check preserves $\mathbf{z}^{\pm}$ is
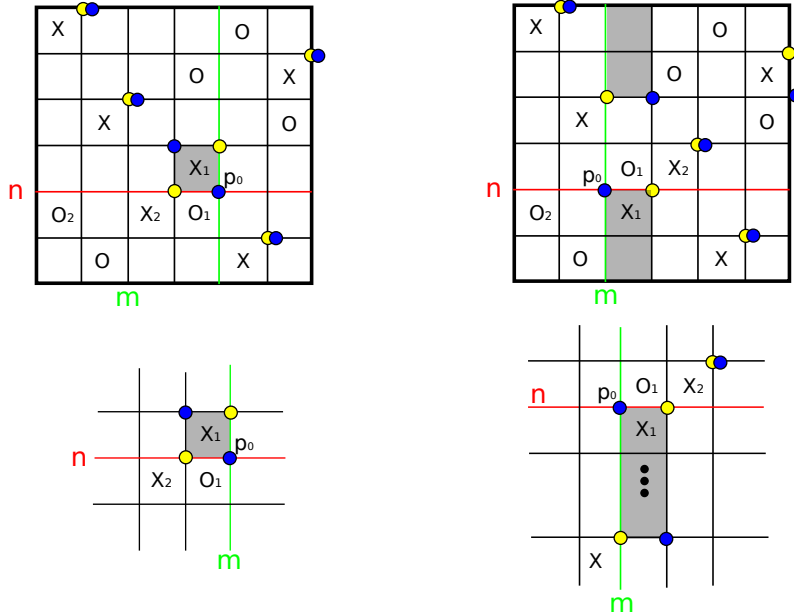
FIGURE 65. The unique region of type R for the $X\colon NW$ stabilization (left) and $X\colon SE$ stabilization (right). An explicit example is shown on the top, and the needed local data which is completely general is extracted below. The yellow dots make up $\mathbf{z}^+ \in \mathbf{S}(H)$. The blue dots represent $\mathbf{y} \in \mathbf{I}$, which is identified with $\mathbf{z}^{+\prime} \in \mathbf{S}(G)$.

$\phi \circ F : C_H \to C_G$. Notice that

$$\phi \circ F(\mathbf{x}) = \phi(F^R(\mathbf{x}))$$

where $\phi(F^R(\mathbf{x}))$ is an element in C_G obtained by identifying each generator $\mathbf{y} \in \mathbf{I}$ with the corresponding generator in C_G and substituting U_2 for any cases of U_1. Therefore we need to simply count the R domains from $\mathbf{z}^\pm \in \mathbf{S}(H)$ which do not contain any X's except X_1. Using a similar argument as commutation invariance, it is clear that there is only one way to form a region from $\mathbf{z}^\pm$ that does not contain any of $\{X_2, \cdots, X_n\}$, since any other region would have an unwanted X in the upper right (or lower left for $\mathbf{z}^-$) corner. This unique region of type R for $X\colon SE$ is shown in figure 65.

For the stabilization of type $X\colon NW$ we rotate the diagram by $180°$, so a type R region for this stabilization corresponds to a region with local multiplicity one greater in the upper left adjacent rectangle. The unique region in this case is shown in figure 65.

In both cases, the unique $\mathbf{y} \in \mathbf{I}$ to which $\mathbf{z}^+$ has a region is identified with $\mathbf{z}^{+\prime} \in \mathbf{S}(G)$, after grid lines m and n are collapsed and X_1 and O_1 are removed. Therefore the image of $\mathbf{z}^+$ under the chain map corresponding to destabilization is $\mathbf{z}^{+\prime}$. A symmetric argument works for $\mathbf{z}^-$.

Because these chain maps are quasi-isomorphisms, this completes the proof that $\lambda^\pm$ are invariants of Legendrian knots.
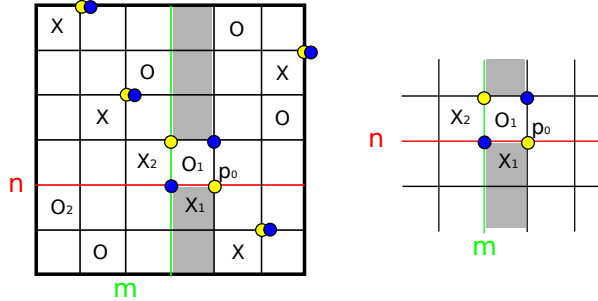
FIGURE 66. The unique type R region from $\mathbf{z}^+$ under $X\colon SW$ stabilization. The yellow dots are $\mathbf{z}^+$ in the stabilized diagram. The blue are $\mathbf{y}$ which is identified with $\mathbf{z}^{+\prime}$ in the destabilized diagram.

7.1.3. *The transverse invariant.* By analyzing the domains corresponding to $X\colon SW$, we can show that λ^+ is invariant under negative stabilizations. As in the proof of invariance under $X\colon NW$ and $X\colon SE$ stabilizations, there is a unique region from $\mathbf{z}^+$ which does not contain any of $\{X_2, \cdots, X_n\}$. This is shown in figure 66.

Since λ^+ is invariant under negative stabilizations, it provides a well-defined invariant of transverse knots. For any transverse knot, find a Legendrian approximations and compute λ^+ to get a transverse invariant. This is independent of the choice of Legendrian approximation by theorem 16.

Note on mirror images: Because of the convention that the grid diagram actually gives the mirror image of the knot, one might be concerned that we are not getting information about the knots we are thinking of, but rather of their mirror images. However, these Legendrian and transverse invariants are preserved by taking the mirror image of a knot with opposite orientation [24], so results distinguishing mirror image grid diagrams of knots with opposite orientation are equivalent to results distinguishing the knots themselves.

7.2. **Using the invariants to distinguish transverse knots.** These invariants would be considerably less interesting if they were unable to actually distinguish Legendrian and transverse knots that cannot be distinguished through knot type and their classical invariants. Fortunately, these invariants are quite effective at distinguishing Legendrian and transverse knot types. Furthermore, they are computable invariants. The C program [23] computes these invariants and some of their variations. This program adapts the computation of the entire knot Floer homology from [2] to simply computing whether the transverse invariant (and some of its variations) are trivial. There are many examples of knots which are distinguishable through these invariants. See [22], [18], and [1] for individual examples and some infinite families of nonsimple transverse knots.
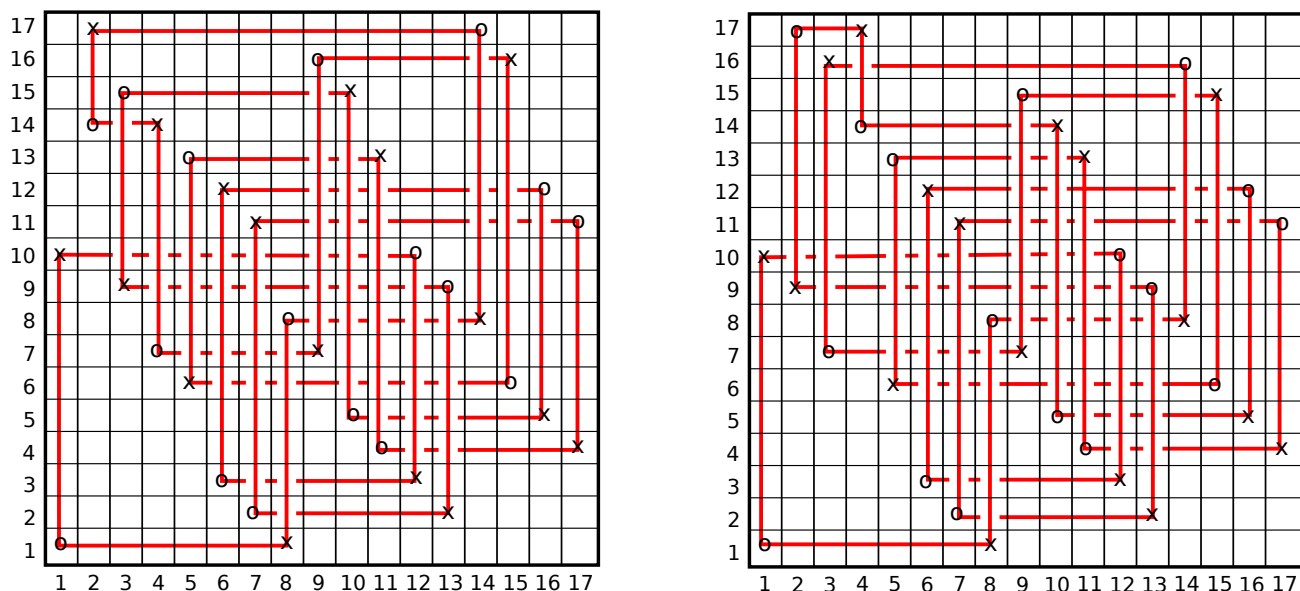
FIGURE 67. The grid diagrams for the two stably distinct versions of the $(2,3)$ cable of the $(2,3)$ torus knot. The diagram on the left is L_1 and the diagram on the right is L_2.

To compute these invariants, we need grid diagrams for two candidates which represent the same topological knot type with the same classical invariants, but are not stably isotopic. While the geometric methods developed in the previous sections were able to generate large classes of transversely non-simple knots, they did not generate explicit diagrams for these knots. Using techniques that come from braid theory, Matsuda and Menasco [21] generated grid diagrams for the $(2,3)$ cable of the $(2,3)$ torus knot. L_1 corresponds to the (mirror image with opposite orientation of the) $(2,3)$ cable of the $(2,3)$ torus knot of $tb = 5$, $r = 2$ which destabilizes, and L_2 corresponds to the (mirror image with opposite orientation of the) knot with the same classical invariants that does not destabilize. These are the explicit diagrams for the (mirror images with opposite orientations of the) Etnyre-Honda pair. The grids are 17×17 and are shown in figure 67.

After running these grid diagrams through the C program, one finds that the transverse invariant for L_1 is null-homologous while the transverse invariant for L_2 is not null homologous. This provides a purely computational proof that the $(2,3)$ cable of the $(2,3)$ torus knot is transversely nonsimple. However, the theory that went into generating these particular diagrams was based in the geometric constructions of Etnyre and Honda, and the braid theory of Birman, Matsuda, and Menasco. What we still need to understand is exactly how these vastly different techniques relate to each other to provide these classification results.

7.3. **Conclusion.** While the computation of the transverse invariant for the diagrams for the $(2,3)$ cable of the $(2,3)$ torus knot takes some time even with the C program, they can be done, and indeed the invariant distinguishes them. However, performing the computation with much more complicated examples requires significant computing power. Furthermore, unless there is a fairly nice pattern in the grid diagrams, only finitely many examples can be computed at a time. While the geometric proof is less explicit and requires careful argumentation in convex surface theory, it proves the existence of infinitely many transversely nonsimple knots for which we cannot compute the algebraic invariants. On the other hand, the algebraic invariants can identify many other transversely nonsimple knots besides cables of torus knots. The introduction of various techniques, geometric cut-and-paste arguments and algebraic transverse invariants, has provided greatly increased knowledge of knots within contact structures. While there were no examples of transversely nonsimple knots before about 2006, we now have a wealth of examples. The next step is to try to understand the connections between these varied techniques to gain a better understanding of why transversely nonsimple knots exist, so we might find a more careful characterization of exactly when transversely nonsimple knots appear.

References

1. J.A. Baldwin, *Comultiplication in link Floer homology and transversely non-simple links*. arxiv:0910.1102v1[math.GT]

2. J.A. Baldwin and W.D. Gillam. *Computations of Heegaard-Floer knot homology*. arxiv:0610167v3[math.GT]

3. Y.V. Chekanov, *Invariants of Legendrian knots*. Proceedings of the ICM, Vol. II (Beijing, 2002), 385–394, Higher Ed. Press, Beijing, 2002.

4. P.R. Cromwell, *Embedding knots and links in an open book. I. Basic properties*, Topology Appl. 64: 37–58, 1995.

5. Y. Eliashberg, *Classification of overtwisted contact structures on 3-manifolds*. Invent. Math. 98(3):623–637, 1989.

6. Y. Eliashberg, *Contact 3-manifolds twenty years since J. Martinent's work*. Ann. Inst. Fourier (Grenoble) 42(1-2):165–192, 1992.

7. J.B. Etnyre, *Introductory lectures on contact geometry*. Topology and geometry of manifolds (Athens, GA 2001), 81–107, Proc. Sympos. Pure Math., 71, 2003.

8. J.B. Etnyre, *Legendrian and transversal knots*. Handbook of knot theory, 105–185, *Elsevier B.V.*, Amsterdam, 2005.

9. J.B. Etnyre and K. Honda, *Knots and contact geometry. I. Torus knots and the figure eight knot*. J. Symplectic Geom. 1(1): 63–120, 2001.

10. J.B. Etnyre and K. Honda, *Cabling and transverse simplicity*. Ann. of Math. 162(3):1305–1333, 2005.

11. H. Geiges, *An Introduction to Contact Topology*. Cambridge Stud. Adv. Math., vol. 109. Cambridge. University Press, Cambridge, 2008.

12. E. Giroux, *Convexité en topologie de contact*. Comment. Math. Helv. 66(4):637–677, 1991.

13. K. Honda, *Gluing tight contact structures*. Duke Math. J. 115(3): 435–478, 2002.

14. K. Honda, *On the classification of tight contact structures. I*. Geom. Topol. 4:309–368, 2000.

15. K. Honda, *On the classification of tight contact structures. II*. J. Differential Geom. 55(1):83–143, 2000.

16. Y. Kanda, *The classification of tight contact structures on the 3-torus*. Comm. Anal. Geom. 5(3):413–438, 1997.

17. Y. Kanda, *On the Thurston-Bennequin invariant of Legendrian knots and nonexactness of Bennequin's inequality*. Invent. Math. 133(2):227–242, 1998.

18. T. Khandhawit and L. Ng, *A family of transversely nonsimple knots*. arxiv:0806.1887v2 [math.GT]

19. C. Manolescu, P. Ozsváth, S. Sarkar, *A combinatorial description of knot Floer homology*. Ann. of Math. 169(2): 633–660, 2009.

20. C. Manolescu, P. Ozsváth, Z. Szabó, D. Thurston, *On combinatorial link Floer homology*. Geom. Topol. 11: 2339–2412, 2007.

21. W.W. Menasco and H. Matsuda *On rectangular diagrams, Legendrian knots and transverse knots* arxiv: 0708.2406v1 [math.GT].

22. L. Ng, P. Ozsváth and D. Thurston, *Transverse knots distinguished by knot Floer homology*. J. Symplectic Geom. 6(4): 461–490, 2008.

23. L. Ng, P. Ozsváth and D. Thurston, *TransverseHFK.c: A program for computing the transverse invariant from knot Floer homology*. www.http://www.math.columbia.edu/ petero/transverse.html

24. P. Ozsváth, Z. Szabó and D. Thurston, *Legendrian knots, transverse knots and combinatorial Floer homology*. arxiv:0611841[math.GT]

25. O. Plamenevskaya, *Transverse knots and Khovanov homology*. Math. Res. Lett., 13(4):571–586, 2006.

26. P. Scott, *The geometries of 3-manifolds*. Bull. London Math. Soc. 15: 401–487, 1983.